# UTILIZING LANDSAT IMAGERY, AERIAL PHOTOGRAPHS, AND TOPOGRAPHIC MAPS FOR DETECTING AREA AND LENGTH PARAMETRIC CHANGES TO FIVE ALPINE GLACIERS NEAR SKAGWAY, ALASKA, 1948-2011

A THESIS PRESENTED TO
THE DEPARTMENT OF HUMANITIES AND SOCIAL SCIENCES
IN CANDIDACY FOR THE DEGREE OF
MASTER OF SCIENCE

By
JEREMY C. SMITH

NORTHWEST MISSOURI STATE UNIVERSITY
MARYVILLE, MISSOURI
APRIL, 2013

# GLACIER CHANGE ANALYSIS

Utilizing Landsat imagery, aerial photographs, and topographic maps

for detecting area and length parametric changes

to five alpine glaciers near Skagway, Alaska, 1948-2011

Jeremy C. Smith

Northwest Missouri State University

THESIS APPROVED

| | |
|---|---|
| Thesis Advisor, Dr. Ming-Chih Hung | Date |
| Dr. Yi-Hwa Wu | Date |
| Dr. John Pope | Date |
| Dean of Graduate School, Dr. Gregory Haddock | Date |

Utilizing Landsat imagery, aerial photographs, and topographic maps
for detecting area and length parametric changes
to five alpine glaciers near Skagway, Alaska, 1948-2011.

## Abstract

The study of glacier dynamics, locally and globally, has become a topic of increasing interest and importance in assessing the effects of climate change, and previous research has demonstrated that analysis of glacier parameters provides valuable information regarding the various consequences of this change. The purpose of this research was to detect temporal change in two specific glacier parameters: glacier extent (total area) and total length along with identifying the rates and direction/trend for the Laughton, Carmack, Cleveland, Saussure, and Irene Glaciers, all situated within the vicinity of Skagway, Alaska. Landsat TM and ETM+ image scenes from 1984-2011 were utilized in addition to aerial photographs and topographic maps from as early as 1948 to identify glacier parametric changes and trends. Furthermore, specific processing techniques were applied for the purpose of accurately mapping glaciers, including manual extraction, calculating the Normalized Difference Snow Index statistic, band ratioing, and performing a supervised classification.

Results of the analysis indicated that the total areas and lengths for all five glaciers experienced significant change during the period of 1948-2011. All glaciers individually decreased in area by approximately 31% - 65% and retreated in length by

approximately 19% - 43%; whereas collectively the trend of all glacier areas and lengths were found to be decreasing by approximately 42% and 31%, respectively. Although there were some image years that experienced substantial glacier advancement during this time period, the overall trend was clearly shown to be moving in the negative direction. In addition, the results of this study provided an even more current and comprehensive assessment of five Southeast Alaska glaciers and contributed to the state of Alaska's glacier inventory. Eventually it was determined that this study could be expanded on in the future specifically by analyzing each glacier's mass balance and elevation change in addition to examining and quantifying the correlation between climate change and glacier parametric changes.

TABLE OF CONTENTS

## LIST OF FIGURES

## LIST OF TABLES

## ACKNOWLEDGMENTS

I would like to express my gratitude and appreciation first and foremost to Dr. Ming Hung, who chaired my thesis committee and offered encouragement, editing and formatting remarks, and valuable feedback throughout the thesis process. I would also like to recognize and thank the two other members of my committee, Dr. Yi-Hwa Wu and Dr. John Pope, in addition to Dr. Patty Drews, Graduate GIScience Program Director, all who made thoughtful and meaningful inquiries of my research and provided opportunities for me to defend my methods, findings, and conclusions.

Furthermore, I feel that it is necessary recognize the source of inspiration for the subject of my research with its associated study area. I lived and worked in Skagway, Alaska during the summer months of 2000-2007 and developed a knowledge and fascination of the surrounding temperate rain forests, alpine and tidewater glaciers, and abundant wildlife. Lastly, I would especially like to thank my mother and father for their continual interest in my graduate studies and frequent words of encouragement that provided me with extra motivation to persevere through the graduate program.

## LIST OF ABBREVIATIONS

AOI: Area of Interest

ASTER: Advanced Spaceborne Thermal Emission and Reflection Radiometer

DEM: Digital Elevation Model

ERDAS: Earth Resources Data Analysis System

ESRI: Environmental Systems Research Institute

ETM+: Enhanced Thematic Mapper Plus

GIS: Geographic Information Systems

GPS: Global Positioning Systems

IHS: Intensity Hue Saturation

JIRP: Juneau Icefield Research Program

MODIS: Moderate Resolution Imaging Spectroradiometer

MSS: Multi-Spectral Scanner

NASA: National Aeronautics and Space Administration

NDSI: Normalized Difference Snow Index

PCA: Principal Component Analysis

TM: Thematic Mapper

SAR: Synthetic Aperture Radar

USGS: United States Geological Survey

## GLOSSARY OF TERMINOLOGY

| Term | Definition |
|---|---|
| Ablation | All processes that reduce glacier mass, including melting and calving. |
| Accumulation | All processes that add to glacier mass, including snowfall. |
| Albedo | Portion of incident radiation (such as light) reflected by a surface or body. |
| Equilibrium Line Altitude | The elevation above which snow and ice cover the ground year-round. |
| Frontal Termini | Leading edge or front of the glacier. |
| Geomorphology | The study and interpretation of the earth's relief features. |
| Mass Balance | The change in glacier mass as a difference between accumulation and ablation. |
| Transient Snowline | The boundary between the previous winter's snow and older ice and snow. This boundary moves up the glacier during the summer melting season. |

Definitions for Ablation, Accumulation, Equilibrium Line Altitude, and Mass Balance were acquired from the University of Alaska, Fairbanks Geophysical Institute website. The definitions for Albedo, Frontal Termini, and Transient Snowline were acquired from the Merriam-Webster Dictionary website, United States Geological Survey website, and the National Aeronautical Space Administration website, respectively. The definition for Geomorphology was acquired from the Merriam-Webster Dictionary website.

# CHAPTER 1: INTRODUCTION

The study of glacier dynamics, locally and globally, has become a topic of increasing interest and importance in assessing the effects of climate change. A multitude of research (Solomon et al., 2007; Paul, 2002; Schoner et al., 2000; Haeberli and Hoelzle, 1995) demonstrates that analysis of glaciers provides valuable information regarding the various consequences of climate change (such as glacier retreat and subsequent rises in sea levels) in addition to ecological processes in the earth's environment. When examining glacier advance/retreat rates, specific changes to one or more parameters are typically analyzed, including glacier area, thickness, elevation, volume, length, velocity, and geomorphology.

The state of Alaska contains a sizeable percentage of all glaciers in the Western Hemisphere, and it has been well documented that there has been a significant overall retreat of glaciers in the state over the last 30+ years. The southeast part of the state, commonly referred to as the Alaska Panhandle, contains an abundance of both alpine and tidewater glaciers—particularly within the Coast Mountains. "Alpine glaciers" denote areas of glacier ice formed among mountain summits that descend through high valleys. Often such glaciers consist of one or more distributaries (glacier areas that move away from the primary glacier body). "Tidewater glaciers" denote glaciers that contain termini ending in a tidally-influenced water body (such as an ocean or lake) and are often evidenced by icebergs resulting from glacier calving (United States Geological Survey, 2013). A vast majority of glacier change studies in southeast Alaska have been limited to the Juneau Icefield, an expanse of alpine and tidewater glaciers extending from just south of the city and borough of Juneau to just south of the borough of Skagway.

There is a demonstrated need for inventorying glaciers in Alaska in order to evaluate the consequences of climate change in North America. There has never been a comprehensive inventory of all glaciers in the state, and a relatively large proportion of Alaska's glaciers reside within the Alaska Panhandle—either within the Coast Mountains along the eastern boundary of the state or within mountain ranges found throughout the archipelago of the Inside Passage. In addition, much of the current statewide glacier baseline data is derived from Landsat Multi-Spectral Scanner (MSS) false-color composite images collected between 1972 and 1981 and 1:250,000 scale topographic maps. However, many of the topographic maps are derived from data collected between 1949 and 1979 by the Unites States Geological Survey (USGS), the National Geospatial Intelligence Agency (NGA, formerly known as the National Imagery and Mapping Agency), and other organizations.

The use of remote sensing technology has proven to be an efficient method for inventorying glaciers; and Geographic Information Systems (GIS) have commonly been incorporated for the purpose of analyzing the resulting geometry, statistics, and other calculations of the various glacier parameters. Digital image processing techniques have shown to be particularly adept at processing the remotely-sensed data (e.g., image enhancement, classification, and change detection) and for improving the ease and accuracy of mapping glaciers. Many remote sensing techniques also offer the major advantage of deriving spectral characteristics of glaciers in various regions of the electromagnetic spectrum that are not discernable to the naked eye (e.g., infrared and thermal bands). Glaciers have their own unique spectral signature, and images recorded

by various remote sensing platforms allow for detailed image analysis of glacier parameters.

Landsat Thematic Mapper (TM) and Enhanced Thematic Mapper Plus (ETM+) images have often been utilized for identifying glaciers on the earth's surface remotely, and they specifically have demonstrated their ability for delineating glacier areas from other land cover types through the application of various band ratio and image classification techniques. Landsat image analysis is not without its share of major challenges, however. Often problems in glacier delineation arise when there are glacier areas covered by glacier debris, shadow areas (particularly areas adjacent to mountain ridges), and prominent cloud cover over the analysis area. Over the years, a variety of methods for mapping glaciers under these conditions have been developed that focus on using specific Landsat image analysis methods.

A particular advantage of using Landsat ETM+ and TM imagery for inventorying glaciers in southeast Alaska is the excellent availability of annual image scenes from 1984-present. In addition, some aerial photographs and topographic maps are readily available for assisting with the inventorying process. Having a near complete collection of useable imagery on an annual basis allows one to study not only the aforementioned glacier parameters, but glacier trend and variability as well. However, although there is a relatively large collection of Landsat TM/ETM+ scenes, there are some considerable issues with cloud cover, shadow areas, and seasonal snow variability that still need to be overcome during the glacier change detection process.

Multi-temporal Landsat TM/ETM+ imagery are particularly suitable as primary data sources for detecting change in land cover classification. Change detection is a

critical component in the study of specific changes to glacier parameters on an annual basis over a specified time period. In addition, the success of any remote sensing change detection project is significantly affected by the spatial, temporal, spectral, and radiometric resolution of the remotely-sensed data. Accuracy assessments for land cover classification and change detection techniques are commonly performed in order to evaluate the effectiveness of the selected technique when analyzing glacier parametric changes and trends. This thesis incorporates a thorough review of the literature concerning change detection/analysis methods employed on remotely-sensed glacier data.

### 1.1 Research Objective

The research objective of this study is to detect temporal change in two specific glacier parameters: glacier extent (total area) and total length along with identifying the rates and direction/trend of glacier change for five southeast Alaska glaciers that are in relatively close proximity to each other. This study focused on the Laughton, Carmack, Cleveland, Saussure, and Irene Glaciers. Annual Landsat TM and ETM+ image scenes from 1984-2011 were utilized in addition to aerial photographs and topographic maps from earlier dates (as early as 1948). Specific image processing techniques were employed on the satellite imagery in order to overcome glacier mapping challenges attributed to cloud cover and shadow areas, and a post-classification change detection method was used for evaluating the changes in the aforementioned glacier parameters. Glacier areas extracted from aerial photographs and topographic maps were also incorporated in to the change analysis. This research generally identified what glacier changes have occurred through time, the direction of change, the locations of greatest/least change, and a comparison of the changes between the five glaciers.

Therefore, by utilizing annual Landsat TM/ETM+ image scenes for 1984-2011 (in addition to earlier aerial photographs and topographic maps) an even more current and comprehensive assessment of five southeast Alaska glaciers can contribute to the state's glacier inventory—particularly by examining change during an almost 30-year period widely believed to have experienced the greatest degree of climate change and subsequent glacier retreat.

**1.2 Study Area**

The five named glaciers analyzed in this study are situated at the northern terminus of the Coast Mountains at the head of the Taiya Inlet (see Figure 1), and include the Laughton, Carmack, Cleveland, Saussure, and Irene Glaciers. All five are categorized as alpine glaciers, and a sizeable area of the eastern portion of the study area (including the Laughton Glacier) lies within the Tongass National Forest. The study area bounding box for all five glaciers extends from 59°45'16"N, 135°31'39"W at the northwest corner to 59°26'25"N, 135°04'08"W at the southeast corner, a total land area of approximately 284mi$^2$ (736km$^2$). The topography is quite varied, ranging from sea level at the Taiya Inlet to approximately 7,000ft (2,134m) at the peaks of the Sawtooth Range above the Laughton Glacier. The general climate of the area can be considered primarily humid continental (warm summer subtype), as summer high temperatures typically range between 60 to 80 degrees Fahrenheit and winter high temperatures range between 15 to 30 degrees Fahrenheit, with heavy snowfall in the surrounding Coast Mountains, particularly in areas above 500ft (152m) in elevation. Seasonal snow in the mountains typically lasts well into June, whereas areas of lower elevation (<500ft/152m) are typically clear of snow by the beginning of May.

The closest settlement in the proximity of the study area is the borough of Skagway, which has a year-round population of 920 (United States Census Bureau, 2010). However, this number tends to increase by several thousand during the summer tourism season, as the borough is major port of call for prominent cruise lines. The Laughton Glacier is situated approximately five miles northeast of Skagway, whereas the four other glaciers in this study are located 7-20 miles north of the borough in mountain areas of highest elevation. All snow/glacier water runoff tends to flow into two primary rivers in the region: the Skagway River (with several forks) and the Taiya River.

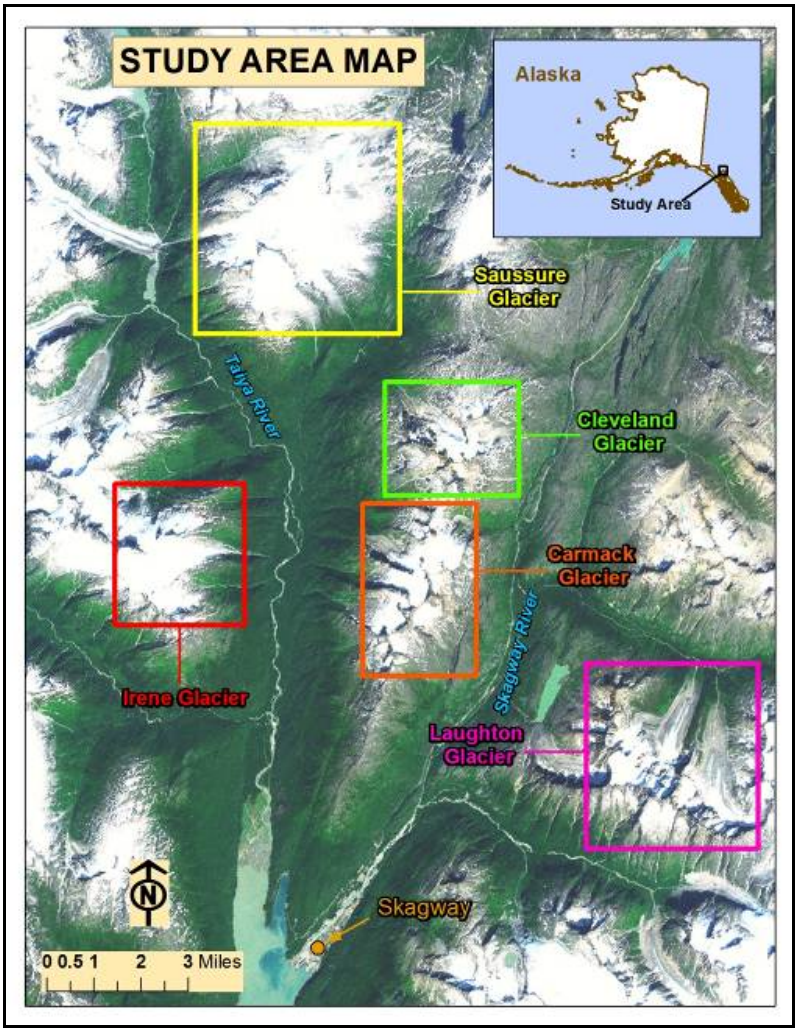


Figure 1. Study Area Map

### 1.3 Description of Data Sources

All topographic maps (see Table 1), aerial photographs (see Table 2), and Landsat imagery (see Table 3) utilized in the glacier change analysis were selected and retrieved through the USGS Earth Explorer application (URL: www.earthexplorer.usgs.gov). Reference and ground truth imagery used for geo-referencing and thematic accuracy assessment, respectively, were obtained from DigitalGlobe, Inc. (see table 4).

Table 1. Topographic maps utilized in the study.

| Map Name | Date | Scale | Full Coverage |
|---|---|---|---|
| Skagway C-1 | 07/1948 | 1:63,360 | Carmack, Cleveland |
| Skagway C-1/C-2 Mosaic | 07/1948 | 1: 63,360 | Irene |
| Skagway C-1/B-1 Mosaic | 07/1948 | 1:63,360 | Laughton |
| Skagway C-1/C-2 Mosaic | 07/1948 | 1:63,360 | Saussure |
| Skagway | 07/1961 | 1:250,000 | All |

Table 2. Aerial photographs utilized in the study.

| Entity ID | Date | Scale | Full Coverage | RMSE |
|---|---|---|---|---|
| AR5790028056746 | 08/11/1979 | 1:123,214 | Carmack, Cleveland, Irene, Laughton | 3.98m |
| AR5790028056747 | 08/11/1979 | 1:123,214 | Saussure | 6.02m |

Table 3. Landsat satellite imagery utilized in the study.

| Satellite | Date | % Cloud Cover | Acceptable Imagery |
|---|---|---|---|
| Landsat TM | 09/25/1984 | < 1 | All Glaciers |
| Landsat TM | 09/12/1985 | < 2 | None |
| Landsat TM | 09/06/1986 | 0 | All Glaciers |
| Landsat TM | 08/24/1987 | < 1 | All Glaciers |
| Landsat TM | 08/19/1988 | 35 | None |
| Landsat TM | 08/13/1989 | 5 | All Glaciers |
| Landsat TM | 09/26/1990 | 10 | All Glaciers |
| Landsat TM | 08/28/1991 | 40 | None |
| Landsat TM | 08/30/1992 | 10 | All Glaciers |
| Landsat TM | 08/08/1993 | 20 | Carmack, Cleveland, Irene, Saussure |
| Landsat TM | 08/11/1994 | 50 | Carmack, Cleveland |
| Landsat TM | 09/24/1995 | 0 | All Glaciers |
| Landsat TM | 08/16/1996 | < 2 | All Glaciers |
| Landsat TM | 09/13/1997 | 20 | Carmack, Cleveland, Saussure |
| Landsat TM | 09/16/1998 | 10 | All Glaciers |
| Landsat TM | 08/18/1999 | 5 | All Glaciers |
| Landsat ETM+ | 08/15/2001 | < 2 | Carmack, Irene, Laughton |
| Landsat TM | 09/05/2003 | 10 | Carmack, Cleveland, Irene, Laughton |
| Landsat TM | 08/22/2004 | 5 | Carmack, Cleveland, Irene, Laughton |
| Landsat TM | 08/09/2005 | 5 | All Glaciers |
| Landsat TM | 08/28/2006 | 55 | All Glaciers |
| Landsat TM | 08/15/2007 | 3 | All Glaciers |
| Landsat TM | 08/10/2008 | 25 | None |
| Landsat TM | 09/14/2009 | < 2 | Carmack, Cleveland |
| Landsat TM | 08/16/2010 | 20 | Laughton |
| Landsat TM | 09/11/2011 | < 2 | All Glaciers |

Table 4. Reference and ground truth imagery utilized in the study.

| Satellite | Date | Spatial Resolution | Coverage |
|---|---|---|---|
| Worldview-1 | 09/15/2006 | 0.8m | Irene |
| Worldview-1 | 09/29/2009 | 0.6m | Laughton |
| Worldview-1 | 09/16/2010 | 0.6m | Cleveland, Irene |
| Worldview-1 | 09/16/2010 | 0.6m | Saussure |
| Worldview-1 | 09/21/2010 | 0.6m | Carmack |

# CHAPTER 2: LITERATURE REVIEW

## 2.1 Climate Change and Glaciers

There has been an increasing interest, particularly within the physical and environmental sciences, in the effects of climate change. Research has shown that glaciers, ice caps, and ice sheets can be considered "sensitive indicators" of climate change (Zemp et al., 2008; Haerberli, 1998); and studies focusing on glacier change have often provided valuable insights in to changes in climate (Solomon et al., 2007; Paul, 2002; Schoner et al., 2000; Haeberli and Hoelzle, 1995). These variables typically include precipitation and air temperature, and analyses such as a specific one involving glaciers on Kenya's Mt. Kilimanjaro performed by Kaser et al. (2004) often examine modern glacier recession rates in order to gain greater insight in to the interactions between these climate variables and glaciers. For example, Schoner et al. (2000) studied climate change variability and subsequent glacier response in the Austria eastern Alps, and they discovered a positive correlation between glacier mass balance and summer air temperature and winter glacier accumulation. Indeed, there has been remarkable progress in recent years in modeling the response of glaciers to the assortment of climate change variables (Barry, 2006).

Changes in the area extent of glaciers provide evidence of the glaciers' response to past changes in climate; and climate conditions can not only be studied to understand the spatial distribution of glacier areas, but also to quantify long-term climate controls on glacier health over a broad area (Shea et al., 2004; Paterson, 1994). Furthermore, Oerlemens (1994) concluded that the most effective method for examining the relationships between climate change and glacier activity is to annually monitor the

losses or gains of the glaciers at the surface. Climate variability can particularly be examined not only by studying such glacier geometric parameters as area, volume, and length, as emphasized in the Global Climate Observation System (Haeberli et al., 2000), but also through utilizing a collection of regional glacier data over a time period of several decades—specifically for analyzing climate change and subsequent glacier responses in small alpine glaciers. There is significant importance in studying glacier changes' responses to climate change over the last approximately 30 years, as there has been a demonstrated increase in glacier recession globally and locally during this period more than any other since the last ice age (Barry, 2006).

Peduzzi et al. (2010) elaborated further on glacier and climate change relationships in noting that glacier volume worldwide is currently on a downward trajectory at an accelerating rate, and Moore et al. (2009) examined changes in western North America glaciers and found consistent recession of glaciers in western Canada and the conterminous United States over the last several decades. A particular consequence of great concern with glacier recession is that approximately $1/6^{th}$ of the world's population depends on glacier and snow melt to supply their water needs (Bradley et al., 2006). Consequently, it has been demonstrated that another one of the consequences of glacier recession is an increase in stream temperatures which greatly affect hydrological systems, and therefore glaciers significantly influence the relationship between climate change and streamflow (Moore et al., 2009). In addition, Barnett et al. (2005) analyzed impacts of warming climates on the availability of freshwater in areas dominated by snow and glaciers and noted that serious water supply shortage risks were prevalent during dry seasons, particularly in areas that heavily depend on glacier meltwater.

Furthermore, Dyurgerov (2002) temporally evaluated 280 glaciers worldwide from 1945 to 1998 and concluded that annual meltwater production (glacier ablation) increased by approximately 5.6ft (1.7m)/year in water equivalent. Moreover, Meier and Bahr (1996), while inventorying all small glaciers worldwide (excluding the two major ice sheets of Greenland and Antarctica), calculated a total glacier area of at least 262,550$mi^2$ (680,000$km^2$). However, although this area only comprises approximately four percent of all land ice area, glaciers collectively contributed up to 30 percent of changes in sea levels during the 20$^{th}$ century as a consequence of shrinking ice volumes and warming climates (Meier, 1984).

Although the collection of glaciers, ice caps, and ice sheets at small and large scales have shown to be important evidences of climate change, it has also been believed that inland/valley glaciers and small ice caps contribute significantly to sea level fluctuations on a global scale—one of the major consequences of climate change (Oerlemans, 2001). The study of mountain/alpine glaciers specifically for the purpose of analyzing parametric changes has shown to be of great importance. Barnett et al. (2005) noted that alpine glaciers are "key indicators" of climate change, also taking in to consideration the varying contributions of climatic variables, regionally and globally. In fact, while analyzing small glaciers (specifically alpine glaciers), Wood (1988) determined that not only are alpine glaciers good indicators of climate change, but they are also believed to be particularly sensitive to long-term trends in temperature and precipitation. Dyurgerov and Meier (1999) studied the relationship between small glacier changes for the purpose of isolating evidences of past climate change in addition to projecting the potential effects that future global warming might have on such glaciers.

Furthermore, Luckman and Kavanagh (2000) examined alpine glaciers in the Canadian Rockies and discovered that such temporal glacier changes provided critical evidence of climate change in mountainous areas. This concept was furthered by Oerlemans (2001) as he stated that alpine glaciers (rather than ice caps) are especially sensitive to climate changes because of the generally warmer and wetter climate conditions of their local environment (mountain ranges). In addition, changes in alpine glacier sizes have been shown to be a positive indicator of changing air temperatures that may or may not be caused by human activities (Haeberli et al., 2000).

**2.2 Glaciers of Alaska**

Approximately 5 percent of the state of Alaska is covered by glaciers (roughly 29,000$mi^2$/75,000$km^2$ as estimated by several scientists), and only about 600 of the estimated 100,000+ glaciers have been officially named by the U.S. Board of Geographic Names, including many in the Coast Mountains of southeast Alaska. Furthermore, Alaska contains the greatest number and total volume of non-polar glaciers in the world (Motyka et al., 2002). There have been a myriad of major glacier studies that have been conducted concerning Alaska's glaciers, primarily over the last 30 years; and the majority of these analyses identified a general recession trend. However, there has never been a recorded, detailed glacier inventory that has been compiled for Alaska (Molnia, 2008); although a relatively recent Landsat-based inventory of glaciers in western Canada (1985-2005) was conducted by Bolch et al. (2010) that included portions of the Coast Mountains.

One of the earliest temporal mapping studies performed on glaciers in Alaska was undertaken by Field (1947), in which he examined changes to glacier termini in Prince

William Sound, and Molnia (2008) presented a map compiled by Field in 1964 showing changes in the position of glacier termini in Yale Arm, Prince William Sound between 1910 and 1964. Krimmel and Meier (1989) studied the Columbia Glacier specifically for the purposes of enlarging the understanding of glacier activity, assessing the feasibility of the glacier as a water source, documenting glacier parametric changes over time, and analyzing specific hazards posed by the glacier. The research performed by Krimmel and Meier further built upon the base of knowledge that was possessed by the United States Geological Survey, as this agency had been studying the Columbia glacier (among others in Alaska) for several decades prior. Krimmel (2001) followed up on this analysis by utilizing stereo vertical photographs of the Columbia Glacier for 119 different image dates between 1957 and 2000, specifically looking at temporal changes in length, velocity, surface elevation, and calving rates of the glacier. Krimmel also noted that between 1982 and 2000 the greatest amount of recession occurred.

Glaciers within the Wrangell Mountains and College Fjord were examined by Sturm et al. (1991), specifically evaluating changes to the termini of 15 glaciers between 1960 and 1990 through the use of surveying, photogrammetry, and satellite imagery techniques. It was discovered that most of the glaciers in these two regions were either receding or stationary during the study period, with a couple of the glaciers exhibiting slight advancement.

Glacier Bay in southeast Alaska contains a particularly high number of both tidewater and alpine glaciers. Hall et al. (1995) performed a comprehensive inventory and change analysis on several of the area's major glaciers for the period of 1966 to 1986 and noted that many of the area's glaciers had been retreating very quickly since the late

1700's, with the most prominent glacier in the region, the Muir Glacier, actually advancing sporadically over time. In addition, Landsat imagery was utilized specifically for studying change rates of the Muir Glacier over the time period, and it was determined that the glacier experienced the greatest rate of retreat between 1973 and 1980—with an overall glacier retreat rate of 4.5mi ± 259ft (7.3km ± 79m). Also discovered was that many other Glacier Bay glaciers had significantly retreated (average of 4.3mi/7km) based on measurements recorded through the use of Landsat imagery, including the Burroughs, Casement, Cushing, McBride, Plateau, and Morse Glaciers. Furthermore, other glaciers had slightly advanced (<0.6mi/1km), while only the Carroll Glacier advanced significantly (3.2mi/5.1km) during the study period. A major conclusion presented in this study by Hall et al. (1995) denoted that the Glacier Bay region of Alaska provides an excellent example of rapid glacier retreat even though they did confess that it was not readily apparent as to what degree climate change caused the glacier recession and as to what degree such changes were caused by tidewater cycles which are known to be independent of short-term, regional climate. Available readings of average air temperatures showed a general warming trend, particularly over the time period of 1975-1995, and there was the possibility that the recession of Glacier Bay's non-tidewater glaciers at that time could have been explained by this warming trend.

Bitz and Battisti (1999) performed a more general glacier change analysis concerning six glaciers located within the Coast Mountains at various locales between Washington and Alaska with a primary purpose of looking at changes in mass balance between the 1960s and the 1990s. This analysis also examined the potential correlation between glacier mass balance changes (positive or negative) and climate variability.

Another prominent glacier in southeast Alaska is the Mendenhall Glacier, located within the city and borough of Juneau. Motyka et al. (2002) explained how the extensive research on this glacier has demonstrated that it is receding and thinning very rapidly, and that such a substantial recession could be attributed to a trend of warming climate especially over the previous three decades. The Mendenhall Glacier is a particularly important glacier to analyze in southeast Alaska because there is a highly detailed record concerning its retreat that has been derived from terminal and recessional moraines, topographic maps produced in 1909, 1948, and 1982, and especially in the great quantity of aerial photographs and surveys dating back to as early as 1895 (Motyka et al., 2002).

Arendt et al. (2002) conducted a two-part volume change analysis of Alaska glaciers through the use of airborne laser altimetry, specifically measuring average annual changes in thickness over two separate time periods: 1950s to 1990s and mid-1990s to 2001. Findings for 67 glaciers monitored from the 1950s to the 1990s were extrapolated to all glaciers statewide and estimated an annual total glacier volume loss of $12.5mi^3 \pm 530ft^3$ ($52km^3 \pm 15m^3$) water equivalent. Parametric measurements were taken again for 28 glaciers from the mid-1990s to 2001, and these finding were again extrapolated to all Alaska glaciers and approximated an annual total glacier volume loss of $23mi^3 \pm 1{,}236ft^3$ ($96km^3 \pm 35m^3$), indicating an increase in the average rate of glacier thinning. In fact, this thinning estimate was found to be substantially higher than estimates produced in earlier Alaska glacier studies. An additional Alaska glacier change analysis that centered on thinning rates was conducted by Berthier and Toutin (2007). Digital Elevation Models from February 2000 and May 2004 were applied for monitoring glacier elevation changes, particularly thickness change rates of glaciers within southeast Alaska, and it

was determined that low elevation glaciers in the region experienced thinning of up to 33ft ± 8.2ft (10m ± 2.5m) per year.

The Nabesna Glacier in Alaska's Wrangell Mountains was recently studied by Li et al. (2008) through the use of Synthetic Aperture Radar (SAR) images for the period of 1994 to 1996. This particular glacier is the longest valley glacier in North America.

Another pertinent study of Alaska's glaciers was performed on the Taku Glacier, in the Juneau Icefield of southeast Alaska, by Pelto (2011). Ablation rates were specifically analyzed through the use of Landsat TM imagery (bands 4 and 7) in addition to MODIS imagery for the primary purpose of delineating transient snowline of the glacier for the period of 2004 to 2010. The Taku Glacier was selected for this study primarily as a consequence of a detailed glacier mass balance record that has been kept by the Juneau Icefield Research Program (JIRP) that dates back to 1946.

Finally, a most recent glacier change study involving Alaska's glaciers was conducted by Heid and Kääb (2012), involving alpine glaciers within the Alaska Range. This multi-temporal analysis focused specifically on velocities of broader areas of glaciers (not individual glaciers) for the purpose of detecting change through the use of repeat optical satellite images during the time period of 1953 to 2004.

**2.3 Remote Sensing of Glaciers**

Optical and microwave remote sensing have become well-recognized for playing a major role in mapping, inventorying, and monitoring glacial parameters in many regions across the globe (Romshoo and Rashid, 2010). Such parameters typically include mass balance, area, length, velocity, geomorphology, thickness, and volume. In addition, multi-spectral satellite imagery along with aerial photographs have proven to be valuable

in remotely identifying glacier features such as spatial extent, transient snowline, equilibrium line elevation, accumulation and ablation zones, and ice/snow differentiation. Moreover, digital image processing (e.g., image enhancement, spectral ratioing, and classification) makes it possible to map these glacier features and assess the parameters more easily and accurately (Binaghi et al., 1993). However, Gao and Liu (2001) noted that the feasibility of utilizing remotely-sensed imagery for studying glacier dynamics is largely dependent on a unique spectral signature and sufficient spectral, spatial, and temporal resolution of the data. Furthermore, any remotely-sensed glacier data will have its limitations without the inclusion of associated ground measurements (Williams et al., 1991).

*2.3.1 Utility of Landsat Imagery*

The use of Landsat multi-spectral imagery, specifically the visible and near-infrared spectral bands, have proven to be adept at observing and inventorying glacier surfaces and their associated dynamics due to the sensors' generally adequate spatial resolutions, high revisit rates, and relatively large areas of coverage in each scene (Frey et al., 2012). Additionally, Sidjak and Wheate (1999) noted that each Landsat TM image scene covers an area that encompasses hundreds of aerial photograph frames, minimizes effects caused by relief displacement, and often has satisfactory spatial and spectral resolutions for extracting image features of interest. In addition, Landsat scene availability dates back to 1972, the images are capable of being geo-coded and ortho-rectified, and the images can be combined with digital elevation data for subsequent integration in to a database for image processing (Sidjak and Wheate, 1999).

Furthermore, Landsat image scenes have specifically been utilized for measuring glacier changes through the use of sequential images (Lucchita et al., 1993; Knight et al., 1987; Williams et al., 1974) and also to conduct initial glacier inventories (Williams, 1986). Binaghi et al. (1993) further identified the values of Landsat and other remotely-sensed imagery in glacier monitoring and mapping by explaining that data acquired through remote sensing methods can be effectively incorporated in to GIS and GPS for further analysis. An additional benefit of Landsat remotely-sensed imagery is that it has proven to be a valuable tool for overcoming inherent inaccuracies in typical glacier baseline data that has been generated through direct human methods and with other various instruments (Romshoo and Ramshid, 2010).

Landsat imagery has also shown to be advantageous when conducting analyses in both small and large scale areas of glacier change, primarily because since 2008 the imagery has been available in an ortho-rectified format at no cost from the NASA Landsat Program. Internet applications such as the USGS EarthExplorer make it possible for the user to easily query and retrieve image scenes for their area of interest; and thus Landsat imagery has become the most frequently utilized remotely-sensed data for mapping glaciers (Frey et al., 2012). Another specific advantage of performing glacier mapping/change analyses with Landsat imagery (particularly when analyzing relatively large areas of glacier fluctuations with Landsat MSS) is the ease at which the user can take full advantage of the radiometric and spatial resolution of the images when working with the digital data (Dowdeswell, 1986). Although Landsat imagery offers a multitude of advantages for analyzing glaciers, it is also important to consider the critical need for

applying local knowledge of the glacier when utilizing the imagery for accurate delineation of its boundaries (Williams et al., 1997).

*2.3.2 General Glacier Monitoring and Inventorying*

Much of the previous research concerning the utilization of Landsat imagery for studying glacier dynamics has been conducted primarily for the purpose of inventorying glaciers generally—essentially for glacier boundary delineation. Specific glacier features such as glacial frontal termini, summer snowline accumulation, and ablation zones can easily be identified through the use of remotely-sensed imagery such as Landsat scenes, and glacier detection is most useful when there is minimal seasonal snow cover (Gao and Liu, 2001). For example, Della Ventura et al. (1987) found that Landsat MSS image scenes were effective for delineating small alpine glacier surfaces in the Alps systematically and specifically noted that such glaciers often experience major shadow influences, which is typical of their morphology.

Gratton et al. (1990) applied a multi-spectral classification of Landsat MSS and Landsat TM imagery for delineating ablation zone covers of the Columbia Glacier in Alaska, and from this study they were able to explore the possibility of creating a glaciological database for the purpose of studying alpine glacier variations. Williams et al. (1991) also utilized Landsat MSS and Landsat TM image scenes, specifically examining glaciers by applying the images' visible and near-infrared data. Sidjak and Wheate (1999) combined regional elevation data with Landsat TM imagery for mapping and classifying the Illecillewaet Icefield in Glacier National Park, British Columbia, Canada. In an earlier study by Aniya et al. (1996), it was determined that a mosaicked Landsat TM image was effective for using as a basemap when inventorying outlet

glaciers in the Southern Patagonia Icefield and, in combination with stereo-interpreted aerial photographs, for identifying glacier divides and basins. In this case, this imagery was particularly valuable because the icefield lacked complete topographic map coverage. More recently, Paul and Andreeson (2009) created a new inventory of 489 glaciers in Norway through the use of Landsat ETM+ images that spanned the time period of 1999 to 2008 (in connection with multi-spectral image classification techniques).

Landsat imagery has also been examined for the purpose of analyzing the spectral reflectance of glacier surfaces. Landsat 5 Digital Numbers (DNs) were analyzed by Hall and Chang (1988) for the purpose of identifying and comparing satellite image reflectance on glacier areas in Alaska and Austria that contained spectral similarities. In the following year, Hall et al. (1989) utilized Landsat TM data for calculating glacier spectral reflectance values in the Wrangell Mountains of Alaska; and band 4 was specifically used for analyzing snow and ice albedo.

An additional application of Landsat imagery is for analyzing relationships between specific glacier parameters, including mass balances, equilibrium line altitudes, morphology, and topography. One example of this application can be found in a study by Allen (1998), where he utilized multi-temporal Landsat TM imagery and aerial photography (integrated in to a GIS) for showing how the glacier parameters of equilibrium line altitude, topography, and glacier morphology were interrelated. Hall and Chang (1988) focused their study on the comparison between spectral reflectance values obtained from analyzing Landsat 5 imagery to other spectral reflectance methods applied to various glacier parameters. Moreover, they found that by looking at previous work in

locating areas of similar reflectance on glaciers in Austria and Alaska he was able to establish a relationship between specific glacier areas and glacier sedimentation, and noted that such information is critical when examining glacier mass balance.

Finally, Landsat imagery has also proven to be useful for comparing the accuracies of different glacier extraction methods. A good example of this application is found in the work performed by Paul (2000), as he utilized Landsat TM image scenes for comparing the accuracy of glacier extraction methods, including manual, ratio image segmentation, and supervised classification methods. Subsequently, Landsat MSS was combined with false color composite images derived from Landsat TM imagery when analyzing the accuracy of manual glacier extraction.

*2.3.3 Glacier Parametric Changes*

Landsat TM (and on occasion MSS) with its various spectral bands has shown to be especially useful for generating data regarding such specific glacier surface parametric changes as area extents, length, recession/advancement rates, margins, velocity, and overall trends—with area extent change appearing to be the most common parametric change examined in the research. Dowdeswell (1986) measured changes in glacier margins of 22 outlet glaciers in Svalbard, Norway utilizing Landsat MSS images and 1:50,000 scale aerial photographs for the period of 1969 to 1981. Dowdeswell also analyzed the overall glacier trends in determining whether the glaciers were retreating, advancing, or static in addition to quantifying the minimum and maximum distances of such trends. When studying changes to aerial extents of 11 small alpine glaciers (also in the Alps of Austria), Della Ventura et al. (1987) also utilized Landsat MSS images. Bayr et al. (1994) assessed glacier area retreat rates in two glaciers located in the eastern Alps

of Austria through the use of Landsat TM data from 1984 to 1990. Hall et al. (2003) measured both glacier recession rates and area extent changes of the same two glaciers using Landsat ETM+ data from 1976 to 2001 along with topographic maps from as early as 1893 and IKONOS (4 m spatial resolution) images from 2000 to 2001, and compared accuracies between topographic-derived glacier areas and those areas derived from satellite images.

While comparing frontal positions of 11 specific outlet glaciers in Iceland, Williams et al. (1997) utilized Landsat MSS and Landsat TM imagery for identifying glaciers that had experienced the largest change in area in addition to specific areas that had experienced the greatest fluctuation in area extent from 1973 to 1992. Jacobs et al. (1997) used Landsat TM imagery and incorporated 1:50,000 scale topographic maps (based on 1961 photogrammetry) for updating the glacier area boundary of the Barnes Ice Cap in Baffin Bay, Canada.

Landsat TM scenes from 1987 and 2000 were utilized for identifying and quantifying changes to glacier area coverage as well by Ouma and Tateishi (2005), although the primary purpose of this study was to introduce a particular glacier extraction method for identifying glacier changes on Mount Kenya through the use of the Landsat TM satellite data in addition to analyzing the potential for predicting future glacier change. Furthermore, the use of Landsat TM imagery continues to be a popular method for identifying changes to glacier parameters. Erdenetuya et al. (2006) utilized Landsat TM and ETM+ image scenes from 1990 to 2002 along with other extraction and classification techniques to calculate changes in area extent. They also emphasized the point that the great advantages of remotely-sensed data (including Landsat TM and

ETM+ imagery) are that it is capable of providing real estimations of spatial and temporal condition of glaciers in addition to changes in glacier surface areas. In even more recent studies, Narama et al. (2010) examined changes to glacier area extent through the use of Landsat 7 ETM+ in order to analyze changes that transpired between 1999 and 2002. Moreover, Bolch et al. (2010) found that by using a Landsat MSS image scene from 1976 along with Landsat TM and ETM+ scenes from 1991, 2001, 2005, and 2009, along with other sensor data, he was able to effectively analyze changes to glacier area extent in the Himalayas of Tibet.

### 2.4 **Normalized Difference Snow Index**

The Normalized Difference Snow Index (NDSI) was first coined as such by Hall et al. (1995) as a statistic that has since proven to be a valuable tool in analyzing glaciers in remotely-sensed imagery—particularly in Landsat TM image scenes. This statistic is essentially the normalized difference of two Landsat TM bands (bands 2 and 5), with one in the visible and the other in the near-infrared part of the electromagnetic spectrum. However, the concepts behind the NDSI were being examined in the literature dating back to the 1970s, and the original intent was to create an automated algorithm to distinguish snow from cloud cover in satellite images (Hall and Riggs, 2010). For example, research performed by Barnes and Smallwood (1975) utilized Landsat MSS data for the purpose of examining snow cover reflectance characteristics in many of the spectral bands within the imagery. They discovered that the use of a visible spectral band in conjunction with a near-infrared spectral band made it possible to perform snow mapping by discriminating between snow and clouds. Further studies in later years made use of the increasing availability and advancement of satellite data for making important

adjustments to the visible/NIR ratio (Rosenthal and Dozier, 1996; Hall et al., 1995; Dozier, 1989; Crane and Anderson, 1984).

The NDSI can also be used to delineate snow and ice on a glacier from clouds (Irish et al., 2006), especially in areas of mountainous terrain (Hall et al., 1995). In addition, analyzing glaciers with the assistance of the NDSI allows for the subsequent use of a fairly simple set of decision rules that are applied to snow/ice and can be automatically applied to any Landsat TM image without requiring a priori knowledge of the glacier surface characteristics (Hall and Riggs, 2010). Moreover, and perhaps most importantly, this statistic (with its underlying algorithm) produces consistent discrimination of snow/ice from clouds in a wide variety of Landsat TM image scenes (Hall and Riggs, 2010). However, there are a couple of factors that can decrease the overall effectiveness of the NDSI statistic. One factor is that the threshold value for the statistic can vary from image to image depending on such image variables as sun elevation angle, atmospheric conditions, and season, whereas the other factor is that the near-infrared reflectance of snow/ice increases as the size of the snow grain increases, thus potentially making the discrimination between snow/ice and clouds more difficult (Choi and Bindschadler, 2004).

The NDSI is calculated by utilizing a Landsat TM visible band (band 2) and near-infrared band (band 5), as shown in the following equation:

$$NDSI = (TM2-TM5)/(TM2+TM5)$$

Dozier (1989; 1987) developed and introduced this normalized difference of Landsat TM bands 2 (0.52μm – 0.60μm) and band 5 (1.55μm – 1.75μm) as a more advanced application of Landsat TM band ratioing. One particular reason why bands 2 and 5 are

incorporated in to this statistic is that while clouds and snow/ice spectral reflectance are similar in the visible band (band 2), they are widely dissimilar in the near-infrared band (band 5)—as in this band there is high cloud reflectance but low snow/ice reflectance (Irish et al., 2006). Another reason why these two bands are applied in the NDSI is that although the clouds can be delineated by their high reflectance in the visible spectrum and colder temperatures, there are often times when localized temperature inversions in the lower atmosphere can cause the ice/snow surface to temporarily have colder temperatures than the surrounding clouds. Therefore, the NDSI statistic takes in to account the concept that while band 2 contains both highly reflective snow/ice and highly reflective clouds, cloud reflectance in band 5 decreases at a slower rate than snow reflectance does (Choi and Bindschadler, 2004).

There are a number of glacier inventory and change studies that have incorporated the use of the NDSI statistic for discriminating between snow/ice and clouds. An earlier example of this was in the study by Sidjak and Wheate (1999), in which the NDSI was applied to Landsat TM imagery for the purpose of delineating glacier areas of the Illecillewaet Icefield in Glacier National Park, British Columbia, Canada—an area of rugged terrain that often times contains persistent cloud cover. In a subsequent study by Choi and Bindschadler (2004), it was noted that the NDSI was previous employed specifically for the purpose of identifying possible cloud pixels that were among ice sheet pixels. During their research concerning glacier area changes and recession rates on Mount Kenya, Ouma and Tateishi (2005) utilized the NDSI to assist in extracting the overall glacier, snow/ice, and water mass of specific glaciers. Finally, another research study that made considerable use of this statistic was conducted by Erdenetuya et al.

(2006). This study showed that utilizing all Landsat TM bands along with the NDSI statistic (when appropriate) as input to a maximum likelihood classification algorithm can be effective for classifying glaciated areas in remotely-sensed imagery. They were specifically applying the NDSI for distinguishing snow from similarly bright soil, rock, and cloud for the purpose of classifying alpine glaciers in Mongolia.

### 2.5 **Landsat TM 4/5 Band Ratio**

Band ratioing has been a particularly helpful technique during image processing, as it has shown to enhance the contrast between image features (Moik, 1980). Hall et al. (1987) performed much of the early research concerning the effectiveness of a Landsat TM 4/5 band ratio for enhancing glacier, snow, and ice features, and Paul et al. (2002) introduced this as a method for segmenting ratio images. Hall et al. (1987) specifically noted that snow and ice features in Landsat TM imagery have substantial spectral response differences between bands 4 and 5 (both near-infrared bands), as band 4 contains high spectral reflectance, whereas band 5 contains low reflectance of snow and ice. Furthermore, they concluded that the glacier accumulation areas typically show the effects of contrast enhancement through 4/5 band ratioing, as these areas usually contain the greatest difference in spectral responses between bands 4 and 5. Sidjak and Wheate (1999) expounded on this research by identifying an additional advantage of utilizing the TM 4/5 band ratio for glacier studies: for delineating ice/snow in the shadow areas of glaciers. Their research also found that the problems of shadow areas on glaciers are typically attributed to cloud cover and topography, and that there is less spectral reflectivity variation in these areas versus illuminated areas—thus resulting in a more difficult glacier classification process.

In addition, Paul et al. (2004) explained the rationale for using a TM 4/5 band ratio image for glacier mapping by noting that TM band 5 is particularly applied because shadow areas of glaciers typically contain a low spectral reflectance that is quite similar to glaciers in the mid-infrared band and that subsequently there are visible differences in responses that vary based on differing illumination conditions. Ouma and Tateishi (2005) explained how using the TM 4/5 band ratio in glacier classification is particularly useful due to the low reflectivity of snow and ice in the mid-infrared portion of the electromagnetic spectrum. In fact, Paul (2000) compared results of several different glacier classification methods (e.g., manual, band ratioing, and unsupervised classification) and determined that utilizing a TM 4/5 band ratio (following an application of the NDSI statistic) achieved the optimal results with respect to the classification accuracy.

The TM 4/5 band ratio technique has often been combined with other methods during image processing and subsequent glacier classification. Several studies have specifically coupled this technique with the NDSI statistic for delineating glaciers in shadow areas and discriminating snow/ice from clouds for a more accurate glacier classification. Hall et al. (1987), while conducting a glacier change analysis for glaciers in the Chugach Mountains and Brooks Range of Alaska in addition to the Noric Alps of Austria, found the TM 4/5 band ratio image particularly advantageous for enhancing spectral reflectivity response differences on the glaciers. In a study conducted a few years later by Williams et al. (1991), glacier boundaries were delineated through the use of Landsat MSS and TM imagery of the Brúarjökull Glacier in Iceland, and it was determined that the reflectivity of ice and snow could be detected in individual bands and

especially in ratioed TM bands. Moreover, the TM 4/5 ratio allowed for very clear delineation between glacier boundaries (Williams et al., 1991). Williams and Hall (1998) found the TM 4/5 band ratio technique to successfully perform a multi-spectral classification of glaciers areas.

Another study that incorporated the use of this band ratio technique was performed by Sidjak and Wheate (1999), and it found that the optimal glacier area classification results were achieved by combining the TM 4/5 ratio, the NDSI, the $2^{nd}$, $3^{rd}$, and $4^{th}$ components of a Principal Component Analysis (PCA), and a supervised classification when quantifying glacier area changes of the Illecillewaet Glacier. Furthermore, a primary benefit of the TM 4/5 band ratio technique was identified in this study as being the effectiveness of the technique (in concert with the NDSI) at thoroughly encompassing most if not all glacier area. Sidjak and Wheate also noted that an additional benefit of applying the TM band 4/5 ratio technique in their study was that it resulted in superior classification results compared with just using unprocessed TM bands for glacier area classification (1999).

As part of a comprehensive examination and comparison of image ratioing and segmentation techniques, Paul et al. (2002) applied a segmentation of ratio images using the TM 4/5 band ratio technique for determining the effectiveness of classifying glaciers on a 1985 Landsat image scene of glaciers in Switzerland. The highest classification accuracy was obtained by utilizing a 3X3 median filter on the TM 4/5 ratio image in addition to applying a threshold to raw digital number values for TM bands 4 and 5 for the purpose of obtaining a glacier mask (Bayr et al., 1994). In comparing these classification results with other results derived from such different methods as TM 3/5

band ratioing and an unsupervised classification (ISODATA clustering of bands 1, 4, and 5), it was determined that the most accurate classification results were obtained from the TM 4/5 band ratio image that had been combined with the NDSI, PCA components 2 and 4, and a supervised classification method that utilized the maximum likelihood algorithm. Paul et al. (2002) also specifically emphasized the effectiveness of this method for accurately classifying glaciers within shadow areas.

When mapping glaciers and glacier debris, Paul et al. (2004) again utilized a TM 4/5 ratio image for classifying glacier areas and divided the subsequent classes in to 'glacier' and 'other' in addition to incorporating an ASTER-derived DEM, an Intensity Hue Saturation (IHS) color space transformation, and a 3X3 median filter (specifically for minimizing the number of misclassified pixels and reducing noise). Ouma and Tateishi (2005) also applied the TM 4/5 band ratio technique, preceded by the implementation of the NDSI statistic, for accurately classifying glacier areas in multi-temporal Landsat TM, ETM+, and MSS image scenes (1976-2000). Furthermore, in a very recent study, Veettil (2012) applied a TM 4/5 band ratio as a first step in mapping glacier debris area changes in the Himalayas through the use of Landsat TM and ETM+ image scenes along with a DEM from 1990 to 2010.

## 2.6 **Digital Image Classification and Change Detection**

### *2.6.1 Supervised Classification*

Supervised classification is a commonly utilized method for extracting land cover spectral information based on statistical pattern recognition techniques (Narumalani et al., 2002). This particular image classification method is favored over an unsupervised classification approach specifically when there are land cover types that are generally

known a priori through field work, aerial photograph interpretation, and personal experience (Jensen, 2007). During this process, training sites are selected. Training sites are specific sites within the image scene that represent image pixels (with spectral information) of known land cover types and are utilized as the subsequent input in to the classification algorithm for mapping the land cover across the rest of the image. Two of several methods are commonly utilized for collecting training site data (image pixels): on-screen selection of training data polygons and on-screen training data seeding, and statistical information such as means, standard deviations, and covariance matrices are calculated for each training site before all image pixels are subsequently evaluated and assigned to a specific land cover class (Jensen, 2007).

The maximum likelihood algorithm is a widely used supervised classification algorithm that is based on statistical probability (McIver and Friedl, 2002; Wu and Shao, 2002). In addition, this algorithm assesses the variance and covariance values within the spectral response information of unknown image pixels (Lillesand and Kiefer, 2000) and recognizes land cover class spectral information from the statistical data retrieved from the training sites previously identified (Richards and Jia, 1999).

*2.6.2 Accuracy Assessment*

A classification accuracy (or error) assessment for remotely-sensed data is commonly performed on the classified image and primarily involves comparing classified pixels in the remotely-sensed image with ground (or reference) data (Jensen, 2007). The error matrix (or confusion matrix) is utilized for summarizing these sets of information and is considered to be the standard image classification accuracy assessment method (Jensen, 2007; Morisette and Khorram, 2000; Congalton, 1991). The error matrix is also

known to provide an ideal means for describing image classification accuracy and characterizing errors (Foody, 2002; Wu and Shao, 2002). When performing an accuracy assessment, certain standard procedures are typically followed, as identified by Jensen (2007): having a knowledge of possible inherent training site weaknesses due to the absence of actual ground truth/reference data, determining sample size for each land cover category, utilizing an appropriate training data sampling scheme to locate ground reference test pixels (if feasible) that are within close proximity to the images' acquisition dates, and applying the appropriate statistics (fuzzy or normal) during the accuracy assessment. It is also important to note that ideal sample sizes for training sites for the image accuracy assessment can be determined primarily by analyzing the image pixel data distribution (Jensen, 2007).

However, there are times when it is just not practical to obtain ground reference data for test sites. Therefore, high spatial resolution, remotely-sensed imagery is often substituted for ground reference data (Morisette et al., 2003). Additionally, it is widely understood that imagery substituted for ground reference data should have considerably higher spatial and/or spectral resolution than the original imagery utilized for extracting thematic information (Jensen, 2007). He also provided an example of this by noting that a multitude of studies have incorporated high spatial resolution imagery (<1 m) for collecting ground reference data to compare with land cover classes extracted from 30 m X 30 m spatial resolution Landsat TM imagery.

*2.6.3 Change Detection*

The general process of change detection involves delineating what changes or differences have been observed in an object at various times (Singh, 1989). In fact,

remotely-sensed data, including data acquired from Landsat TM imagery, have shown to be valuable sources of data for applying change detection techniques over the last several decades primarily due to the wide availability of annual image scenes, a synoptic view, and digital formats that are compatible for computer processing of remotely-sensed data (Lu et al., 2004).

A variety of change detection techniques can be employed in remote sensing/imagery analysis, and virtually all glacier studies analyzing parametric changes have utilized one or more techniques. Research has shown that what constitutes a "good" change detection analysis includes several parameters including area change, change rate, the spatial distribution of changes, change direction (trend), and, if possible, a change detection accuracy assessment. Furthermore, a successful change detection analysis particularly relies on remotely-sensed imagery that is of sufficient temporal, spatial, spectral, and radiometric resolutions (Lu et al., 2004). In addition, the accuracy of the change detection technique utilized in these types of studies (when feasible) depends on a number of factors, including: precise geometric registration between the multi-temporal images, normalization between the images, availability of high-quality ground truth data, the change detection method employed, the skill and expertise of the analyst, time and cost restrictions, and classification methods (Hung and Wu, 2005; Lu et al., 2004).

*2.6.4 Post-Classification Method*

A significant number of change detection studies have utilized the post-classification technique for quantifying changes to specific objects or parameters (Hung and Wu, 2005; Arzandeh and Wang, 2003; Civco et al., 2002; Song et al., 2001; Maas, 1999; Yuan et al., 1998; Jensen et al., 1995). This particular technique performs a pixel-

by-pixel comparison through the use of a change detection matrix and requires that each remotely-sensed image has been previously rectified and classified (Jensen, 2007; Lu et al., 2004). In addition, there are several advantages to utilizing the post-classification technique in a glacier change detection analysis. Such advantages include: there is no requirement for the images to be atmospherically-corrected, the result involves intuitive "from-to" classification information, it minimizes environment differences between multi-temporal images, and it provides a complete change detection matrix (Jensen, 2007; Lu et al., 2004). Jensen (2007) and Lu et al. (2004) also identified specific disadvantages in using this change detection technique, including: the dependence on single image dates' classification accuracy, the need to perform two separate classifications, and the great need for sufficient time and expertise for classifying the imagery.

## 2.7 Glacier Change Analysis

### *2.7.1 Data Sources*

The vast majority of recent glacier change studies have utilized some combination of data sources that include remotely-sensed imagery (particularly multi-spectral Landsat image scenes), aerial photographs, and topographic maps and/or other maps. There have been very recent studies that have effectively utilized Landsat imagery in combination with historic aerial photographs for glacier delineation and a subsequent glacier change analysis (Lopez et al., 2010) in addition to recent studies that have used historic aerial photographs in conjunction with other image formats such as ASTER and SAR (Tennant et al., 2012; Solomina et al., 2004). Topographic maps (typically created from pre-1980 imagery) have also been effectively utilized along with Landsat image scenes for

contributing valuable glacier boundary data for glacier change studies (Kulkarni et al., 2011; Lopez et al., 2010; Peduzzi et al., 2010; Erdenetuya et al., 2006; Paul, 2000). There have also been a good number of other recent glacier change studies that have not incorporated Landsat image scenes but have used other image formats in connection with topographic maps for successfully conducting a glacier change analysis (Li et al., 2011; Raj, 2010; Solomina et al., 2004).

*2.7.2 Glacier Change Parameters*

A glacier change analysis has typically assessed changes to specific parameters, including changes in glacier area and length along with such measurements as changes in glacier size, rate of change, percentage change, absolute percentage change, and relationships between changes and glacier size. There have been number of recent studies that have specifically focused on analyzing each of the following four glacier area change parameters: area change amount, area change percentage, retreat/advance rate, and absolute percentage change (Li et al., 2011; Bolch et al., 2010; Narama et al., 2010; Peduzzi et al., 2010; Ouma and Tateishi, 2005). There have also been a couple of recent studies that have just centered on the three change parameters of area change amount, area change percentage, and retreat/advance rate (Tennant et al., 2012; Kulkarni et al., 2011), one study that just assessed changes in glacier area amount, percentage change, and absolute percentage change (Paul, 2000), a study that only determined glacier area amount change (Raj, 2010), and additionally one that that only measured percent area change (Erdenetuya et al., 2006). Moreover, Bolch et al. (2010) broke down changes in glacier areas by specific time periods within the entire time period for a particular set of glaciers within a detailed study area (e.g., 1976-2001, 2001-2009, and 1976-2009).

Concerning the analysis of glacier length change (from classified imagery, aerial photographs, and topographic and other maps), Lopez et al. (2010) calculated length according to the following five specific criteria: "1) Glacier length is represented by a line which corresponds to the longest distance followed by the glacier; 2) The length is measured from the lowest to the highest point of the glacier; 3) The origin is the central position of the glacier's front; 4) The length/distance follows the central position of the glacier tongue; and 5) The length follows surface flow trajectories if they are identifiable on the satellite image."

A very recent study specifically assessed changes in glacier length by focusing on all of the following four glacier change parameters: change in length, length change rate, and length change in relation to glacier size (Lopez et al., 2010). In addition, a very recent study specifically determined changes in length change amount, length change percentage, and length change rate (Li et al., 2011). And finally, another recent study evaluated changes in the glacier length change parameters of only length change amount and length change rate (Bolch et al., 2010).

# CHAPTER 3: METHODOLOGY

## 3.1 Overview

For inventorying the five glaciers of interest, detecting area and length parametric change on an annual basis (when available), and summarizing overall trends, a series of steps were applied including: topographic map processing, aerial photograph processing, imagery pre-preprocessing, image processing techniques, change detection, and a glacier change analysis (see Figure 2).

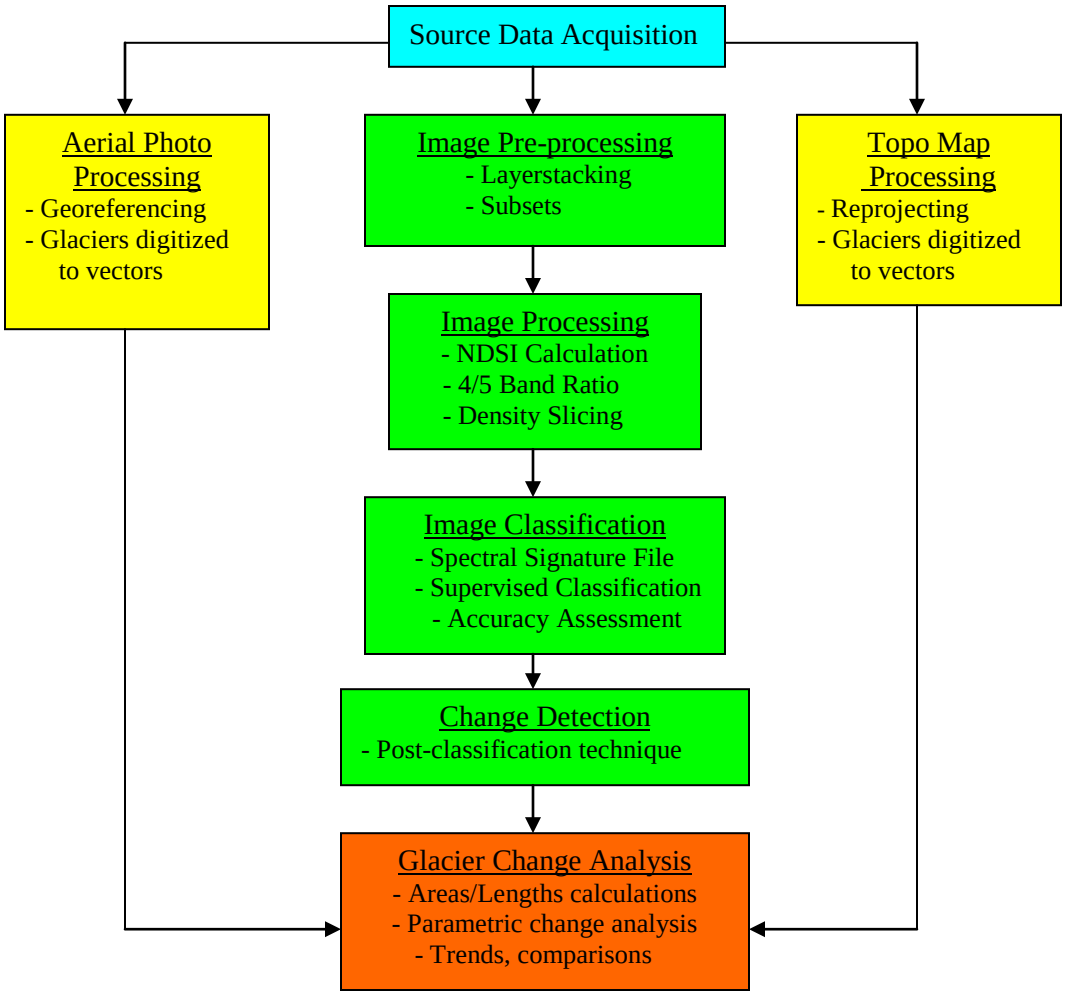


Figure 2. Methodology Flow Chart

### 3.2 Topographic Map Processing

1:63,360 and 1:250,000 scale topographic maps for the years 1948 and 1961, respectively, were acquired from the USGS and did not require additional pre-processing beyond reprojection. All topographic maps were initially reprojected from UTM Zone 8/Clarke 1866 to UTM Zone 8/WGS 84N—the projected coordinate system utilized for the glacier change analysis. For glaciers with only partial coverage in the single 1:63,360 scale topographic maps (including the Saussure, Laughton, and Irene Glaciers), the additional requisite maps were clipped and subsequently mosaicked utilizing the ERDAS Imagine Mosaic Pro tool. Glacier areas were then extracted as polygon features for all five glaciers from 1948 and from 1961 through on-screen digitizing utilizing ArcGIS10 software. These polygon features were then incorporated in to the glacier change analysis.

### 3.3 Aerial Photograph Processing

123,214 scale aerial photographs for the year 1979 were acquired from the USGS and did require additional pre-processing. The aerial photographs were geo-referenced through the use of mosaicked, high-spatial resolution (0.6m) satellite imagery (Digital Globe Worldview-1 imagery, dated Sept. 16, Sept. 21, and Sept. 29, 2010). The aforementioned reference imagery was initially reprojected to the projected coordinate system utilized in the study (UTM Zone 8/ WGS84 N). Complete coverage in aerial photographs was available for all five glaciers, and glacier areas visually discernable on the photographs were subsequently extracted as polygon features through on-screen digitizing with ArcGIS10 software. These multi-part polygon features were then incorporated in to the glacier change analysis.

### 3.4 Satellite Imagery Pre-processing

All 7-band Landsat TM image tiles (30-meter spatial resolution) for the study were acquired from the USGS by applying following set of criteria in the USGS EarthExplorer application: the bounding box for all image scenes needed to contain all five glaciers of interest, imagery acquisition dates of 1984-present, and only imagery acquired between July and September of each year (in order to minimize seasonal snow variation). This query resulted in acceptable image scenes for all years between 1984 and 2011 except for the years 2000-2003. A Landsat ETM+ image from 2001 was also obtained, although this particular scene only contained full coverage for three of the glaciers of interest (Carmack, Irene, and Laughton). However, not every year's image was determined to be suitable for image processing due to severe cloud cover directly over the glaciers of interest. Consequently, the images for the years 1985, 1988, 1991, and 2008 were omitted from the study.

The retrieved satellite images were all classified as USGS Level 1 products, as all images were previously geometrically and radiometrically corrected and orthorectified. The spatial reference for all scenes was UTM Zone 8/WGS 84N, which was subsequently utilized as the spatial reference for the entire study. All images were then pre-processed in ERDAS Imagine, as all bands but band 6 (thermal) were layerstacked to create a single 6-band image for each date of interest. Subsets were then created for each of the five glaciers for each image scene based on identical inquire boxes for each glacier's AOI for each year. At this point all subset images were ready for processing.

### 3.5 Image Processing

All applicable Landsat TM and ETM+ images were processed for obtaining glacier spectral signatures as input in to a supervised classification (with its subsequent accuracy assessment) and for change detection. Three specific processing techniques were applied for the purpose of accurately mapping glaciers in each image: 1) calculating the NDSI statistic, 2) utilizing a 4/5 band ratio and merging the subsequent image with the NDSI image, and 3) applying a threshold value to the merged images for creating distinct spectral value separation between areas of glacier and areas without glacier in the images (see Figure 3).

The NDSI statistic was first calculated for each original subset image in order to overcome persistent cloud cover, as some of the images contained cloud cover over non-glacier areas of up to 20%. The NDSI was calculated from Landsat TM + band 2 (where snow has bright spectral reflectance) and Landsat TM + band 5 (where snow has dark reflectance) by applying the following calculation in ERDAS Imagine Model Maker to obtain the new NDSI image:

*((100 * TM band 2 – 100 * TM band 5) / (TM band 2 + TM band 5))*

Spectral characteristics of glacier in each subset image was also identified by utilizing a 4/5 band ratio technique. This technique was specifically employed for eliminating snow (patches of snow that are not glacier) from the image, as the middle part of the electromagnetic spectrum (near-infrared) contains low reflectivity of snow and glacier ice—which allows for enhanced glacier classification from the segmented bands 4 and 5. The following calculation in ERDAS Imagine Model Maker was applied to obtain the new 4/5 band ratio images:

*(TM band 4 / TM band 5)*

The resulting image was subsequently combined with the NDSI image in order to further improve glacier mapping accuracy. This was accomplished by applying the following calculation in ERDAS Imagine Model Maker to obtain the merged image:

*(NDSI image * 4/5 band ratio image)*

The final image processing technique utilized for accurate glacier mapping involved the use of density slicing (or thresholding). This was performed by visually analyzing each merged image to determine a brightness value threshold for glacier and non-glacier pixels. This interactive approach was found to be particularly useful for discriminating glacier pixels in shadows (areas of topographic influence) that could potentially be misclassified during the image classification process. In addition, the use of a threshold value subsequently resulted in distinct spectral information in just the two regions of interest (glacier and non-glacier) in the upcoming supervised classification and change detection. For example, it was visually determined that the 1990 Saussure Glacier merged image had a brightness value threshold of 120—and the following calculation (applying a relational function) was applied in ERDAS Imagine Model Maker to obtain the new threshold image:

*1990_Saussure_merge ≥ 120*

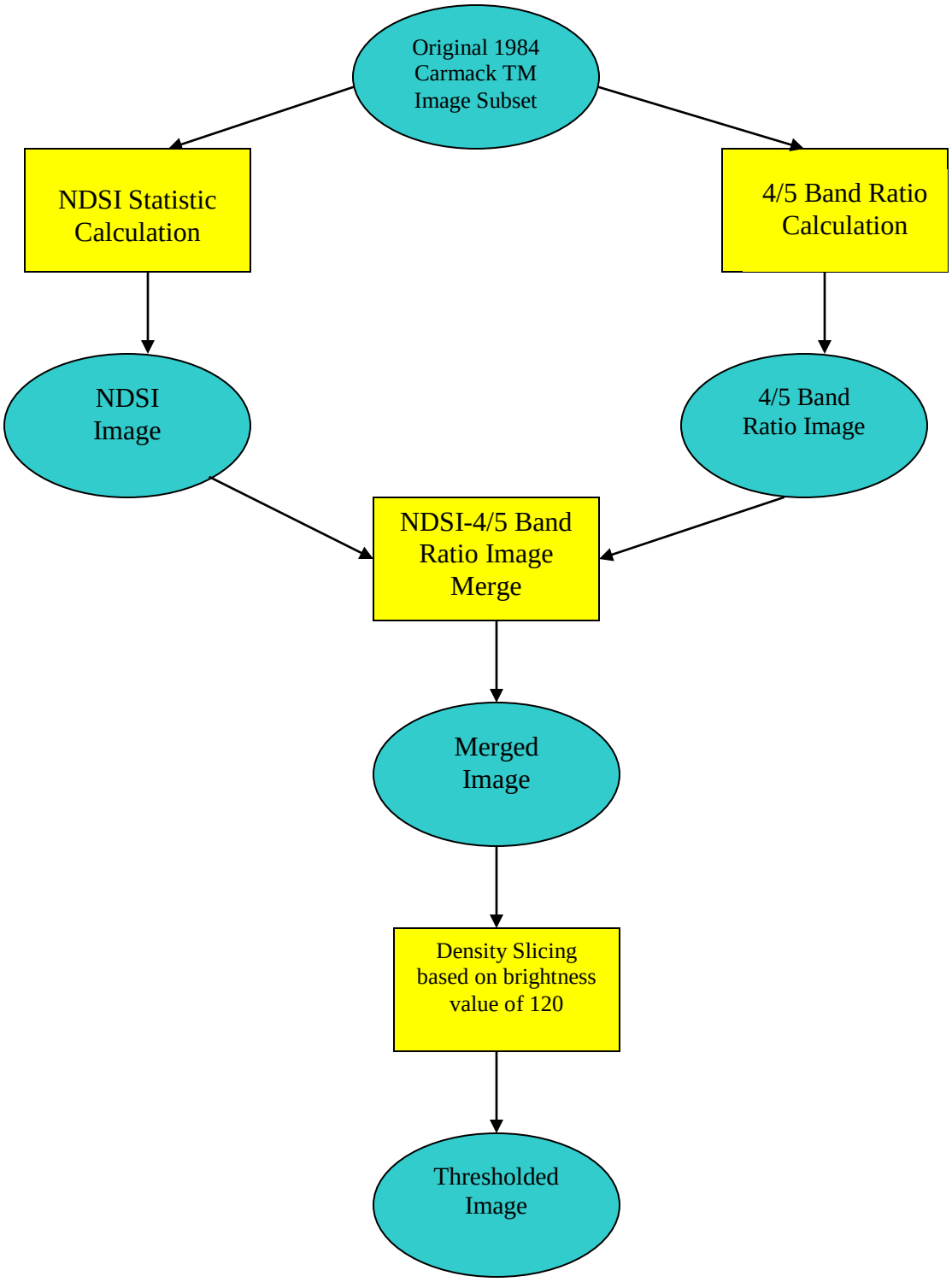


Figure 3. Example of the model created to apply three specific image processing techniques in order to obtain a glacier spectral signature for the 1984 Carmack Glacier Landsat TM image: NDSI, Band 4/5 Ratio (merged with NDSI), and Density Slicing

A supervised classification was then utilized for classifying spectral properties of each threshold image in to their appropriate class: 'Glacier' or 'Not Glacier'. A supervised classification method was appropriate for this analysis due to the familiarity of the study area, a few number of classes (2), and the availability of high-spatial resolution ground truth imagery for assisting with the identification of training sites for the spectral signature file. All image classification was conducted using the maximum likelihood algorithm.

A thematic accuracy assessment was then conducted utilizing high-spatial resolution ground truth imagery, and the subsequent accuracy assessment report was derived. The assessment utilized a 0.8-meter spatial resolution Digital Globe Worldview panchromatic image dated Sept. 15, 2006 as ground truth imagery for the corresponding, classified Irene Glacier subset image dated Sept. 11, 2006. The ground truth image provided full coverage of the Irene Glacier. For conducting the accuracy assessment of the classified image, the sample size for the ground reference test was based on binomial probability theory. This particular theory utilizes a binomial distribution to calculate the assessment's necessary sample sized based on two classes (in this case, 'Glacier' and 'Not Glacier'), desired map accuracy, and desired percentage error (Jensen, 2007).

For this specific thematic accuracy assessment, the Fitzpatrick-Lins equation (1981) was applied for calculating the necessary sample size based on a desired map accuracy of $\geq 85\%$ and a desired percentage error of $\leq 5\%$. The following equation was used:

$$N = \frac{z^2(p)(q)}{E^2}$$

Where N= sample size; z= 2 standard deviations away from mean (for 95% confidence interval); p= expected % accuracy of the entire map; q= 100-p; and E= allowable % error. With a desired map accuracy of ≥ 85% and a percentage allowable error of ≤ 5%, the total necessary sample size was calculated to be 204 pixels. Furthermore, the equalized random sampling method was utilized for the selection of samples in order to ensure an equal number of samples were selected for pixels classified as 'Glacier' and those classified as 'Not Glacier'.

### 3.6 Change Detection

After conducting an accuracy assessment on the classified subset image, change detection was performed utilizing the post-classification technique. This particular technique has been shown to be effective for digitally detecting change in classified land cover classes between images of different dates. This method sought to quantify change in glacier area extent on an annual basis (between consecutive image years, or in the circumstances where there was no available image for a specific year, between the earlier year the next available year) and between the earliest and latest image dates by assessing total pixel change in four categories: 'Glacier' to 'Glacier' (no change), 'Glacier' to 'Not Glacier' (glacier retreat), 'Not Glacier' to 'Glacier' (glacier advancement), and 'Not Glacier' to 'Not Glacier' (no change).

### 3.7 Glacier Change Analysis

Glacier polygons resulting from the classified Landsat TM imagery and digitized aerial photographs and topographic maps were then utilized as input in to a detailed glacier change analysis. Glacier area extent change was analyzed by calculating total glacier area ($mi^2$ and $km^2$) for each classified image's 'Glacier' class and applying the

aforementioned post-classification change detection technique for discovering and quantifying areas of glacier advance or retreat for each of the five glaciers. In addition, total area ($mi^2$ and $km^2$) was calculated for the multi-part glacier polygons derived from the aerial photographs and topographic maps. Furthermore, this study analyzed temporal changes for each of the five glaciers of interest by calculating percent change in total glacier area from year to year (1948 to 2011), including percent area change between the earliest date (1948) and the latest date (2011), identifying subsequent years of greatest fluctuation in glacier areas over the time period, identifying glacier areas that experienced the greatest and least fluctuation (positive and negative) in area extent, calculating area change rate averages (% relative change per year), and identifying retreat or advancement in area extents from year to year.

Changes to glacier lengths were analyzed by initially establishing a reference line based on the earliest glacier inventory year's extent (1948 topographic maps). These reference lines were drawn, and every subsequent year's glacier length based on the topographic maps, aerial photographs, and classified Landsat TM images was measured according to two criteria: 1) glacier length was measured by either shortening or lengthening the reference line to adjust to varying extents of the primary (or largest) glacier of the multi-polygon glacier, and 2) the length/distance followed the visual center of the primary glacier.

In addition, this study analyzed temporal changes in glacier length for each of the glaciers of interest by calculating percent relative change in length extents from year to year (glacier length fluctuations), calculating overall percent change in length extents between the earliest date (1948) and latest inventory date (2011), calculating total

retreat/advancement in glacier length each year (mi and km), identifying subsequent years of greatest fluctuation in glacier length over the time period, calculating length change rate averages (% relative change per year), and identifying retreat or advancement in length extents from year to year.

Finally, the glacier change analysis focused on comparisons and trends in area and length extents across all five glaciers collectively, including: identifying the glacier with the highest area and length change rates, determining the presence of geographical patterns in glacier size fluctuations, comparing overall glacier change rates on an annual basis, identifying glaciers with the least and greatest change in area/length extents over the time period, and evaluating the overall direction (trend) of change for all five glaciers (retreating or advancing).

# CHAPTER 4: ANALYSIS RESULTS AND DISCUSSION

## 4.1 Processing of Topographic Maps and Images

A series of processing techniques were applied for the purpose of inventorying the five glaciers of interest and for performing the subsequent change analysis. First, glacier areas were extracted as polygon features from the 1948 topographic maps (see Figure 4) and from the 1961 topographic maps (see Figure 5) through on-screen digitizing. Second, glacier areas visually discernable on the 1979 aerial photographs were extracted as polygon features through on-screen digitizing (see Figure 6). Third, specific image processing techniques were administered for the purpose of accurately mapping glaciers in each Landsat TM image. These techniques involved calculating the NDSI statistic from the original Landsat TM image (see Figure 7), obtaining the band 4/5 ratio and merging the resulting image with the NDSI image (see Figure 8), and applying a user-defined threshold to each merged image to further isolate glacier areas (see Figure 9). A supervised classification was then utilized for classifying spectral properties of each threshold image in to their appropriate class: 'Glacier' or 'Not Glacier' (see Figure 9). Lastly, glacier lengths were measured in the topographic maps (see Figure 10) in addition to the aerial photographs and classified images (see Figure 11).

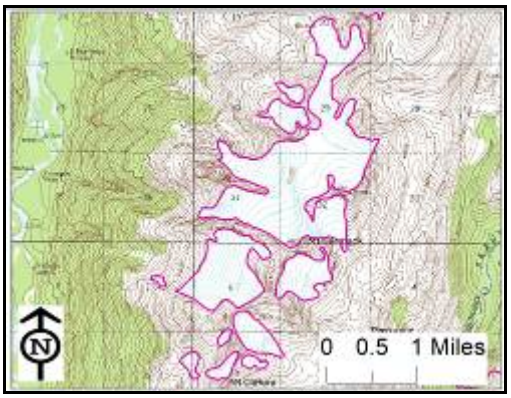


(a)

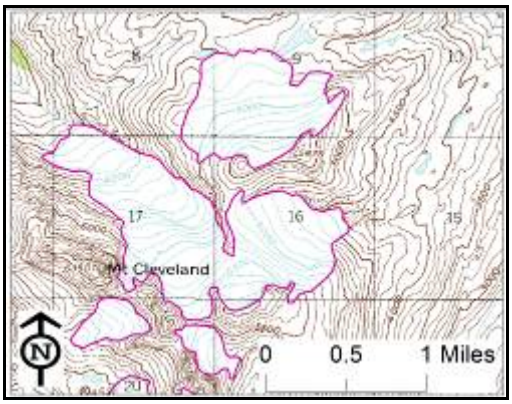


(b)

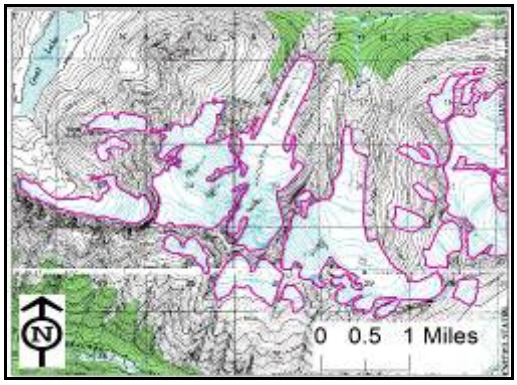


(c)

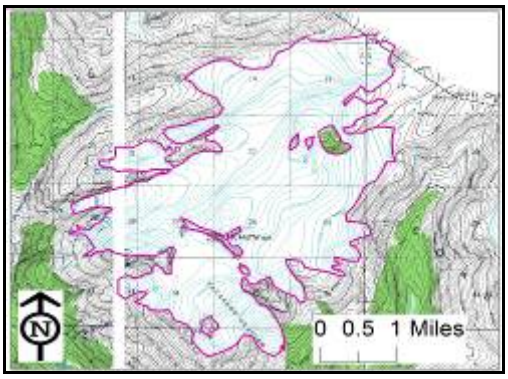


(d)

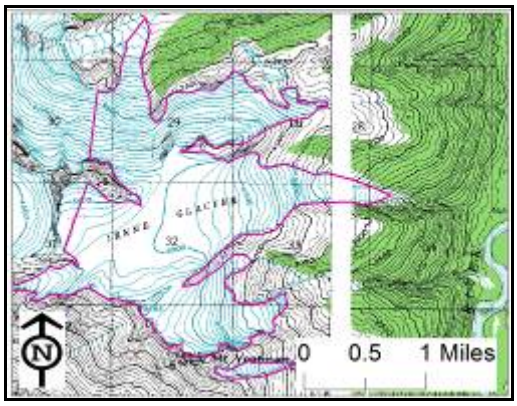


(e)

Figure 4. Digitized 1948 USGS topographic maps (1:63,360 scale) of (a) Carmack; (b) Cleveland; (c) Laughton; (d) Saussure; and (e) Irene Glacier.

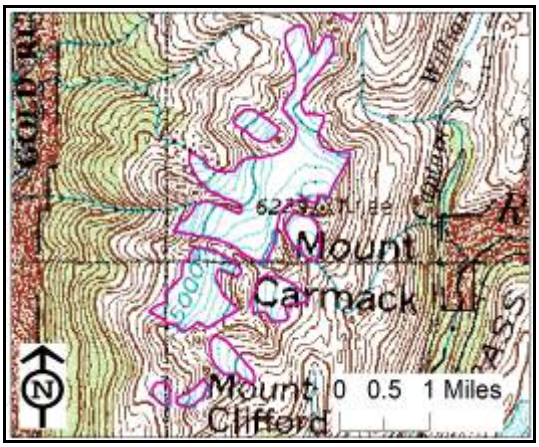


(a)


(b)

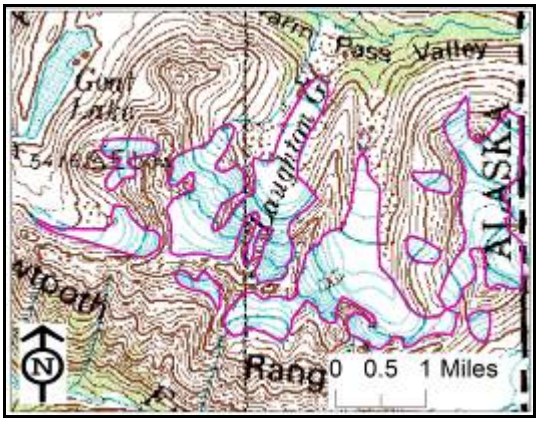


(c)

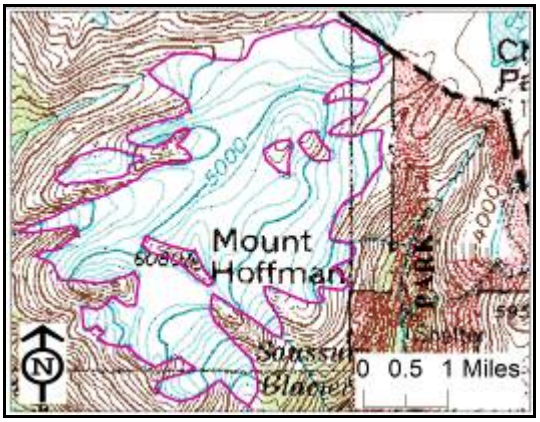


(d)

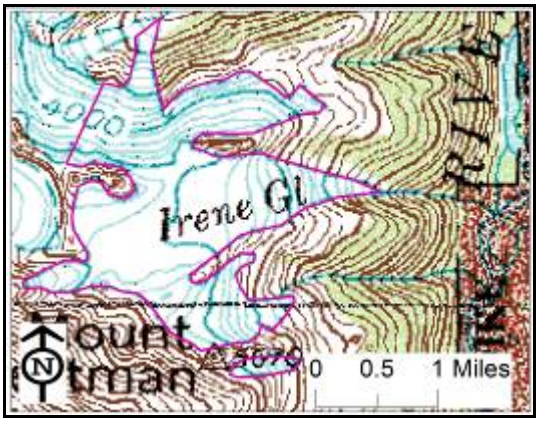


(e)

Figure 5. Digitized 1961 topographic maps (1:250,000 scale) of (a) Carmack; (b) Cleveland; (c) Laughton; (d) Saussure; and (e) Irene Glacier.

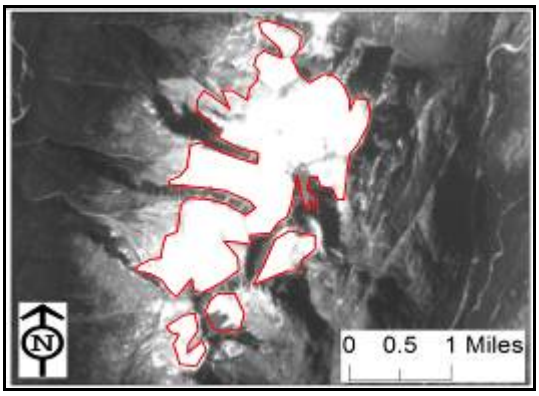


(a)

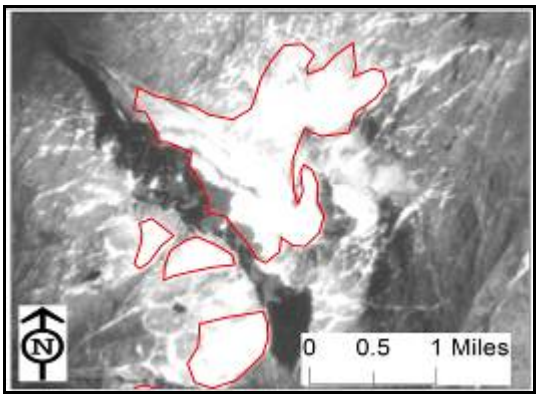


(b)

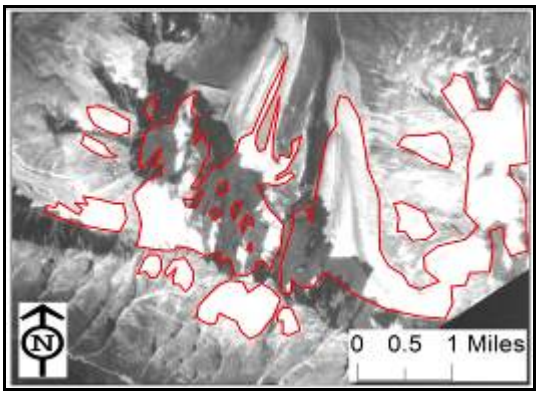


(c)

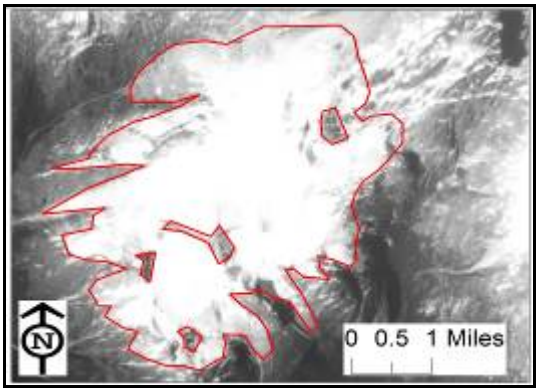


(d)

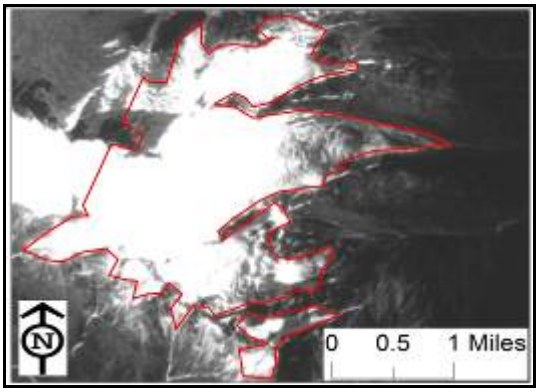


(e)

Figure 6. Digitized 1979 aerial photographs (1:123,214 scale) of (a) Carmack;(b) Cleveland; (c) Laughton; (d) Saussure; and (e) Irene Glacier.

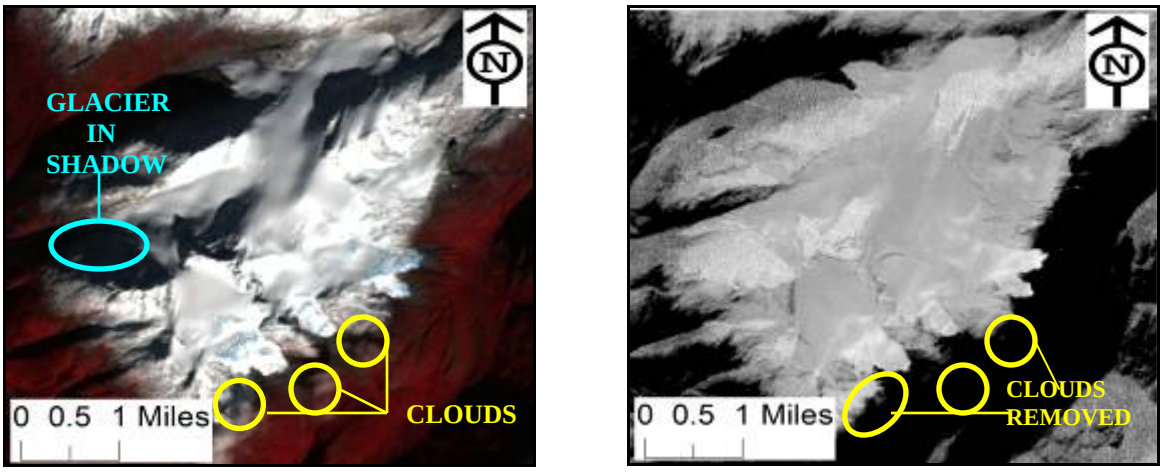


Figure 7. 1990 Saussure Glacier Landsat TM image (left) and the resulting NDSI image with clouds removed (right).

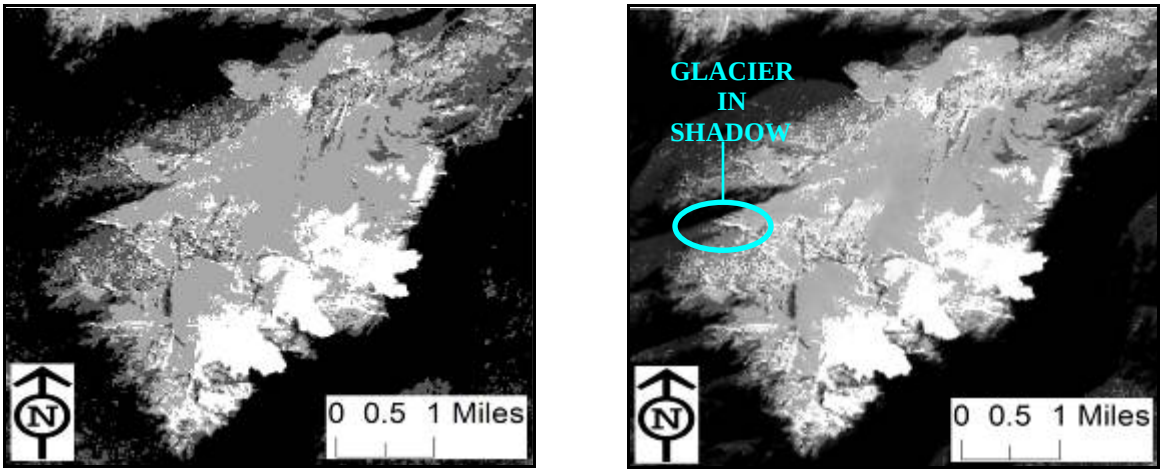


Figure 8. The resulting band 4/5 ratio image (left) and the resulting NDSI/band ratio merged image accounting for glacier in shadow areas (right).

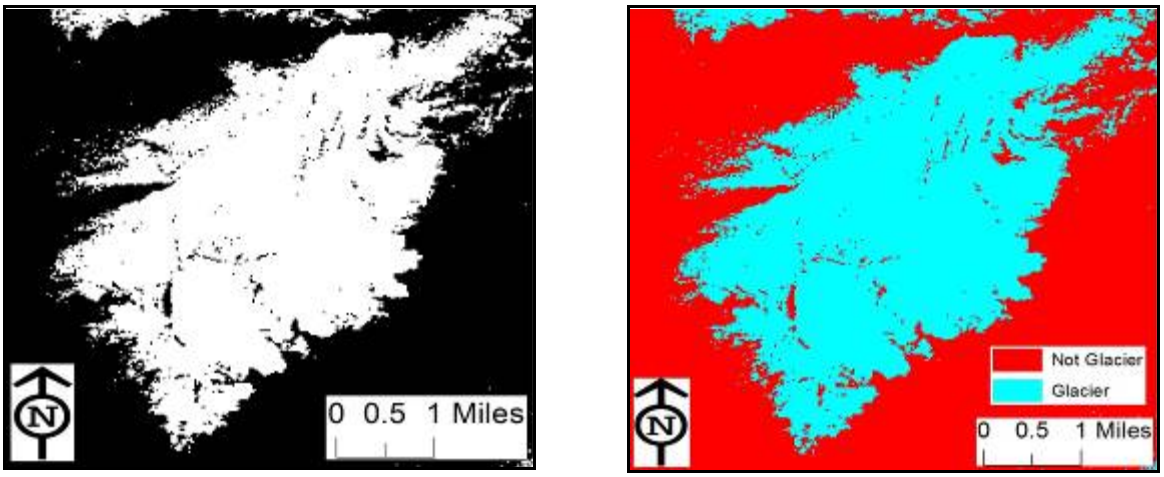


Figure 9. The resulting thresholded image for further isolating glacier areas as input to an image classification (left) and the classified image (right).

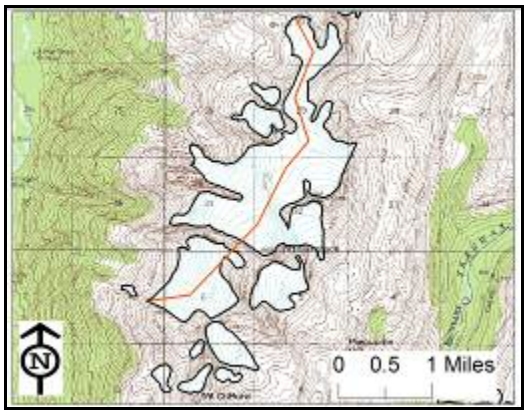


(a)

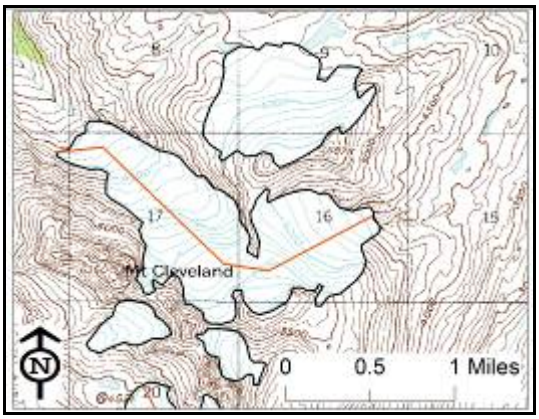


(b)

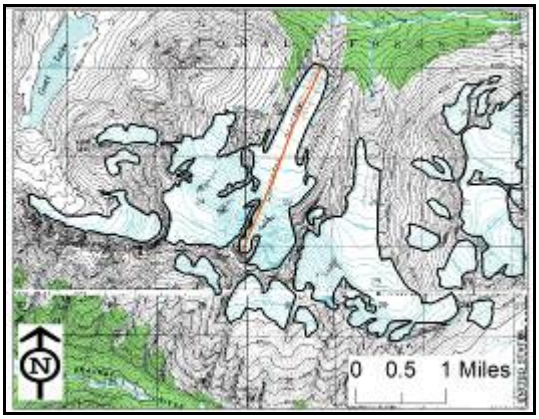


(c)

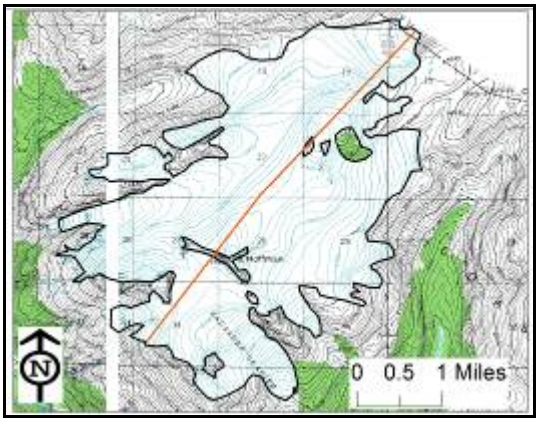


(d)

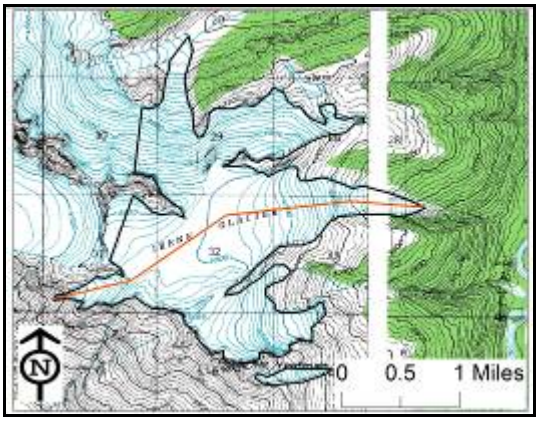


(e)

Figure 10. Glacier reference lines (orange) from digitized 1948 topographic maps- (a) Carmack; (b) Cleveland; (c) Laughton; (d) Saussure; and (e) Irene Glacier.

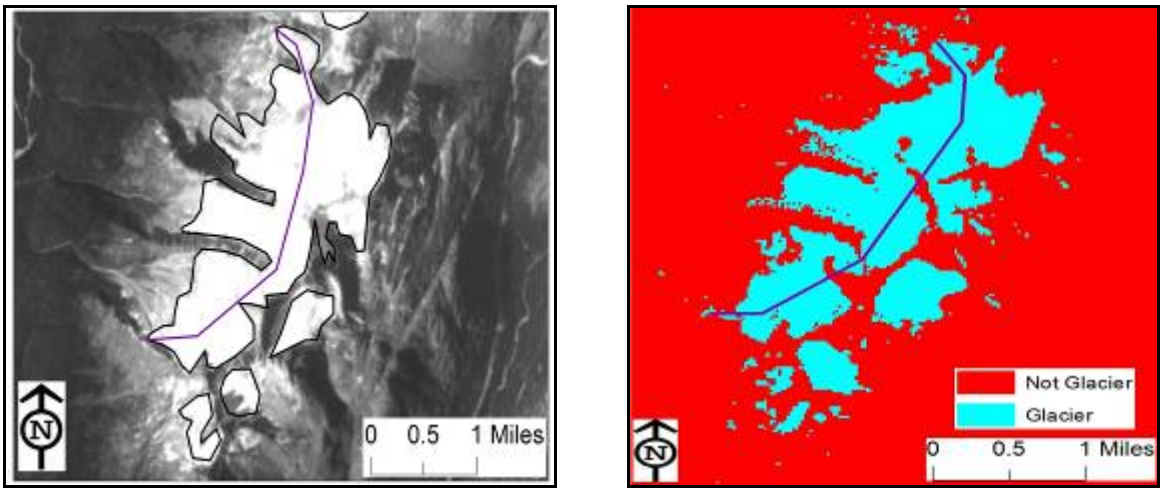


(a) (b)

Figure 11. Examples of glacier length measured from: a) a 1979 aerial photograph of Carmack Glacier (violet line); and b) a 1986 classified Landsat TM image of Carmack Glacier (violet line).

### 4.2 Thematic Accuracy Assessment

The resulting error matrix for the classified Landsat TM image scene (see Table 5) shows that the image processing techniques employed were successful at accurately mapping glacier area boundaries. The 2006 classified Landsat TM image scene of the Irene Glacier had an overall classification accuracy of 94.12%, the user's and producer's accuracy for the 'Not Glacier' class were both 94.12%, and the user's and producer's accuracy for the 'Glacier' class were both 94.12%. Furthermore, the overall Kappa statistic (K^) was determined to be 88.18%. It is also important to note that the image acquisition date for the Landsat TM image (Irene Glacier) was August 28, 2006; whereas the acquisition date for the high-spatial resolution reference image was September 15, 2006. Both image dates were deemed to be satisfactory for minimizing the effects of seasonal snow variation, but there was the potential for some temporal glacier area discrepancies between the ground truth image and the classified Landsat TM image.

Table 5. Thematic Accuracy Assessment Error Matrix: Irene Glacier, 2006

| | REFERENCE DATA | | | | |
|---|---|---|---|---|---|
| CLASSIFIED DATA | Not Glacier | Glacier | Row Total | Producer's Accuracy | Error of Omission |
| Not Glacier | 96 | 6 | 102 | 94.12% | 5.88% |
| Glacier | 6 | 96 | 102 | 94.12% | 5.88% |
| Column Total | 102 | 102 | 204 | | |
| User's Accuracy | 94.12% | 94.12% | | | |
| Errors of Commission | 5.88% | 5.88% | | | |
| Overall Accuracy | 94.12% | | | | |
| Kappa Index | 88.18% | | | | |

## 4.3 Glacier Change Analysis

### *4.3.1 Carmack Glacier Area and Length*

The resulting calculations for temporal changes in total area of the Carmack Glacier (see Appendix) show considerable change during the period of 1948-2011 (see Figure 12), as the total glacier area was greatest in 1948 (3.1$mi^2$/8.04 $km^2$) and was the least in 1995 (1.57$mi^2$/4.07$km^2$). Over the 63 years of interest, the Carmack Glacier total area extent decreased by 38.71% (from 3.1$mi^2$/8.04$km^2$ to 1.9$mi^2$/4.9$km^2$), which equates to an average decrease of 0.019$mi^2$/0.049$km^2$ per year and an average relative percentage change of -0.97%. There was also some considerable fluctuation in the Carmack Glacier area relative percentage change in subsequent image years—in both the positive and negative direction (see Figure 13). The glacier area increased from the previous image year in 1979, 1987, 1990, 1993, 1994, 1996, 1999, 2001, 2005, and 2006, with the years 2001 and 2006 experiencing the greatest increase in glacier area of 50.44% and 57.09%, respectively. The glacier area decreased from the previous image year in 1961, 1984, 1986, 1989, 1992, 1995, 1997, 2003, 2004, 2007, and 2011, with the years 1995 and 2003 experiencing the greatest decrease in glacier area of 35.14% and 35.1%, respectively. There was no change in glacier area from the previous image year in 1998.

Furthermore, the results of the change detection post-classification method for the Carmack Glacier for the Landsat ETM+ and TM images show very few pixels changing from ‘Not Glacier’ to ‘Glacier’ and a great number of pixels changing from ‘Glacier’ to ‘Not Glacier’ (see Figure 14), with the greatest concentration of glacier loss occurring along the western and northeastern margins.

The general trend in the area extent of the Carmack Glacier between 1948 and 2011 is showing to be on a downward trajectory (as shown in Figure 12), with the most recent years' data (1995-2011) showing primarily an average total area of the glacier between 1.5$mi^2$/3.88$km^2$ and 2.0$mi^2$/5.18$km^2$. However, there were considerable spikes in glacier area advancement for the years 2001 and 2006 (with their subsequent large relative percentage change in the preceding and following image years). This could in part be attributed to some patches of snow along the margins of the glacier that may have been the result of lingering seasonal snow that was not identified as such during image processing. However, the image acquisition dates for the 2001 and 2006 Landsat ETM+ and TM images were determined to be satisfactory for attempting to minimize the effects of seasonal snow variation (August 15 and August 28, respectively).

In addition, there were gaps in acceptable satellite imagery for Carmack Glacier for the years 1985, 1988, 1999, 2000, 2002, and 2008-2010; therefore, there was no glacier area extent change data available for several years during the period of interest—which potentially could affect the direction of the general area trend and the average relative change rates per year.

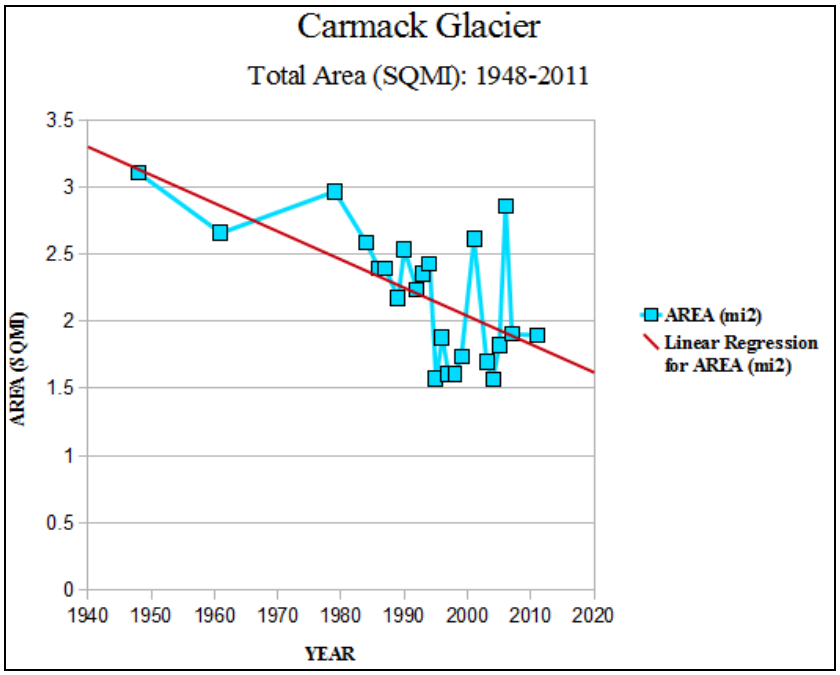


Figure 12. Temporal changes in area extents of the Carmack Glacier.

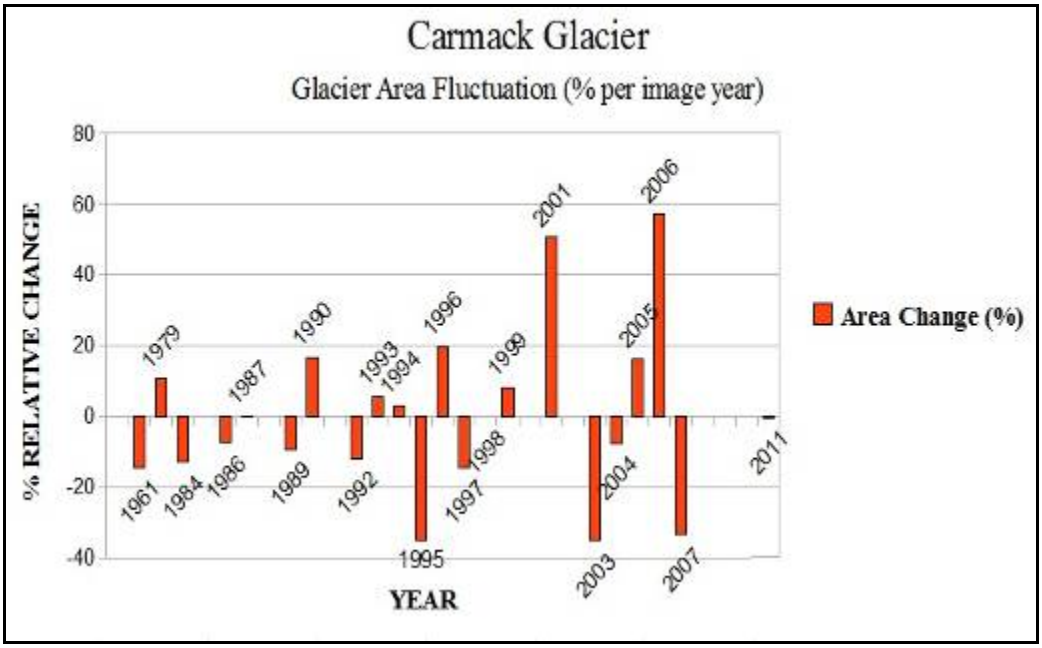


Figure 13. Fluctuation in the Carmack Glacier area relative percentage change.

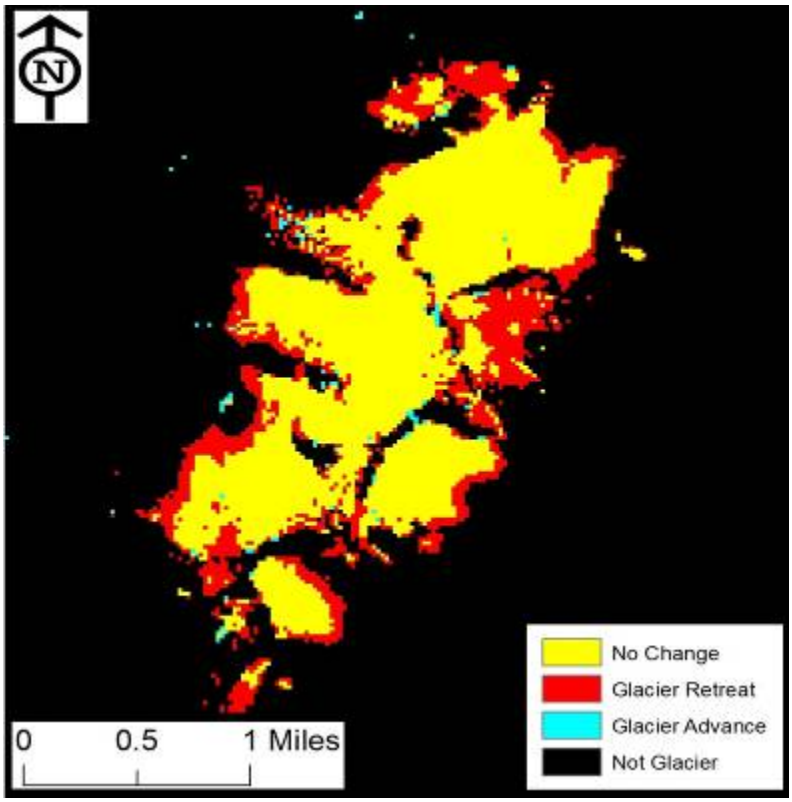


Figure 14. Results of the change detection post-classification method for the Carmack Glacier showing fairly significant glacier area retreat between 1984 and 2011.

The resulting calculations for temporal changes in total length of Carmack Glacier (see Appendix) also shows considerable change during the period of interest (see Figure 15), as the total measured glacier length was greatest in 1948 (3.97mi/6.39km) and was the least in 1995 (2.57mi/4.13km). Over the 63 years of interest, the Carmack Glacier total length decreased by 29.22% (from 3.97mi/6.39km to 2.81mi/4.52km), which equates to an average decrease of 0.022mi/0.036km per year and an average relative percentage change of -1.03%. There was also considerable fluctuation in the glacier length relative percentage change in subsequent image years—in both the positive and negative direction (see Figure 16). Glacier length increased from the previous image year in 1989, 1990, 1993, 1996, 1999, 2001, 2004, 2005, 2006, and 2011, with the years 1990

and 2006 showing the greatest increase in glacier length of 21.41% and 15.21%, respectively. The glacier length decreased from the previous image year in 1961, 1979, 1984, 1986, 1987, 1992, 1994, 1995, 1997, 1998, 2003, and 2007, with the years 1992 and 1995 experiencing the most significant decrease in total length of 22.34% and 18.96%, respectively.

The general trend in the total length of the Carmack glacier between 1948 and 2011 is also clearly showing to be decreasing (as shown in Figures 15 and 17), with the most recent years' data (1995-2011) showing primarily an average total glacier length between 2.5mi/4.02km and 3.0mi/4.83km. However, there was considerable advancement in length measurements for the years 1993 and 2006 (with the subsequent large relative percentage change in the preceding and following image years).

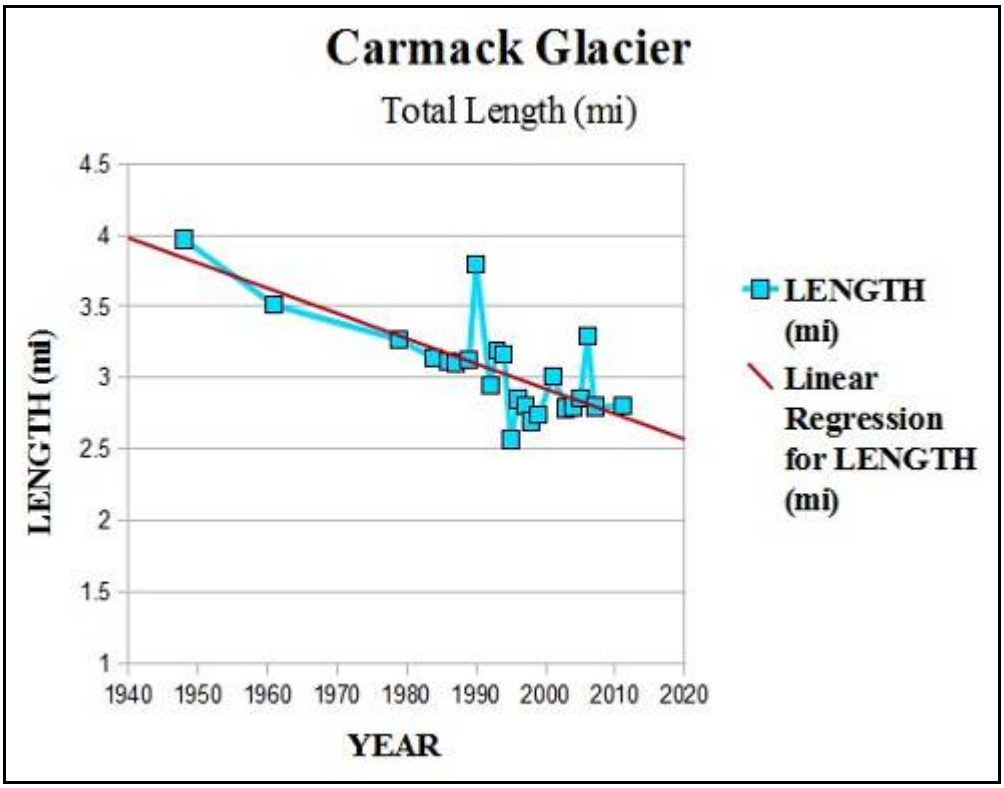

Figure 15. Temporal changes in total lengths of the Carmack Glacier.

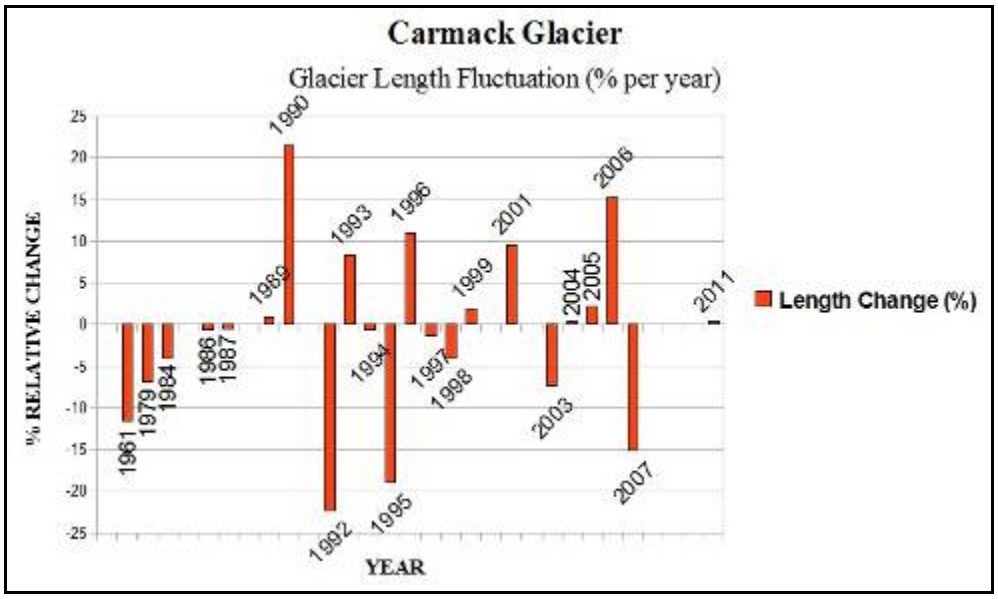

Figure 16. Fluctuation in the Carmack Glacier length relative percentage change.

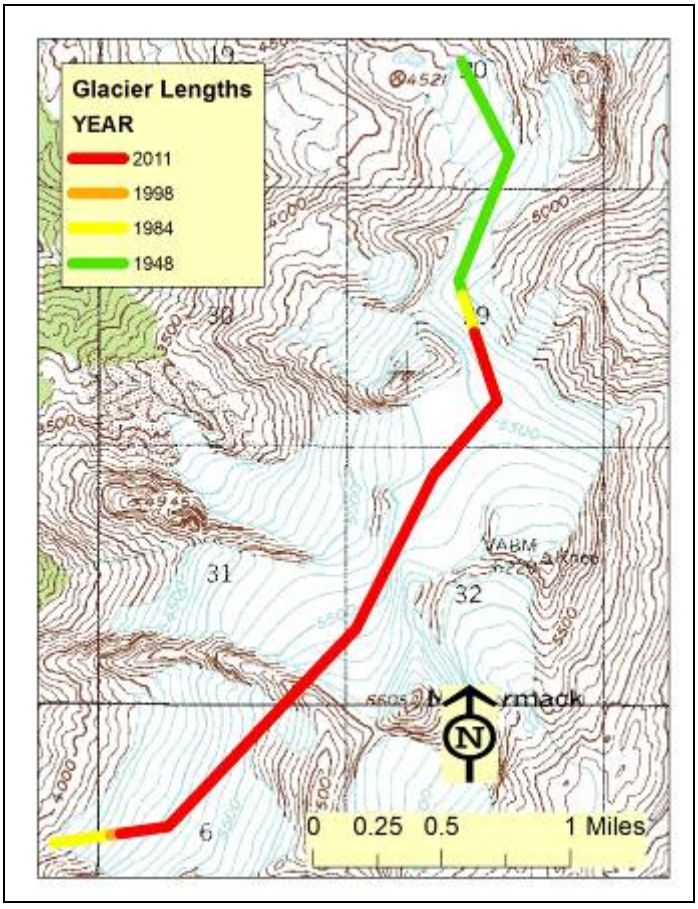

Figure 17. Glacier lengths as measured from the 1948 topographic map and 1984, 1998, and 2011 Landsat TM imagery for Carmack Glacier.

*4.3.2 Cleveland Glacier Area and Length*

The resulting calculations for temporal changes in total area of the Cleveland Glacier (see Appendix) show considerable changes during the period of 1948-2011 (see Figure 18), as the total glacier area was greatest in 2006 (2.34$mi^2$/6.05$km^2$) and was the least in 2004 (0.45$mi^2$/1.16$km^2$). Over the 63 years of interest, the Cleveland Glacier total area extent decreased by 65.48% (from 1.68$mi^2$/4.34$km^2$ to 0.58$mi^2$/1.51$km^2$), which equates to an average decrease of 0.017$mi^2$/0.045$km^2$ per year and an average relative percentage change of -0.55%. There was also considerable fluctuation in the glacier area relative percentage change in subsequent image years—in both the positive and negative direction (see Figure 19). The glacier area extent increased in 1979, 1990, 1993, 1998, 2005, and 2006, with the years 1998 and 2006 experiencing the greatest relative percentage increase in glacier area from the previous image year of 147.26% and 252.86%, respectively. The glacier area decreased from the previous image year in 1961, 1984, 1986, 1987, 1989, 1992, 1994, 1995, 1996, 1997, 1999, 2003, 2004, 2007, and 2011, with the years 1999 and 2007 experiencing the greatest relative glacier area retreat of 64.73% and 70.46%, respectively.

Furthermore, the results of the change detection post-classification method for the Cleveland Glacier for the Landsat ETM+ and TM images show a sparse number of pixels changing from 'Not Glacier' to 'Glacier,' and a great quantity of pixels changing from 'Glacier' to 'Not Glacier' (see Figure 20)—with widespread glacier loss along all sides of the glacier.

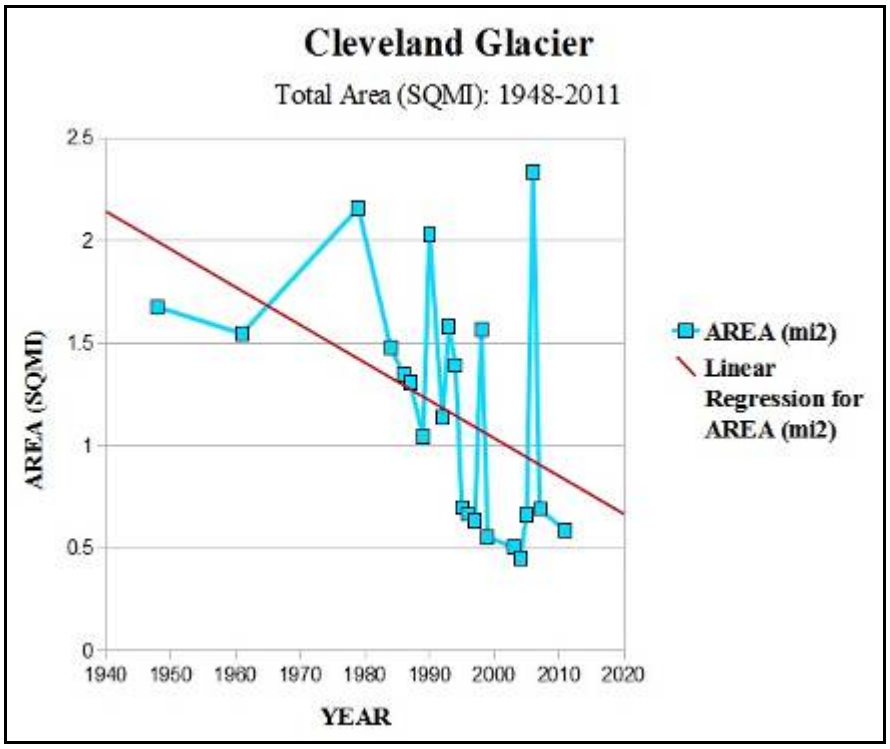


Figure 18. Temporal changes in area extents of the Cleveland Glacier.

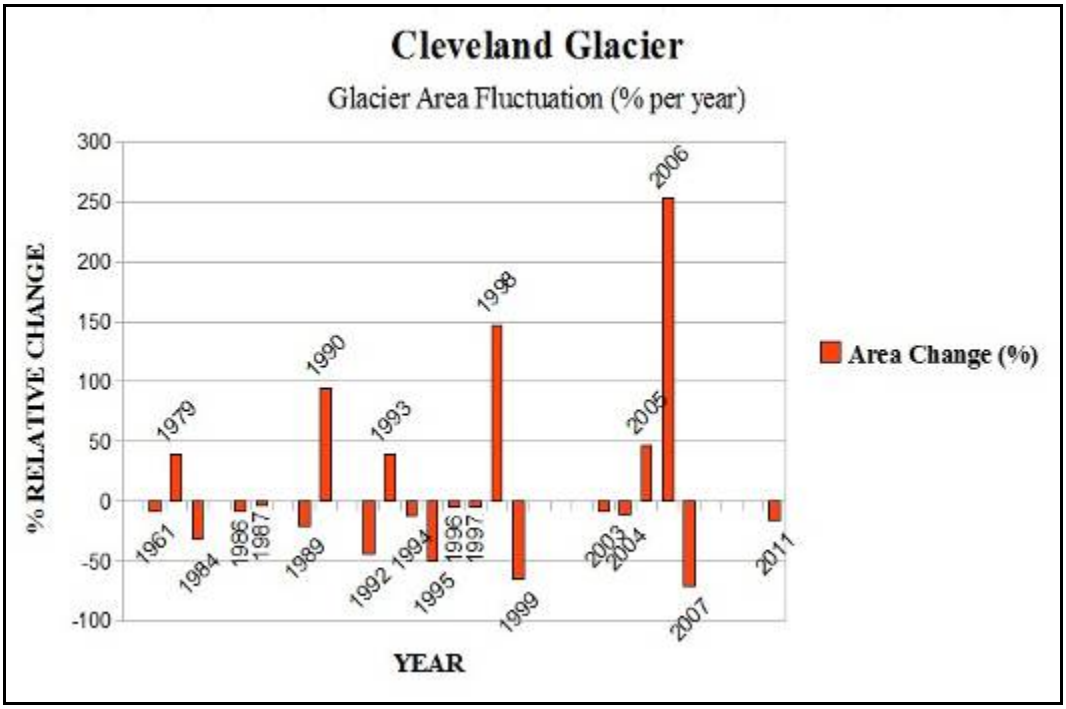


Figure 19. Fluctuation in the Cleveland Glacier area relative percentage change.

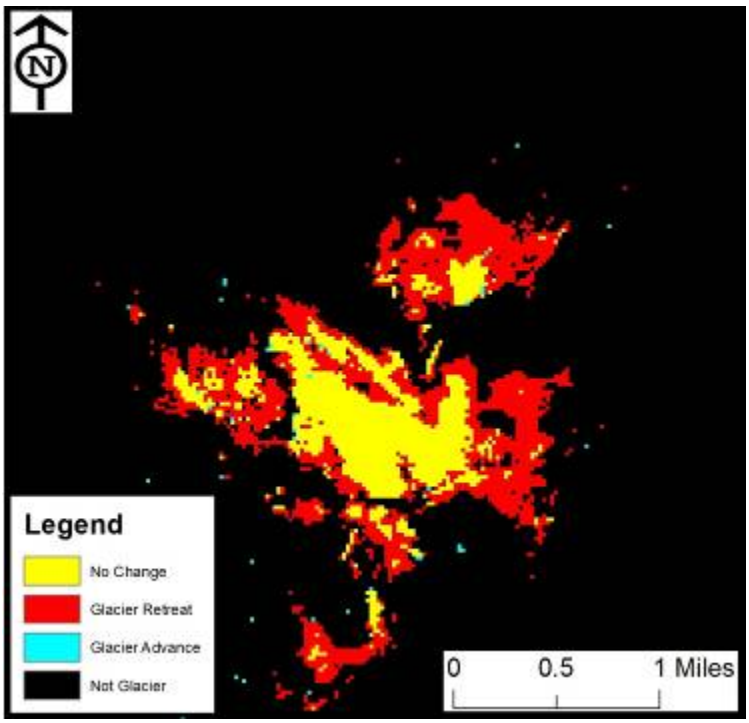

Figure 20. Results of the change detection post-classification method for the Cleveland Glacier showing significant glacier area retreat between 1984 and 2011.

The general trend in the area extent of the Cleveland Glacier is appearing to be on a downward trajectory (as shown in Figure 18), with the most recent years' data (1995-2011) showing primarily an average total area of the glacier between $0.5mi^2/1.29km^2$ and $1.0mi^2/2.59km^2$. However, there were major spikes in glacier area advancement for the years 1998 and 2006, with consistency in major advancement during 2006 for both the Cleveland Glacier and the adjoining Carmack Glacier. This could in part be attributed to some patches of snow along the margins of that glacier that may be a consequence of lingering seasonal snow that was not identified as such during image processing. However, the image acquisition dates for the 1998 and 2006 Landsat TM images were deemed satisfactory for attempting to minimize the effects of seasonal snow variation (September 16 and August 28, respectively).

In addition, there were gaps in acceptable Landsat ETM+ and TM imagery for the glacier for the years 1985, 1988, 1991, 2000-2002, and 2008-2010; therefore, there was no glacier area extent change data for several years during the time period of interest—which potentially could affect the direction of the general area trend and the average relative percentage change rates.

The resulting calculations for the temporal changes in total length of the Cleveland Glacier (see Appendix) also shows considerable change during the period of interest (see Figure 21), as the total measured glacier length was greatest in 1948 (2.24mi/3.6km) and was the least in 2003 and 2004 (both 1.32mi/2.13km). Over the 63 years of interest, the Cleveland Glacier total length decreased by 40.63% (from 2.24mi/3.6km to 1.33mi/2.14km), which equates to an average decrease of 0.014mi/0.023km per year and an average relative percentage change of -0.94%. There was also considerable fluctuation in the glacier length relative percentage change in subsequent image years—in both the positive and negative direction (see Figure 22). Total glacier length increased from the previous image year in 1986, 1990, 1993, 1996, 1997, 1998, 2005, and 2006, with the years 1993 and 2006 experiencing the greatest increase in glacier length of 16.86% and 14.02%, respectively. The glacier length decreased from the previous image year in 1961, 1979, 1984, 1987, 1989, 1992, 1994, 1995, 1999, 2003, 2004, 2007, and 2011, with the years 1984 and 1994 showing the greatest decrease in total length of 16.8% and 23.48%, respectively.

The general trend in the total length of the Cleveland Glacier between 1948 and 2011 is also appearing to be decreasing (as shown in Figures 21 and 23), with the most recent years' data (1995-2011) showing primarily an average total glacier length between

1.3mi/2.09km and 1.6mi/2.57km. However, there was considerable advancement in length measurements for the years 1990, 1993, and 2006 (with subsequent large relative percentage change in the preceding and following image years).

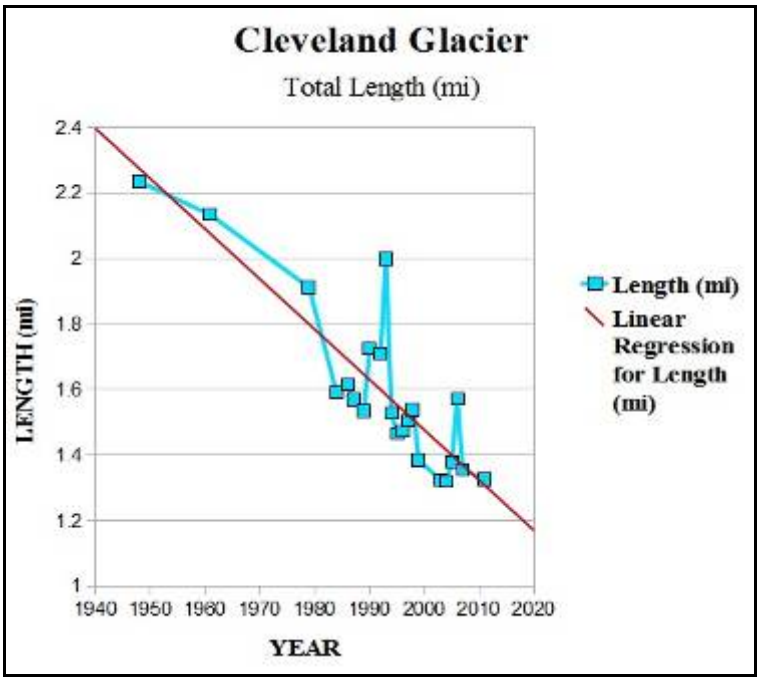


Figure 21. Temporal changes in total lengths of the Cleveland Glacier.

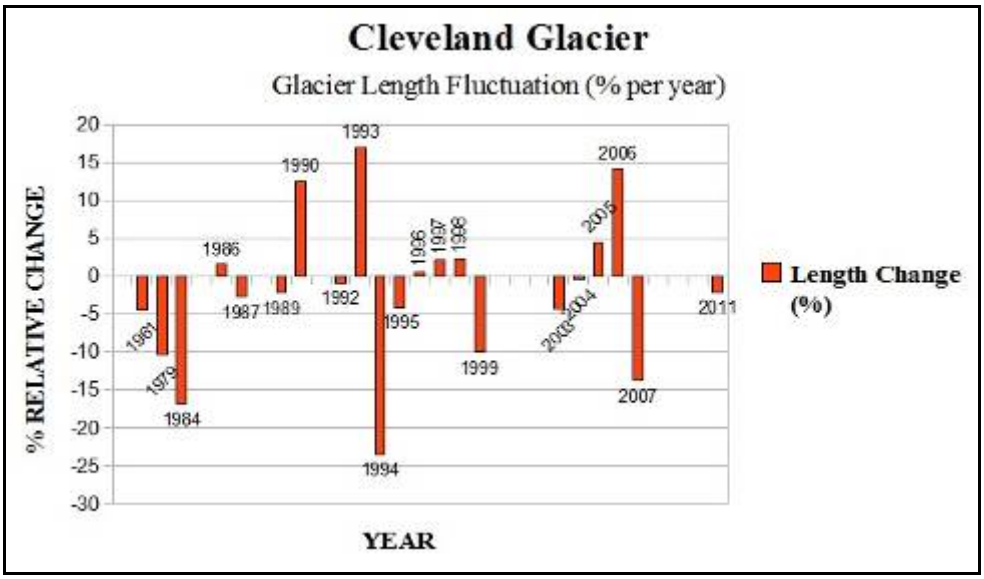


Figure 22. Fluctuation in the Cleveland Glacier length relative percentage change.

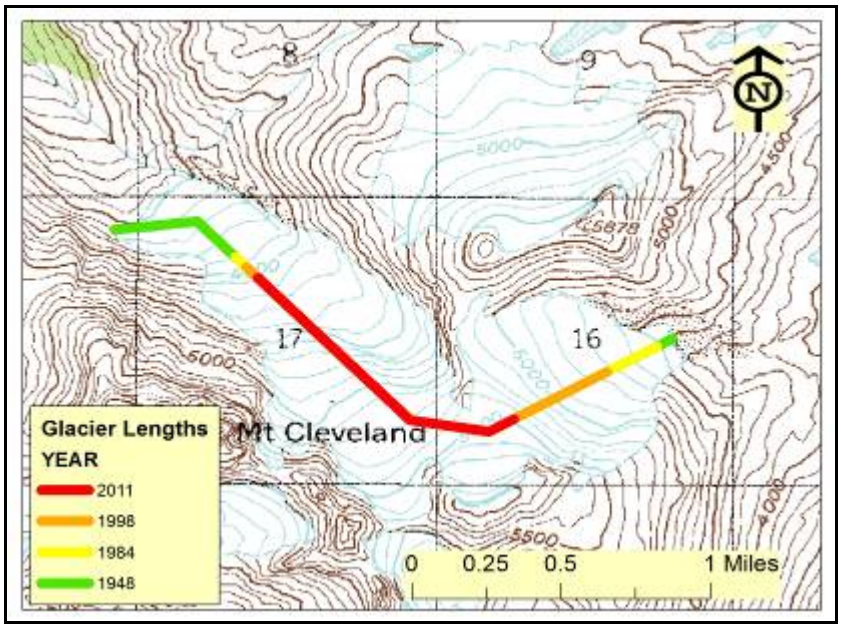

Figure 23. Glacier lengths as measured from 1948 topographic map and 1984, 1998, and 2011 Landsat TM imagery for Cleveland Glacier.

*4.3.3 Irene Glacier Area and Length*

The resulting calculations for temporal changes in total area of the Irene Glacier (see Appendix) show significant change during the period of 1948-2011 (see Figure 24), as the total glacier area was greatest in 1979 (4.11mi$^2$/10.64km$^2$) and was the least in 1995 (2.13mi$^2$/5.51km$^2$). Over the 63 years of interest, the Irene Glacier total area extent decreased by 30.86% (from 3.24mi$^2$/8.4km$^2$ to 2.24mi$^2$/5.79km$^2$), which equates to an average decrease of 0.016mi$^2$/0.041km$^2$ per year and an average relative percentage change of -1.10%. There was also considerable fluctuation in the glacier area relative percentage change in subsequent years—in the positive and negative direction (see Figure 25). The glacier area increased from the previous image year in 1979, 1986 1990, 1993, 1996, 1998, 2001, 2005, 2006, and 2009, with the years 1979 and 2006 showing the greatest increase in glacier area of 26.59% and 26.11%, respectively. The glacier area decreased from the previous image year in 1984, 1989, 1992, 1995, 1999, 2003, 2004,

2007, and 2011, with the years 1984 and 1995 experiencing the greatest decrease in glacier area of 32.71% and 28.3%, respectively. No change in glacier area extent was observed in the years 1961 and 1987.

Furthermore, the results of the change detection post-classification method for the Irene Glacier for the Landsat ETM+ and TM imagery (1984-2011) show a very sparse number of pixels that changed from 'Not Glacier' to 'Glacier' and a large number of pixels that changed from 'Glacier' to 'Not Glacier' (see Figure 26)—with the greatest concentrations of loss occurring along the northern and southeastern margins of the glacier.

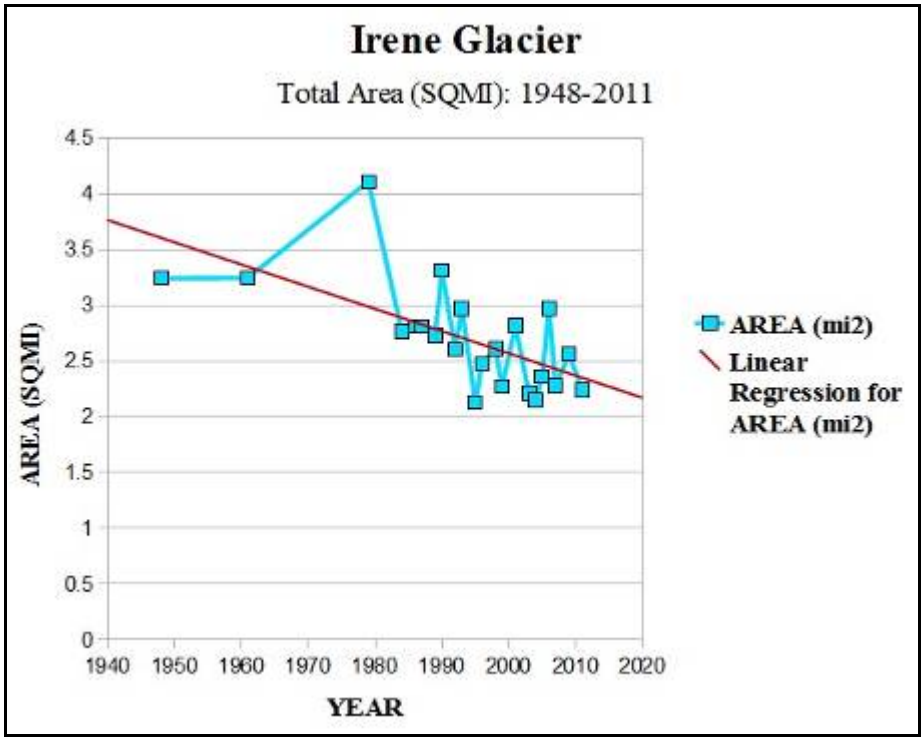

Figure 24. Temporal changes in area extents of the Irene Glacier.

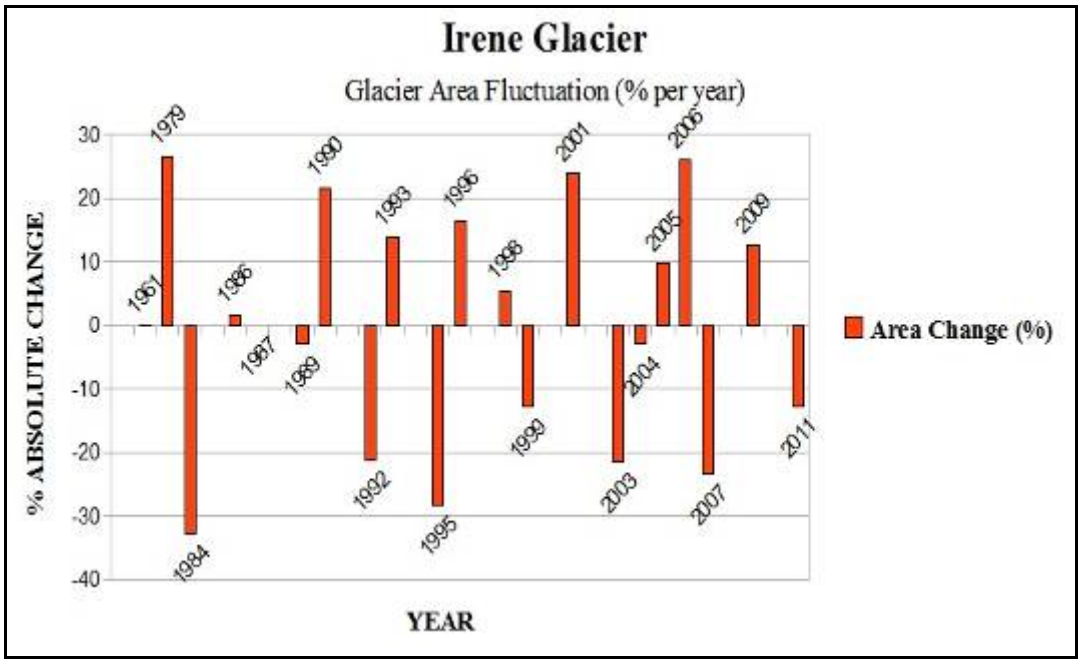

Figure 25. Fluctuation in the Irene Glacier area relative percentage change.

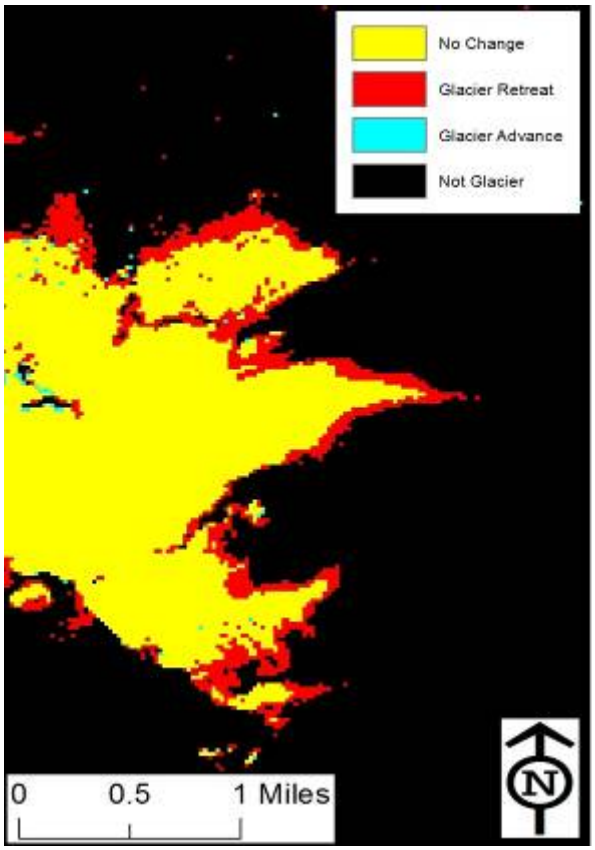

Figure 26. Results of the change detection post-classification method for the Irene Glacier showing fairly significant glacier area retreat between 1984 and 2011.

The general trend in the area extent of the Irene Glacier between 1948 and 2011 is showing to be on a downward trajectory, as shown in Figure 24, with the most recent years' data (1995-2011) showing primarily an average total area of the glacier between $2.0mi^2/5.18km^2$ and $3.0mi^2/7.77km^2$. However, there was a major spike in glacier area advancement for the year 1979 (with the subsequent large relative percentage change in the preceding and following image years). This could in part be attributed to possible unknown positional errors in the original 1979 aerial photograph. In addition, there were gaps in acceptable Landsat TM imagery for the Irene Glaciers for the years 1985, 1988, 1991, 1994, 1997, 2000, 2002, 2008, and 2010; therefore, there was no glacier area extent change data available for multiple years during the time period of interest—which potentially could affect the direction of the general trend and the average relative percentage change rates.

The resulting calculations for temporal changes in total length of Irene Glacier (see Appendix) also shows considerable change during the period of interest (see Figure 27), as the total measured glacier length was greatest in 1948 (3.37mi/5.42km) and was the least in 2001 (1.52mi/2.44km). Over the 63 years of interest, the glacier total length decreased by 43.32% (from 3.37mi/5.42km to 1.91mi/3.08km), which equates to an average decrease of 0.023mi/0.037km per year and an average relative percentage change of -0.90%. There was also considerable fluctuation in the glacier length relative percentage change in subsequent image years—in both the positive and negative direction (see Figure 28). Glacier length increased from the previous image year in 1987, 1989, 1990, 1993, 1996, 1997, 1998, 2003, 2004, 2006, and 2011, with the years 2003 and 2011 exhibiting the greatest increase in glacier length of 13.68% and 14.31%,

respectively. The glacier length decreased from the previous image year in 1961, 1979, 1984, 1986, 1992, 1995, 1999, 2001, 2005, 2007, and 2009, with the year 1984 experiencing the greatest decrease in total length of 29.69%.

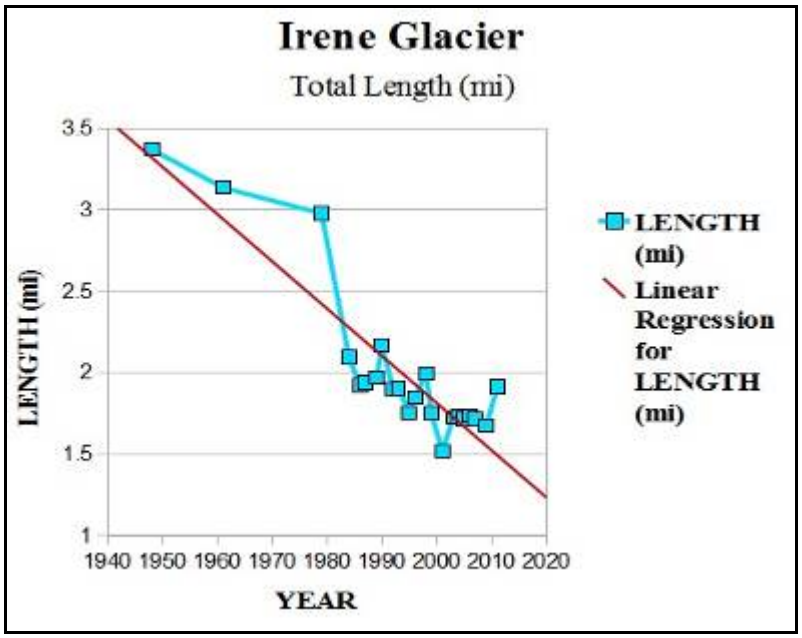


Figure 27. Temporal changes in total lengths of the Irene Glacier.

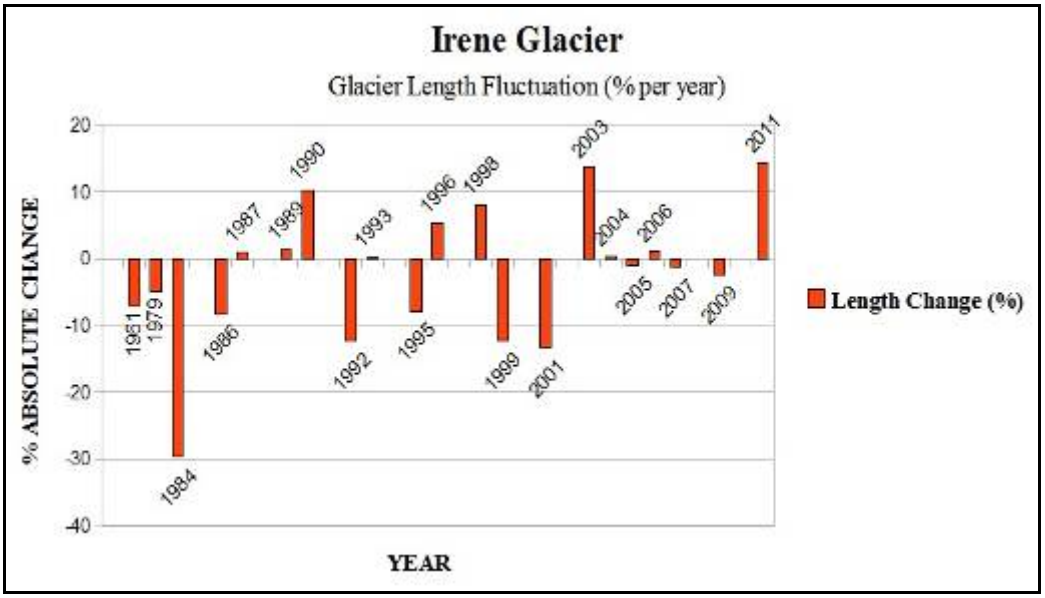


Figure 28. Fluctuation in the Irene Glacier length relative percentage change.

The general trend in total length of Irene Glacier between 1948 and 2011 is also appearing to be decreasing (as shown in Figures 27 and 29), with the most recent years' data (1995-2011) showing primarily an average total glacier length between 1.5mi/2.41km and 2.0mi/3.22km. However, there was a significant retreat in length between the 1979 aerial photograph measurement and the 1984 Landsat TM image calculation (-29.69%).

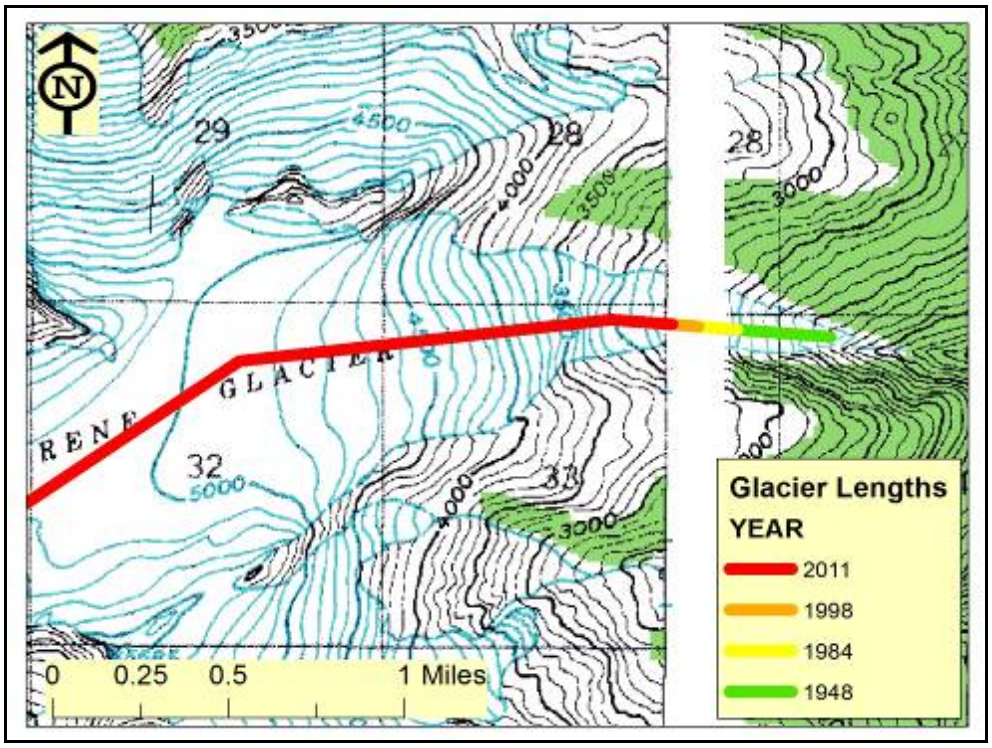


Figure 29. Glacier lengths as measured from the 1948 topographic map and 1984, 1998, and 2011 Landsat TM imagery for Irene Glacier.

*4.3.4 Laughton Glacier Area and Length*

The resulting calculations for temporal changes in the total area of the Laughton Glacier (see Appendix) show considerable change during the period of 1948-2011 (see Figure 30), as the total glacier area was greatest in 2006 ($4.9mi^2/12.69km^2$) and was the least in 1995 ($1.34mi^2/3.47km^2$). Over the 63 years of interest, the glacier total area extent decreased by 52.86% (from $4.37mi^2/11.33km^2$ to $2.06mi^2/5.34km^2$), which equates to an average decrease of $0.037mi^2/0.095km^2$ per year and an average relative percentage change of -0.75%. There was also some considerable fluctuation in the glacier area relative percentage change in subsequent image years—in the positive and negative direction (see Figure 31). The glacier area increased from the previous image year in 1979, 1987, 1990, 1996, 1998, 2001, 2005, 2006, and 2010, with the years 2001 and 2006 experiencing the greatest increase of 101.41% and 95.88%, respectively. The glacier area decreased from the previous image year in 1961, 1984, 1986, 1989, 1992, 1995, 1999, 2003, 2004, 2007, 2009, and 2011, with the years 1995 and 2003 exhibiting the greatest decrease of 56.03% and 49.03%, respectively.

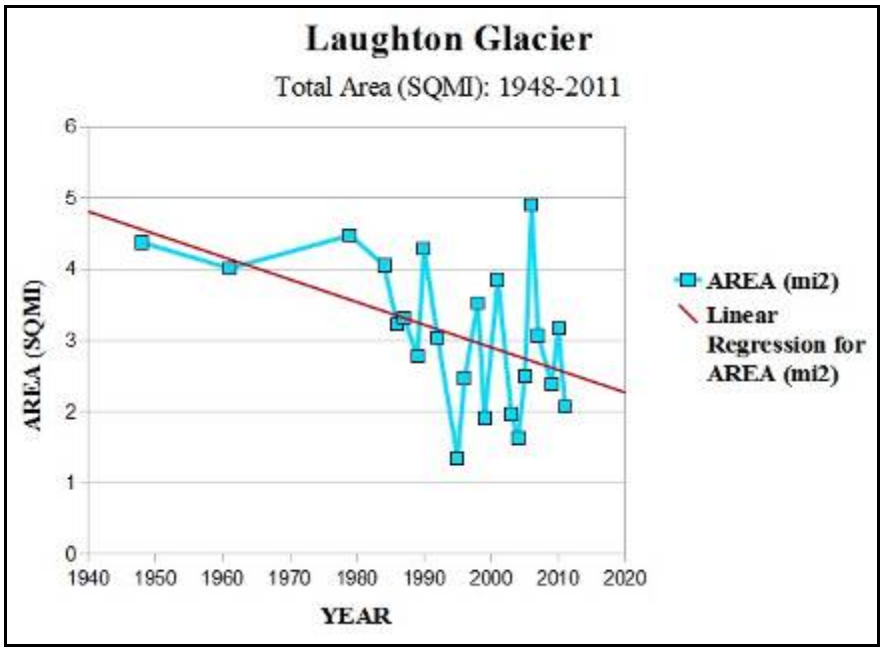

Figure 30. Temporal changes in area extents of the Laughton Glacier.

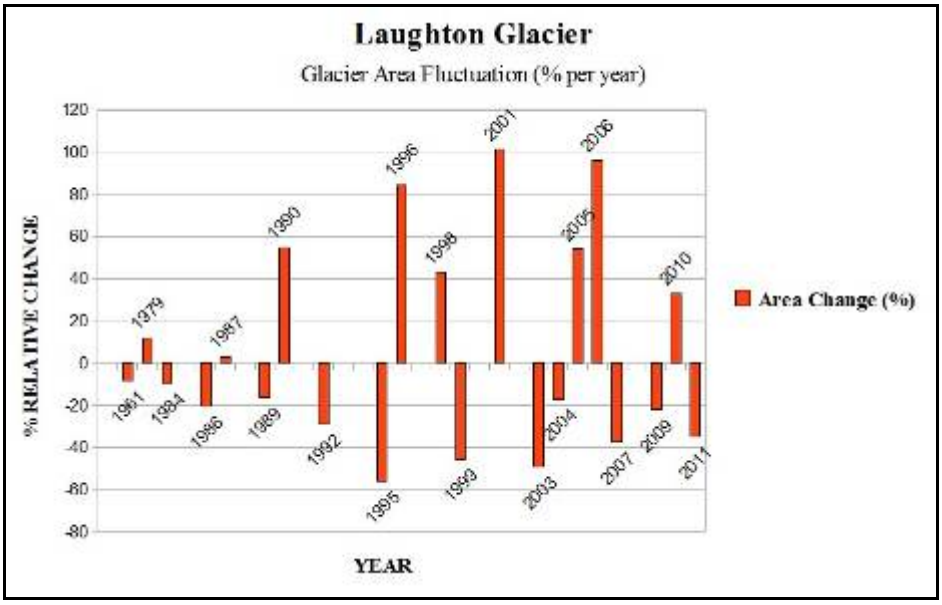

Figure 31. Fluctuation in the Laughton Glacier area relative percentage change.

The results of the change detection post-classification method for the Laughton Glacier show only a few minor clusters of pixels changing from 'Not Glacier' to 'Glacier' and large number of pixels changing from 'Glacier' to 'Not Glacier' (see Figure

32)—with the greatest concentrations of glacier loss occurring along the western and eastern margins.

The general trend in the area extent of the Laughton Glacier is clearly showing to be on a downward trajectory (see figure 30), with the most recent years' data (1995-2011) showing primarily an average total area of the glacier between 2.0mi$^2$/5.18km$^2$ and 4.0mi$^2$/10.36km$^2$. However, there were significant spikes in glacier area advancement for the years 1996, 2001, and 2006 (with their subsequent large relative percentage change in the preceding and following image years). This could be attributed to some patches of snow along the margins of the glacier that may have been the result of lingering seasonal snow that was not identified as such during image processing. However, the image acquisition dates for the 1996, 2001, and 2006 images were deemed satisfactory for attempting to minimize the effects of seasonal snow variation (August 16, 15, and 28, respectively).

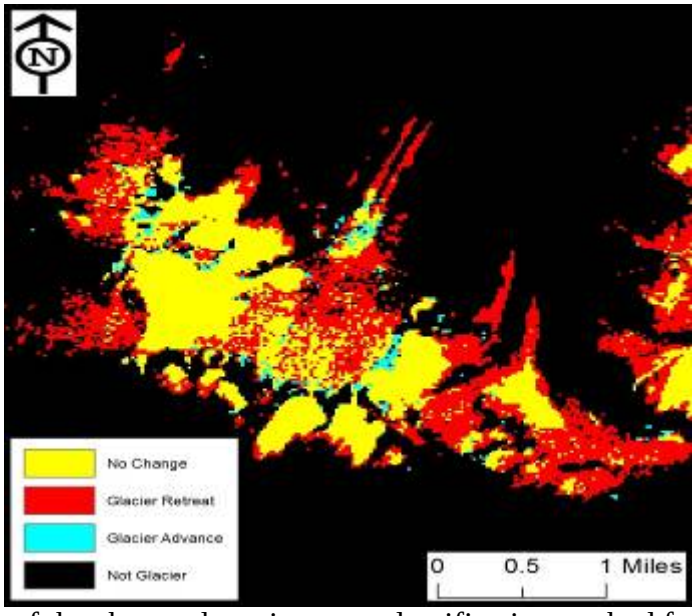


Figure 32. Results of the change detection post-classification method for the Laughton Glacier showing significant glacier area retreat.

In addition, there were gaps in acceptable Landsat TM imagery for Laughton Glacier for the years 1985, 1988, 1991, 1993, 1994, 1997, 2000, 2002, and 2008; therefore, there was no glacier area extent change data available for a number of years during the period of interest—which potentially could affect the direction of the general area trend and the average relative change percentage rates.

The resulting calculations for temporal changes in total length of the Laughton Glacier (see Appendix) also show considerable change during the period of interest (see Figure 33), as the total measured glacier length was greatest in 1979 (2.37mi/3.82km) and was the least in 2009 (1.21mi/1.95km). Over the 63 years of interest, the Laughton Glacier total length decreased by 34.65% (2.28mi/3.67km to 1.49mi/2.41km), which equates to an average decrease of 0.013mi/0.020km per year and an average relative percentage change of -1.04%. There was also considerable fluctuation in the glacier length relative percentage change in subsequent image years—in both the positive and negative direction (see Figure 34). Glacier length increased from the previous image year in 1979, 1990, 1996, 1998, 2001, 2005, 2007, and 2010, with the years 2005 and 2010 showing the greatest increase in glacier length of 25.4% and 39.48%, respectively. The glacier length decreased from the previous image year in 1961, 1984, 1986, 1987, 1989, 1992, 1995, 1999, 2003, 2004, 2006, 2009, and 2011, with the years 2004 and 2009 exhibiting the greatest decrease in total length of 32.73% and 29.24%, respectively.

The general trend in total length of the Laughton Glacier between 1948 and 2011 is clearly showing to be decreasing (as shown in Figures 33 and 35), with the most recent years' data (1995-2011) showing primarily an average total glacier length between

1.2mi/1.93km and 2.0mi/3.22km. However, there was significant retreat in the measured length for the years 2004 and 2009.

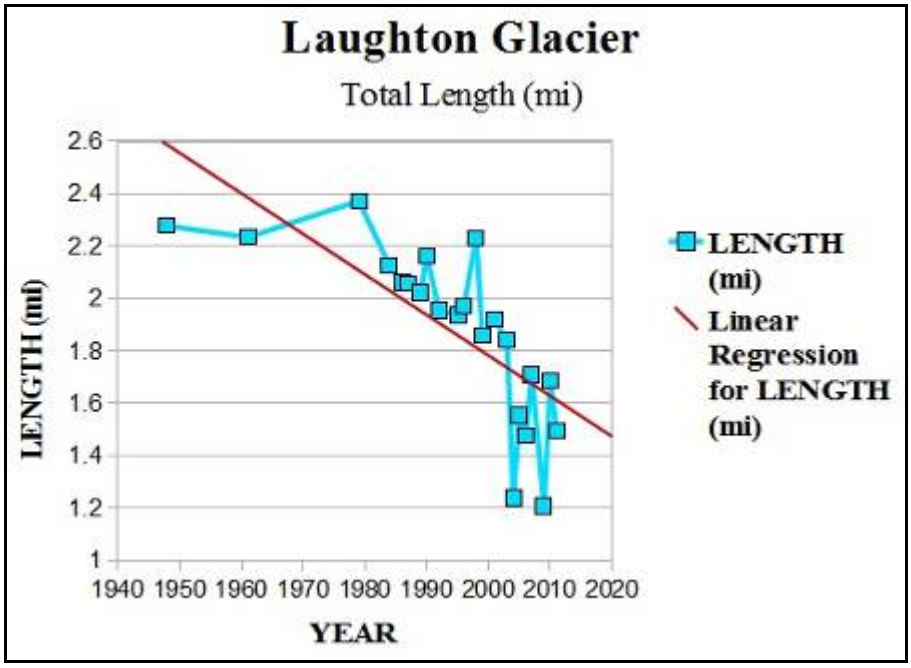


Figure 33. Temporal changes in total lengths of the Laughton Glacier.

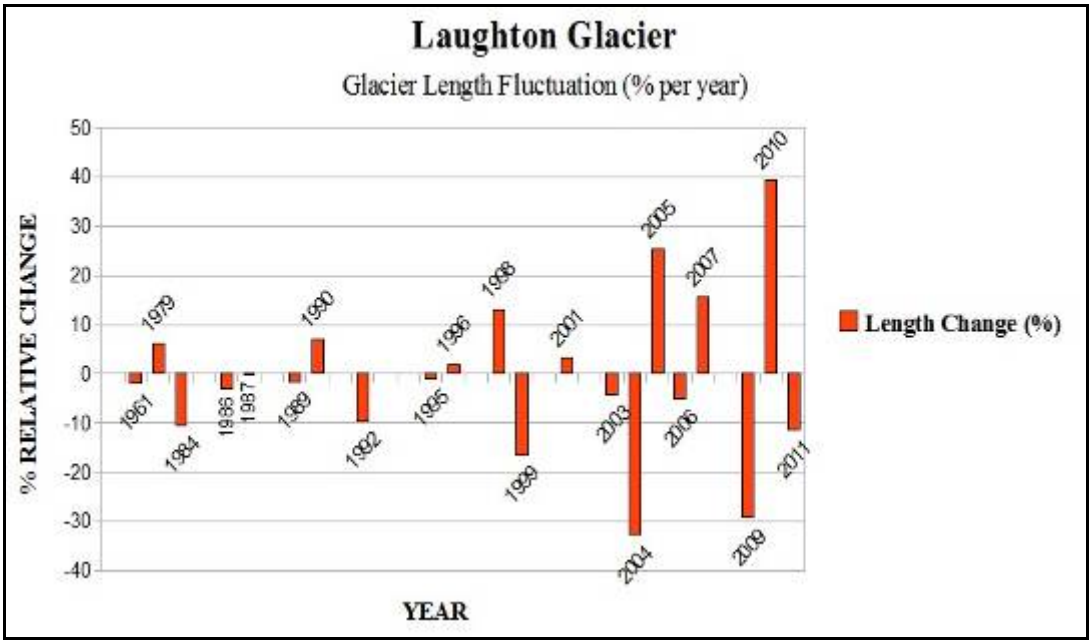


Figure 34. Fluctuation in the Laughton Glacier length relative percentage change.

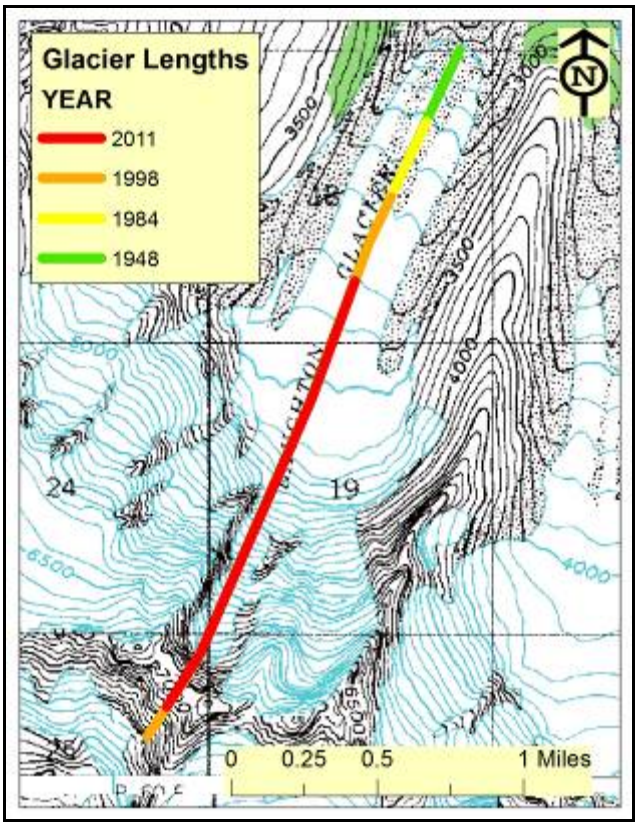

Figure 35. Glacier lengths as measured from the 1948 topographic map and 1984, 1998, and 2011 Landsat TM imagery for Laughton Glacier.

*4.3.5 Saussure Glacier Area and Length*

The resulting calculations for temporal changes in the total area of Saussure Glacier (see Appendix) show considerable change during the period interest (see Figure 36), as the total glacier area was greatest in 1979 (12.05mi$^2$/31.21km$^2$) and was the least in 1995 (6.32mi$^2$/16.36km$^2$). Over the 63 years of interest, the Saussure Glacier total area extent decreased by 38.47% (from 10.32mi$^2$/26.73km$^2$ to 6.35mi$^2$/16.44km$^2$), which equates to an average decrease of 0.063mi$^2$/0.163km$^2$ per year and an average relative percentage change of -0.98%. There was also some considerable fluctuation in the glacier area relative percentage change in subsequent image years—in the positive and negative direction (see Figure 37). The glacier area increased from the previous image

year in 1979, 1986, 1990, 1993, 1996, 1998, 2005, 2006, and 2009, with the years 1990 and 2006 experiencing the greatest increase of 39.52% and 28.68%, respectively. The Saussure Glacier area decreased from the previous image year in 1961, 1984, 1987, 1989, 1992, 1995, 1997, 1999, 2007, and 2011, with the years 1984 and 1992 exhibiting the greatest decrease in glacier area of 33.22% and 29.63%, respectively.

Furthermore, the results of the change detection post-classification method for the Saussure Glacier for the Landsat ETM+ and TM images (1984-2011) show very few pixels changing from 'Not Glacier' to 'Glacier' and a substantial number of pixels changing from 'Glacier' to 'Not Glacier' (see Figure 38)—with the greatest concentrations of glacier loss occurring along the northern and northeastern margins.

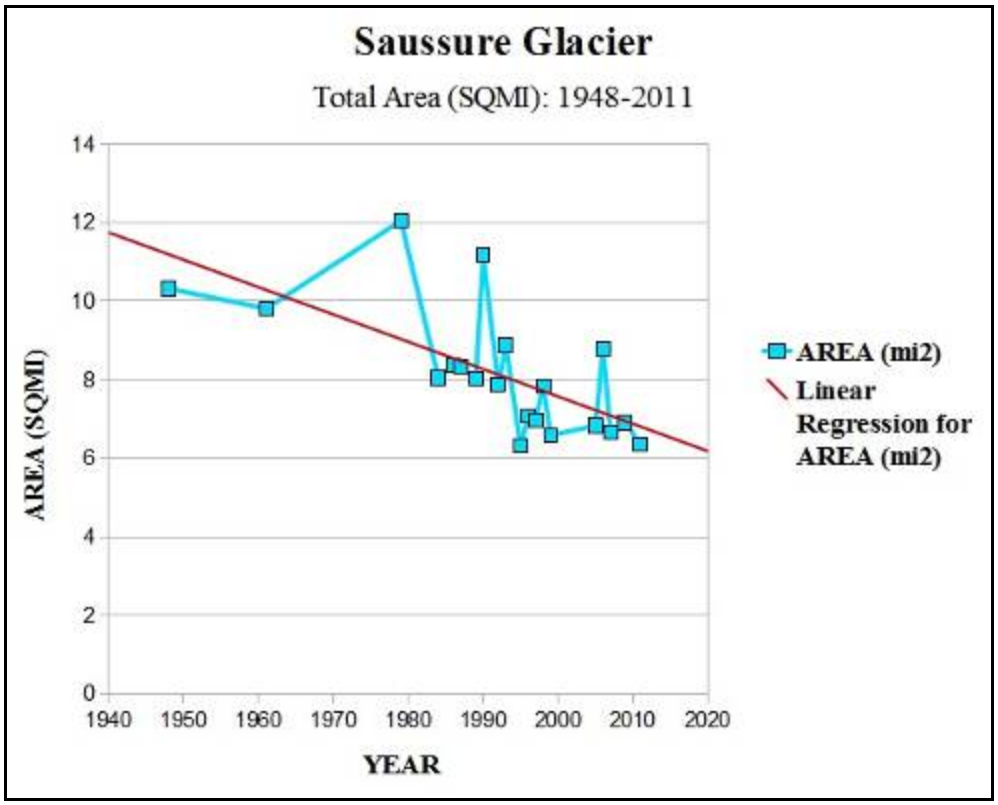

Figure 36. Temporal changes in area extents of the Saussure Glacier.

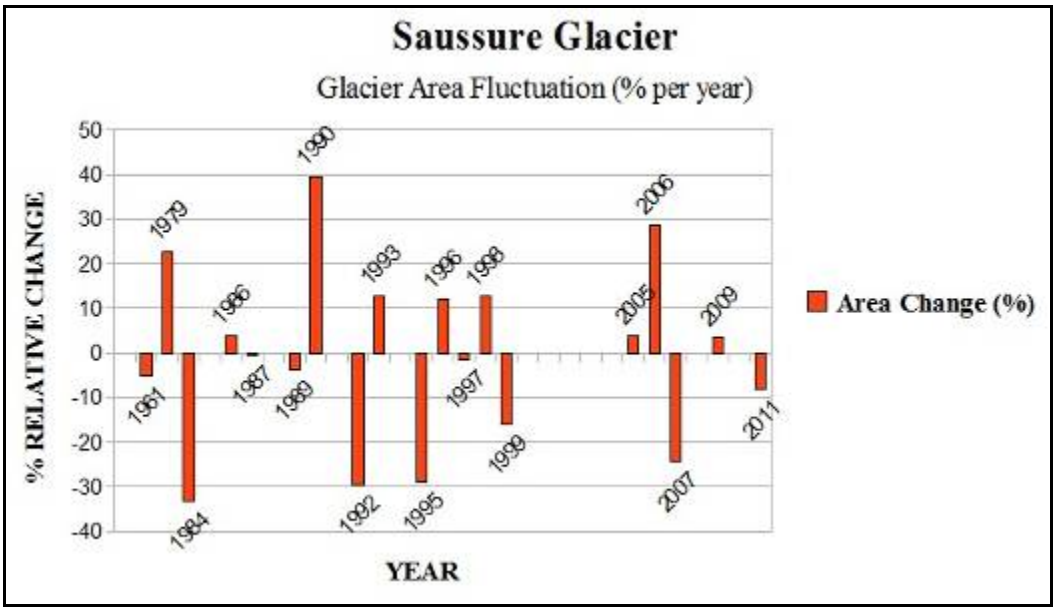

Figure 37. Fluctuation in the Saussure Glacier area relative percentage change.

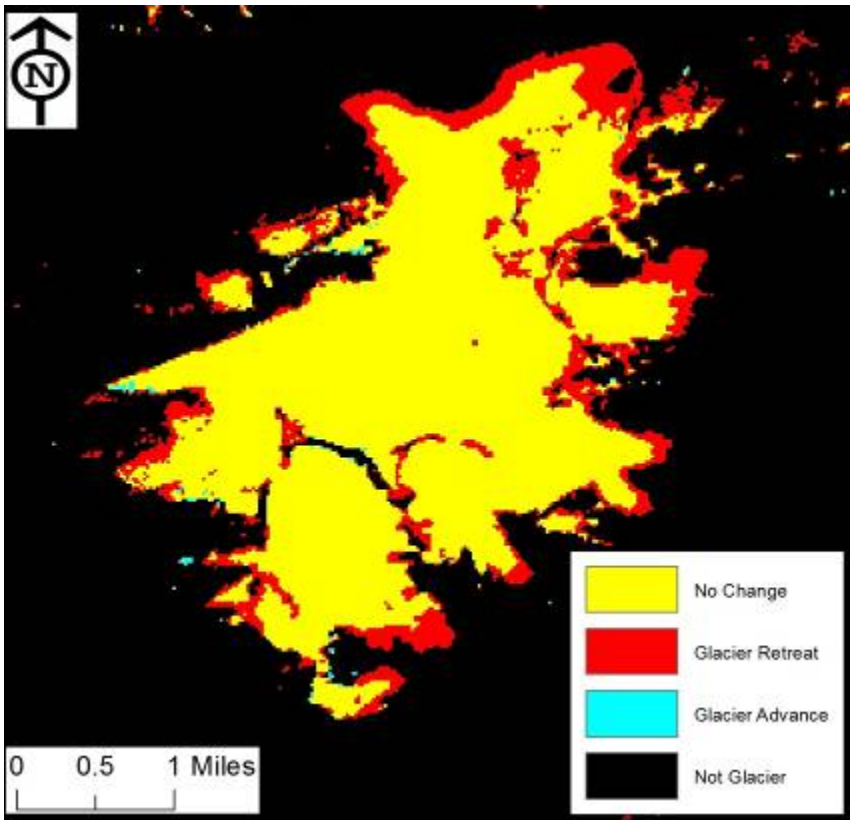

Figure 38. Results of the change detection post-classification method for the Saussure Glacier showing fairly significant glacier area retreat between the years 1984 and 2011.

The general trend in the area extent of the Saussure Glacier between 1948 and 2011 is clearly showing to be on a downward trajectory, as demonstrated in Figure 36, with the most recent years' data (1995-2011) showing primarily an average total area of the glacier between 6.0mi$^2$/15.54km$^2$ and 8.0mi$^2$/20.72km$^2$. However, there were substantial spikes in glacier area advancement for the years 1979, 1990, and 2006 (with their subsequent large relative percentage change in the preceding and following image year). This could be in part be attributed to some patches of snow along the margins of the glacier that may have been the result of lingering seasonal snow that was not identified as such during image processing. However, the image acquisition dates for the 1990 and 2006 Landsat TM images were satisfactory for attempting to minimize the effects of seasonal snow variation (September 26 and August 28, respectively).

In addition, there were gaps in acceptable Landsat TM imagery for the years 1985, 1988, 1991, 1994, 1997, 2000-2004, 2008, and 2010; therefore, there was no glacier area extent change data available for a significant number of years during the period of interest—which potentially could affect the direction of the general area trend and the average relative change percentage rates.

The resulting calculations for temporal changes in total length of the Saussure Glacier (see Appendix) show fairly significant change during the period of interest (see Figure 39), as the total glacier length was greatest in 1948 (4.89mi/7.87km) and was the least in 2011 (3.96mi/6.37km). Over the 63 years of interest, the glacier total length decreased by 19.02% (from 4.89mi/7.87km to 3.96mi/6.37km), which equates to a decrease of 0.015mi/0.024km per year and an average relative percentage change of -1.29%. There was also some minor fluctuation in the glacier length relative percentage

change in subsequent image years—in both the positive and negative direction (see Figure 40). Glacier length increased from the previous image year in 1979, 1986, 1989, 1990, 1993, 1997, and 2009, with the 1990 clearly showing the greatest increase in glacier length of 8.76%. The glacier length decreased from the previous image year in 1961, 1984, 1987, 1992, 1995, 1996, 1998, 1999, 2005, 2006, 2007, and 2011, with the years 1984 and 1992 exhibiting the greatest decrease in total length of 9.36% and 8.47%, respectively.

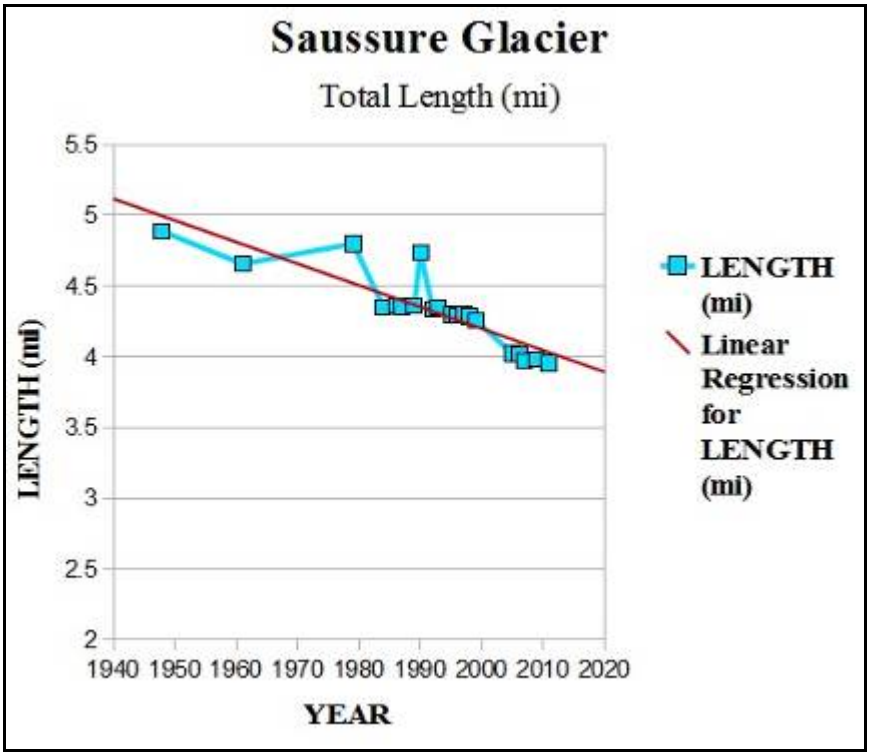


Figure 39. Temporal changes in total lengths of the Saussure Glacier.

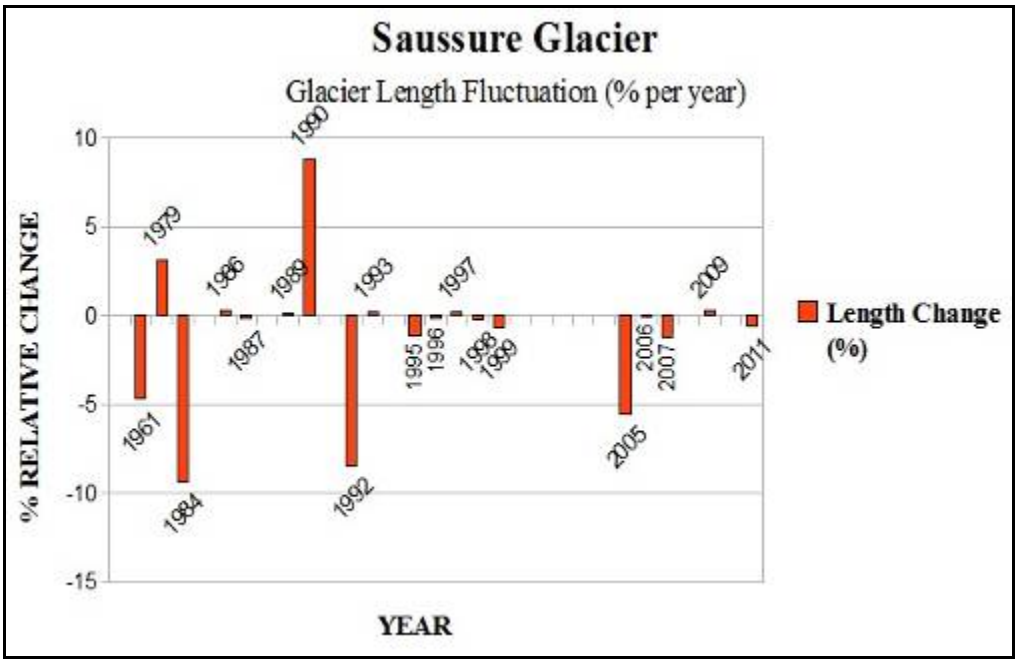

Figure 40. Fluctuation in the Saussure Glacier length relative percentage change.

The general trend in total length of the Saussure Glacier between 1948 and 2011 is clearly showing to be slightly decreasing (as shown in Figures 39 and 41), with the most recent years' data (1995-2011) showing primarily an average total glacier length between 4.0mi/6.44km and 4.5mi/7.24km. There was substantial glacier length advancement for the year 1990 (with the subsequent significant relative percentage change in the preceding and following years).

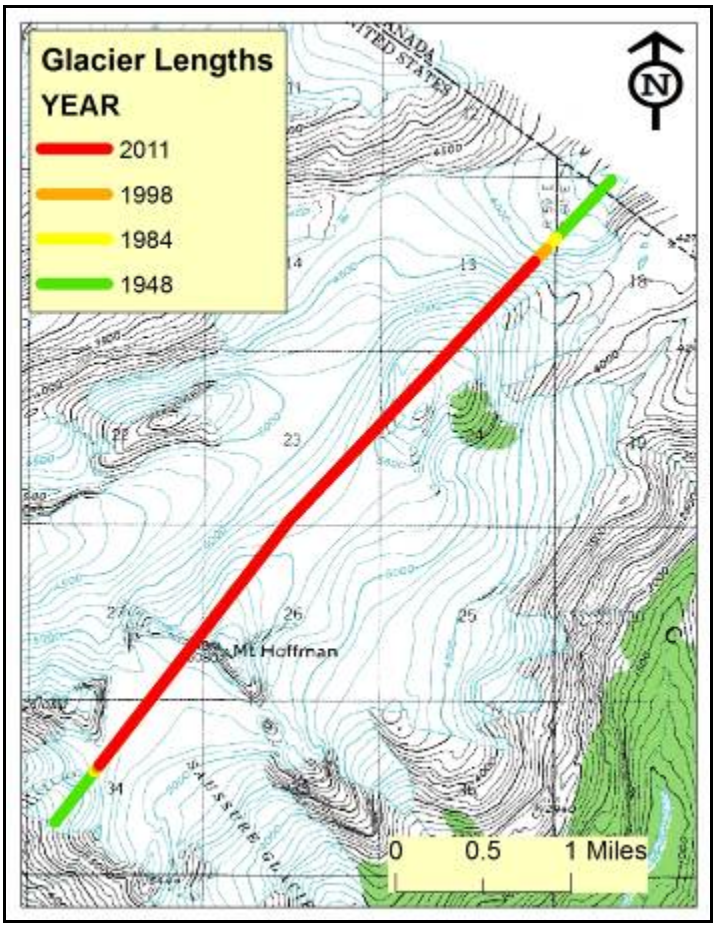


Figure 41. Glacier lengths as measured from the 1948 topographic map and 1984, 1998, and 2011 Landsat TM imagery for Saussure Glacier.

*4.3.6 All Glaciers' Areas and Lengths*

The resulting calculations for temporal changes in total area for all five glaciers of interest, collectively (see Table 6), show significant change during the period of 1948-2011. The collective average relative percentage change for all glaciers for all image years was -42.21%. The general trend in the area extent of all five glaciers of interest is clearly showing to be on a downward trajectory, with the Cleveland Glacier experiencing the highest percentage of area retreat followed by the Laughton, Carmack, Saussure, and Irene Glaciers (see Table 6 and Figure 42).

Table 6. Area extent relative percentage changes for all glaciers (1948-2011).

| GLACIER | Area ($mi^2$) 1948 | Area ($mi^2$) 2011 | Area Change ($mi^2$) | Area Change ($km^2$) | Total Area Change (%) |
|---|---|---|---|---|---|
| Carmack | 3.1 | 1.9 | -1.21 | -3.13 | -38.91% |
| Cleveland | 1.68 | 0.58 | -1.09 | -2.83 | -65.12% |
| Irene | 3.24 | 2.24 | -1.01 | -2.6 | -31.01% |
| Laughton | 4.37 | 2.06 | -2.31 | -5.99 | -52.84% |
| Saussure | 10.32 | 6.35 | -3.97 | -10.29 | -38.49% |
| All | 22.72 | 13.13 | -9.59 | -24.83 | -42.21% |

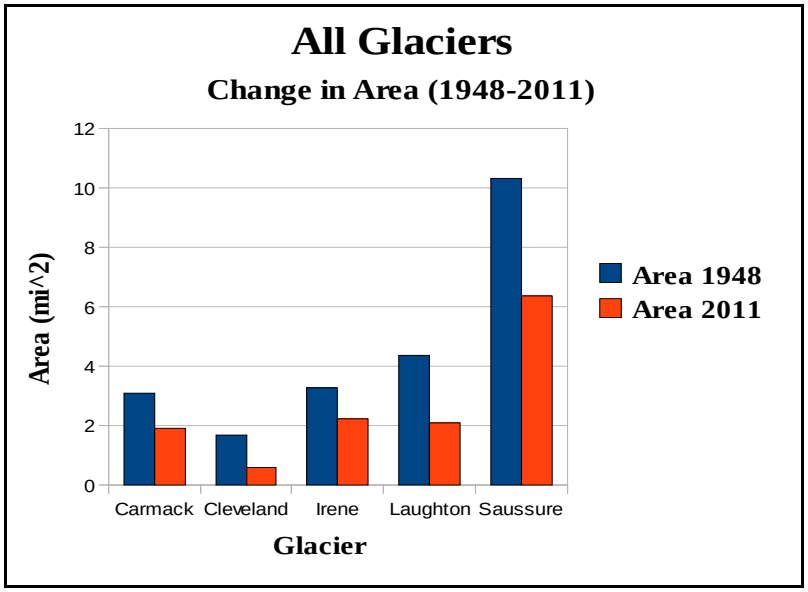


Figure 42. Change in areas for all five glaciers (1948-2011).

The resulting calculations for temporal changes in total length of all five glaciers collectively (see Table 7) also show considerable change during the period of interest. The collective average relative percentage change for all glaciers for all image years was -31.33%. The general trend in the average lengths of all five glaciers of interest is clearly showing to be decreasing, with the Irene Glacier experiencing the highest percentage of length retreat followed by the Cleveland, Laughton, Carmack, and Saussure Glaciers (see Table 7 and Figure 43).

Table 7. Total length relative percentage changes for all glaciers (1948-2011).

| GLACIER | Length 1948 (mi) | Length 2011 (mi) | Length Change (mi) | Length Change (km) | Total Length Change (%) |
|---|---|---|---|---|---|
| Carmack | 3.97 | 2.81 | -1.16 | -1.87 | -29.33% |
| Cleveland | 2.24 | 1.33 | -0.91 | -1.46 | -40.66% |
| Irene | 3.37 | 1.91 | -1.46 | -2.35 | -43.27% |
| Laughton | 2.28 | 1.49 | -0.78 | -1.26 | -34.38% |
| Saussure | 4.89 | 3.96 | -0.93 | -1.5 | -19.03% |
| All | 16.74 | 11.5 | -5.24 | -8.44 | -31.33% |

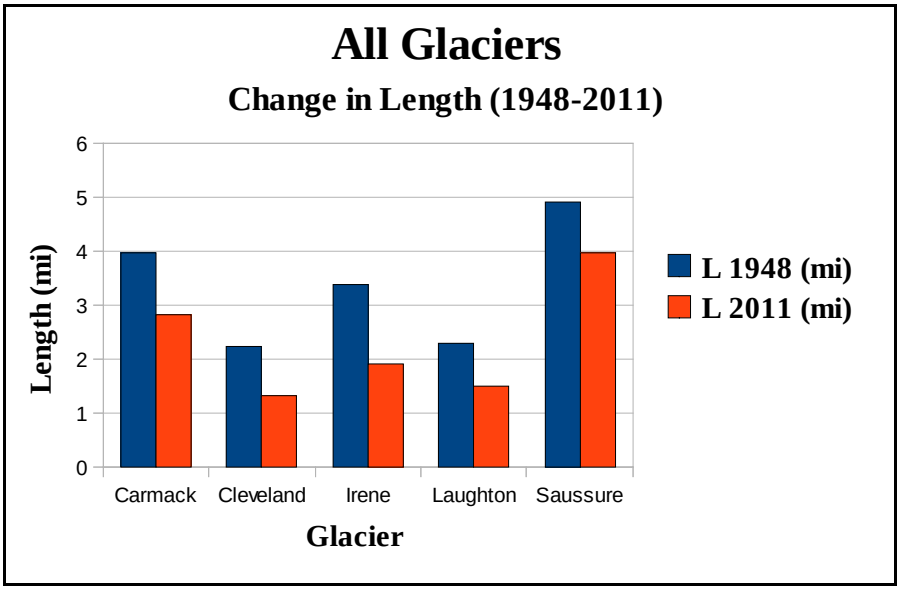


Figure 43. Changes in lengths for all five glaciers (1948-2011).

# CHAPTER 5: CONCLUSION

## 5.1 Summary

The primary objective of this study was to inventory, detect, quantify, and analyze specific parametric changes in glacier area extent and length for five alpine glaciers in Southeast Alaska, individually and collectively, including the Carmack, Cleveland, Irene, Laughton, and Saussure Glaciers all located above the borough of Skagway. The research objective was accomplished primarily by applying remote sensing technology in addition to utilizing historic aerial photographs and topographic maps for the purpose of delineating glacier boundaries over the time period of 1948-2011 and incorporating GIS for analyzing the resulting geometry, statistics, and other parametric calculations.

Furthermore, multi-temporal Landsat ETM+ and TM images were determined to be suitable remotely-sensed data for detecting changes in the glacier area extents (and subsequent lengths), particularly through the use of such image processing techniques as NDSI calculation, band ratioing, and density slicing. These methods proved valuable for overcoming glacier mapping challenges arising from cloud cover, seasonal snow, and topographic influences.

The results of this study provided a detailed analysis of the temporal changes in glacier area extents and lengths and clearly exhibited the trends for all five glaciers, individually and collectively. All glaciers were found to be decreasing in area and length substantially between 1948 and 2011. Although there were some image years experiencing glacier advancement during this time period, the overall trend in the glacier parameters of interest has clearly been moving in the negative direction.

However, this study did present both anticipated and unforeseen challenges. One particular challenge was that there were a fairly large number of years that the Landsat ETM+ and TM imagery were available but contained such persistent cloud cover over the glaciers of interest as to render the images unusable for the study. Fortunately, all images that contained some degree of clouds not covering the glacier of interest were utilized, as the NDSI statistic proved to be largely effective at eliminating these clouds for the subsequent image classification. A second challenge involved the processing of the 1979 123,214 scale aerial photographs acquired from the USGS. The smaller-scale image made it difficult to geo-reference the photographs to the high-spatial resolution satellite imagery; and consequently, the RMSE values (3.98m and 6.02m) were considerably higher than what was preferred ($\leq 1$). A third challenge related to the ground truth imagery utilized in the thematic accuracy assessment of the classified 2006 Irene Glacier image. Only a panchromatic image was available for this specific area of interest, which did present some difficulties when visually interpreting glaciers versus non-glaciers. A multi-spectral, high-resolution image would have been preferable for overcoming this challenge.

An additional challenge involved the subjectivity applied when deriving glacier length reference lines. These lines were drawn primarily based on visual interpretation of the "center" of the alpine glacier, which was difficult to assess (especially in the multi-part Laughton Glacier) particularly due to major inherent differences between alpine and tidewater glaciers. Alpine glaciers often do not contain a primary glacier "tongue," as they typically can advance or retreat at multiple locations and in many directions, and

alpine glaciers often contain multiple glacier areas—not just a single glacier body. Visual interpretation of length lines was performed to the best of the author's ability.

### 5.2 Advantages and Limitations

In analyzing temporal changes to alpine glaciers in Southeast Alaska, a number of advantages and a few limitations were identified. One particular advantage of this glacier change analysis was the relatively large quantity of temporal data that was collected concerning area and length parametric change for five glaciers with no known previous record of inventory. While the region just to the south, known as the Juneau Icefield, has been the location for several extensive glacier studies, the Carmack, Cleveland, Irene, Laughton, and Saussure Glaciers do not contain any previous records involving a change analysis, remotely or *in situ*. Another advantage of this analysis was the further evidence that was provided in regards to the effectiveness of utilizing remotely-sensed imagery for not only inventorying temporal glacier changes economically, practically, and accurately, but also for providing a detailed analysis of what changes have occurred, the location of such changes, the degree or magnitude of change, and the individual and collective trends.

Furthermore, the study opened avenues for further temporal analyses—not only for analyzing changes to other glaciers in the region, but also for incorporating additional change parameters in future glacier studies concerning the five glaciers of interest, including the parameters of mass balance, elevation, and velocity. Moreover, the data compiled in this analysis could be of benefit to the borough of Skagway and associated local tour operations-- particularly the data concerning changes to the area and length of

the Laughton Glacier, which is a glacier that is often incorporated in to multiple tour excursions during the summer seasons.

There are several limitations to this analysis that have been identified, however. One limitation touched on in the results of the glacier change analysis involved the gaps in available/usable satellite imagery between 1984 and 2011. These gaps in acceptable Landsat ETM+ and TM imagery for deriving glacier areas and lengths could potentially affect the direction of the general length trend and the average relative percentage change rates. While some of the lack of acceptable imagery could be attributed to persistent cloud cover over the glaciers of interest, there were also the years of 2000 and 2002 when neither the Landsat TM nor ETM+ were available through the USGS Landsat imagery archive. As noted earlier, without a complete, annual record of glacier change detection there is a possibility that the general individual and collective glacier change trends could lack sufficient representation.

Another limitation involved the 1979 aerial photographs for all five glaciers of interest. The panchromatic image, as opposed to a multi-spectral image, made it difficult to visually assess glacier boundaries. These photographs along with the digitized topographic maps lacked associated metadata detailing estimated error. Therefore, the overall accuracy and error for the topographic maps and aerial imagery were not known. Furthermore, the glacier areas digitized from the 1948 and 1961 topographic maps and the 1979 aerial photograph likely contain some degree of spatial error introduced during the digitizing process in addition to unknown error in the original USGS topographic maps.

Finally, there was some subjectivity in the delineation of the individual glacier boundaries for the Laughton and Irene Glaciers. The Laughton Glacier consists of two primary glacier tongues; however, there are multiple glacier areas in the immediate proximity that are essentially lumped together and called the "Laughton Glacier." The Irene Glacier boundary was even more subjective, as there was a need to arbitrarily limit the boundary of the entire icefield for two primary reasons: 1) the lack of readily-available, high spatial-resolution satellite imagery for groundtruthing the area immediately west of the selected Irene Glacier boundary, and 2) the absence of a digital boundary showing the actual western extent of the glacier.

Lastly, there was unknown spatial and positional error in the USGS topographic map (1948, 1961) glacier boundaries, as these maps lacked associated ground truth data (for field-checking glacier areas represented on the maps), and the 1961 map (a compilation of 1:63,360 scale maps) generalized the glacier boundaries—thus creating the possibility of over or under-representing glacier areas and subsequent lengths for that particular year.

### 5.3 Future Improvements/Studies

Temporal glacier change analysis, specifically in examining parametric changes to the five alpine glaciers in this study, could potentially be expanded. The use of Digital Elevation Models (DEMs) or Shuttle Radar Topography Mission (SRTM) elevation datasets could be incorporated in to a future study for the purpose of analyzing change in the additional glacier parameter of elevation and for delineating debris-covered portions of the glacier that are often misclassified during the image classification process or in the visual analysis of historic aerial photographs. Also, future studies focusing on similar

topics could be undertaken which might create a more complete picture of the changes in not only the glaciers analyzed in this study, but also for others within the Coast Mountains of Southeast Alaska.

Additional change parameters could also be incorporated in to future studies, including glacier thickness/volume (mass balance) and geomorphology. Changes in glacier thickness/volume (mass balance) could provide more important information in regards to the glacier trend (advancing or retreating) and long-term, regional climate trends. The study of glacial geomorphology could provide more in-depth information as to current and future changes in landforms (e.g., moraines, eskers, glacial lakes) through the use of *in situ* observations and measurements. Essentially, future studies concerning the topic of glacier change in the study area could be most benefited from analyzing a multitude of glacier change variables over time.

Finally, future research and analysis could be well-served by further examining and quantifying the correlation between climate change and glacier parametric change in the five glaciers analyzed in this study. This examination could be performed specifically by collecting climate data covering the period of 1948-2011 and comparing the climate trend data with the trends exhibited in the glacier change analysis, specifically examining and comparing the years of fluctuation between glacier advancement and retreat.

## APPENDIX: GLACIER AREA AND LENGTH CHANGE TABLES

Changes in total areas and lengths of Carmack Glacier (1948-2011).

| YEAR | Area ($km^2$) | Area Change ($km^2$) | Area ($mi^2$) | Area Change ($mi^2$) | Area Change (%) | Length (km) | Length Change (km) | Length (mi) | Length Change (mi) | Length Change (%) |
|---|---|---|---|---|---|---|---|---|---|---|
| 1948 | 8.04 | - | 3.1 | - | - | 6.39 | - | 3.97 | - | - |
| 1961 | 6.88 | -1.16 | 2.66 | -0.45 | -14.39% | 5.65 | -0.74 | 3.51 | -0.46 | -11.6% |
| 1979 | 7.68 | 0.8 | 2.97 | 0.31 | 10.42% | 5.26 | -0.39 | 3.27 | -0.24 | -6.9% |
| 1984 | 6.69 | -0.99 | 2.58 | -0.38 | -12.87% | 5.05 | -0.21 | 3.14 | -0.13 | -4.01% |
| 1985 | - | - | - | - | - | - | - | - | - | - |
| 1986 | 6.19 | -0.5 | 2.39 | -0.19 | -7.49% | 5.01 | -0.04 | 3.11 | -0.02 | -0.71% |
| 1987 | 6.2 | 0.01 | 2.39 | 0 | 0.15% | 4.98 | -0.03 | 3.1 | -0.02 | -0.56% |
| 1988 | - | - | - | - | - | - | - | - | - | - |
| 1989 | 5.63 | -0.57 | 2.17 | -0.22 | -9.25% | 5.03 | 0.05 | 3.13 | 0.03 | 0.92% |
| 1990 | 6.56 | 0.94 | 2.53 | 0.36 | 16.62% | 6.11 | 1.08 | 3.79 | 0.67 | 21.41% |
| 1991 | - | - | - | - | - | - | - | - | - | - |
| 1992 | 5.78 | -0.78 | 2.23 | -0.3 | -11.87% | 4.74 | -1.36 | 2.95 | -0.85 | -22.34% |
| 1993 | 6.1 | 0.32 | 2.35 | 0.12 | 5.45% | 5.14 | 0.39 | 3.19 | 0.24 | 8.26% |
| 1994 | 6.28 | 0.18 | 2.42 | 0.07 | 2.94% | 5.1 | -0.04 | 3.17 | -0.02 | -0.7% |
| 1995 | 4.07 | -2.21 | 1.57 | -0.85 | -35.14% | 4.13 | -0.97 | 2.57 | -0.6 | -18.96% |
| 1996 | 4.86 | 0.79 | 1.88 | 0.3 | 19.39% | 4.58 | 0.45 | 2.85 | 0.28 | 10.91% |
| 1997 | 4.16 | -0.7 | 1.61 | -0.27 | -14.37% | 4.52 | -0.06 | 2.81 | -0.04 | -1.4% |
| 1998 | 4.16 | 0 | 1.61 | 0 | 0% | 4.34 | -0.18 | 2.69 | -0.11 | -4.07% |
| 1999 | 4.5 | 0.33 | 1.74 | 0.13 | 7.98% | 4.42 | 0.08 | 2.74 | 0.05 | 1.87% |
| 2000 | - | - | - | - | - | - | - | - | - | - |
| 2001 | 6.76 | 2.27 | 2.61 | 0.88 | 50.44% | 4.84 | 0.43 | 3.01 | 0.26 | 9.62% |
| 2002 | - | - | - | - | - | - | - | - | - | - |
| 2003 | 4.39 | -2.37 | 1.69 | -0.92 | -35.1% | 4.49 | -0.36 | 2.79 | -0.22 | -7.33% |
| 2004 | 4.06 | -0.33 | 1.57 | -0.13 | -7.61% | 4.5 | 0.02 | 2.8 | 0.01 | 0.33% |
| 2005 | 4.71 | 0.66 | 1.82 | 0.25 | 16.16% | 4.6 | 0.1 | 2.86 | 0.06 | 2.22% |
| 2006 | 7.4 | 2.69 | 2.86 | 1.04 | 57.09% | 5.3 | 0.7 | 3.29 | 0.43 | 15.21% |
| 2007 | 4.93 | -2.47 | 1.9 | -0.95 | -33.4% | 4.5 | -0.8 | 2.8 | -0.5 | -15.07% |
| 2008 | - | - | - | - | - | - | - | - | - | - |
| 2009 | - | - | - | - | - | - | - | - | - | - |
| 2010 | - | - | - | - | - | - | - | - | - | - |
| 2011 | 4.91 | -0.02 | 1.9 | -0.01 | -0.38% | 4.52 | 0.01 | 2.81 | 0.01 | 0.31% |
| 1948-2011 | - | -3.13 | - | -1.21 | -38.71% | - | -1.87 | - | -1.16 | -29.22% |
| Rate (+-/yr) | - | -0.049 | - | -0.019 | - | - | -0.036 | - | -0.022 | - |
| Rate (%/yr) | - | - | - | - | -0.97% | - | - | - | - | -1.03% |

Changes in total areas and lengths of Cleveland Glacier (1948-2011).

| YEAR | Area ($km^2$) | Area Change ($km^2$) | Area ($mi^2$) | Area Change ($mi^2$) | Area Change (%) | Len. (km) | Length Chg. (km) | Len. (mi) | Length Chg. (mi) | Length Chg. (%) |
|---|---|---|---|---|---|---|---|---|---|---|
| 1948 | 4.34 | - | 1.68 | - | - | 3.6 | - | 2.24 | - | - |
| 1961 | 4.01 | -0.34 | 1.55 | -0.13 | -7.74% | 3.43 | -0.16 | 2.13 | -0.1 | -4.56% |
| 1979 | 5.59 | 1.59 | 2.16 | 0.61 | 39.64% | 3.08 | -0.36 | 1.91 | -0.22 | -10.4% |
| 1984 | 3.83 | -1.76 | 1.48 | -0.68 | -31.55% | 2.56 | -0.52 | 1.59 | -0.32 | -16.8% |
| 1985 | - | - | - | - | - | - | - | - | - | - |
| 1986 | 3.49 | -0.34 | 1.35 | -0.13 | -8.86% | 2.6 | 0.04 | 1.61 | 0.02 | 1.48% |
| 1987 | 3.39 | -0.1 | 1.31 | -0.04 | -2.91% | 2.53 | -0.07 | 1.57 | -0.04 | -2.77% |
| 1988 | - | - | - | - | - | - | - | - | - | - |
| 1989 | 2.7 | -0.69 | 1.04 | -0.27 | -20.27% | 2.47 | -0.06 | 1.53 | -0.04 | -2.26% |
| 1990 | 5.26 | 2.56 | 2.03 | 0.99 | 94.6% | 2.78 | 0.31 | 1.72 | 0.19 | 12.43% |
| 1991 | - | - | - | - | - | - | - | - | - | - |
| 1992 | 2.94 | -2.31 | 1.14 | -0.89 | -44.03% | 2.75 | -0.02 | 1.71 | -0.01 | -0.86% |
| 1993 | 4.09 | 1.15 | 1.58 | 0.44 | 39.08% | 3.22 | 0.46 | 2 | 0.29 | 16.86% |
| 1994 | 3.6 | -0.49 | 1.39 | -0.19 | -11.98% | 2.46 | -0.76 | 1.53 | -0.47 | -23.48% |
| 1995 | 1.81 | -1.79 | 0.7 | -0.69 | -49.69% | 2.36 | -0.1 | 1.47 | -0.06 | -4.1% |
| 1996 | 1.72 | -0.09 | 0.66 | -0.04 | -5.01% | 2.37 | 0.01 | 1.47 | 0.01 | 0.51% |
| 1997 | 1.64 | -0.08 | 0.63 | -0.03 | -4.76% | 2.42 | 0.05 | 1.5 | 0.03 | 2.11% |
| 1998 | 4.05 | 2.41 | 1.57 | 0.93 | 147.26% | 2.48 | 0.05 | 1.54 | 0.03 | 2.27% |
| 1999 | 1.43 | -2.62 | 0.55 | -1.01 | -64.73% | 2.23 | -0.25 | 1.38 | -0.15 | -10.05% |
| 2000 | - | - | - | - | - | - | - | - | - | - |
| 2001 | - | - | - | - | - | - | - | - | - | - |
| 2002 | - | - | - | - | - | - | - | - | - | - |
| 2003 | 1.31 | -0.12 | 0.5 | -0.05 | -8.68% | 2.13 | -0.1 | 1.32 | -0.06 | -4.31% |
| 2004 | 1.16 | -0.14 | 0.45 | -0.05 | -10.82% | 2.13 | -0.01 | 1.32 | 0 | -0.33% |
| 2005 | 1.71 | 0.55 | 0.66 | 0.21 | 47.22% | 2.22 | 0.09 | 1.38 | 0.06 | 4.42% |
| 2006 | 6.05 | 4.34 | 2.34 | 1.67 | 252.86% | 2.53 | 0.31 | 1.57 | 0.19 | 14.02% |
| 2007 | 1.79 | -4.26 | 0.69 | -1.65 | -70.46% | 2.18 | -0.35 | 1.36 | -0.22 | -13.79% |
| 2008 | - | - | - | - | - | - | - | - | - | - |
| 2009 | - | - | - | - | - | - | - | - | - | - |
| 2010 | - | - | - | - | - | - | - | - | - | - |
| 2011 | 1.51 | -0.27 | 0.58 | -0.11 | -15.26% | 2.14 | -0.05 | 1.33 | -0.03 | -2.11% |
| 1948-2011 | - | -2.83 | - | -1.1 | -65.48% | - | -1.46 | - | -0.91 | -40.63% |
| Rate (+-/yr) | - | -0.45 | - | -0.17 | - | - | -0.014 | - | -0.023 | - |
| Rate (%/yr) | - | - | - | - | -0.55% | - |  | - | - | -0.94% |

Changes in total areas and lengths of Irene Glacier (1948-2011).

| YEAR | Area ($km^2$) | Area Change ($km^2$) | Area ($mi^2$) | Area Change ($mi^2$) | Area Change (%) | Len. (km) | Length Change (km) | Len. (mi) | Length Change (mi) | Length Change (%) |
|---|---|---|---|---|---|---|---|---|---|---|
| 1948 | 8.4 | - | 3.24 | - | - | 5.42 | - | 3.37 | - | - |
| 1961 | 8.4 | 0.01 | 3.24 | 0 | 0.0% | 5.05 | -0.38 | 3.14 | -0.23 | -6.93% |
| 1979 | 10.64 | 2.23 | 4.11 | 0.86 | 26.59% | 4.79 | -0.26 | 2.98 | -0.16 | -5.07% |
| 1984 | 7.16 | -3.48 | 2.76 | -1.34 | -32.71% | 3.37 | -1.42 | 2.09 | -0.88 | -29.69% |
| 1985 | - | - | - | - | - | - | - | | - | - |
| 1986 | 7.27 | 0.11 | 2.81 | 0.04 | 1.56% | 3.09 | -0.28 | 1.92 | -0.17 | -8.25% |
| 1987 | 7.27 | 0 | 2.81 | 0 | 0.0% | 3.12 | 0.03 | 1.94 | 0.02 | 1.0% |
| 1988 | - | - | - | - | - | - | - | | - | - |
| 1989 | 7.05 | -0.22 | 2.72 | -0.08 | -2.98% | 3.17 | 0.04 | 1.97 | 0.03 | 1.41% |
| 1990 | 8.57 | 1.52 | 3.31 | 0.59 | 21.49% | 3.49 | 0.32 | 2.17 | 0.2 | 10.21% |
| 1991 | - | - | - | - | - | - | - | | - | - |
| 1992 | 6.75 | -1.82 | 2.61 | -0.7 | -21.22% | 3.06 | -0.43 | 1.9 | -0.27 | -12.27% |
| 1993 | 7.68 | 0.93 | 2.97 | 0.36 | 13.83% | 3.06 | 0 | 1.9 | 0 | 0.13% |
| 1994 | - | - | - | - | - | - | - | | - | - |
| 1995 | 5.51 | -2.18 | 2.13 | -0.84 | -28.31% | 2.82 | -0.24 | 1.75 | -0.15 | -7.87% |
| 1996 | 6.41 | 0.9 | 2.47 | 0.35 | 16.37% | 2.97 | 0.15 | 1.85 | 0.09 | 5.28% |
| 1997 | - | - | - | - | - | - | - | - | - | - |
| 1998 | 6.75 | 0.34 | 2.61 | 0.13 | 5.35% | 3.21 | 3.21 | 2 | 2 | 8.11% |
| 1999 | 5.88 | -0.87 | 2.27 | -0.34 | -12.87% | 2.82 | -0.4 | 1.75 | -0.25 | -12.36% |
| 2000 | - | - | - | - | - | - | - | | - | - |
| 2001 | 7.29 | 1.4 | 2.81 | 0.54 | 23.85% | 2.44 | -0.37 | 1.52 | -0.23 | -13.28% |
| 2002 | - | - | - | - | - | - | - | | - | - |
| 2003 | 5.73 | -1.56 | 2.21 | -0.6 | -21.38% | 2.78 | 0.33 | 1.72 | 0.21 | 13.68% |
| 2004 | 5.56 | -0.17 | 2.15 | -0.07 | -2.97% | 2.79 | 0.01 | 1.73 | 0.01 | 0.4% |
| 2005 | 6.1 | 0.54 | 2.36 | 0.21 | 9.78% | 2.76 | -0.03 | 1.71 | -0.02 | -0.97% |
| 2006 | 7.7 | 1.59 | 2.97 | 0.62 | 26.11% | 2.79 | 0.03 | 1.73 | 0.02 | 1.05% |
| 2007 | 5.89 | -1.8 | 2.28 | -0.7 | -23.4% | 2.76 | -0.03 | 1.71 | -0.02 | -1.22% |
| 2008 | - | - | - | - | - | - | - | | - | - |
| 2009 | 6.64 | 0.75 | 2.56 | 0.29 | 12.64% | 2.69 | -0.06 | 1.67 | -0.04 | -2.32% |
| 2010 | - | - | - | - | - | - | - | | - | - |
| 2011 | 5.79 | -0.85 | 2.24 | -0.33 | -12.74% | 3.08 | 0.39 | 1.91 | 0.24 | 14.31% |
| 1948-2011 | - | -2.6 | - | -1.01 | -30.86% | - | -2.35 | - | -1.46 | -43.32% |
| Rate (+-/yr) | - | -0.016 | - | -0.041 | - | - | 0.023 | - | 0.037 | - |
| Rate (%/yr) | - | | - | - | -1.10% | - | - | - | - | -0.90% |

Changes in total areas and lengths of Laughton Glacier (1948-2011).

| Year | Area ($km^2$) | Area Change ($km^2$) | Area ($mi^2$) | Area Change ($mi^2$) | Area Change (%) | Len. (km) | Length Change (km) | Len. (mi) | Length Change (mi) | Length Change (%) |
|---|---|---|---|---|---|---|---|---|---|---|
| 1948 | 11.33 | - | 4.37 | - | - | 3.67 | - | 2.28 | - | - |
| 1961 | 10.39 | -0.94 | 4.01 | -0.36 | -8.27% | 3.6 | -0.07 | 2.23 | -0.04 | -1.91% |
| 1979 | 11.6 | 1.2 | 4.48 | 0.46 | 11.57% | 3.82 | 0.22 | 2.37 | 0.14 | 6.2% |
| 1984 | 10.5 | -1.09 | 4.06 | -0.42 | -9.42% | 3.42 | -0.4 | 2.12 | -0.25 | -10.48% |
| 1985 | - | - | - | - | - | - | - | - | - | - |
| 1986 | 8.35 | -2.15 | 3.23 | -0.83 | -20.48% | 3.32 | -0.1 | 2.06 | -0.06 | -3.01% |
| 1987 | 8.6 | 0.24 | 3.32 | 0.09 | 2.89% | 3.31 | -0.01 | 2.06 | 0 | -0.18% |
| 1988 | - | - | - | - | - | - | - | - | - | - |
| 1989 | 7.18 | -1.42 | 2.77 | -0.55 | -16.5% | 3.25 | -0.06 | 2.02 | -0.03 | -1.69% |
| 1990 | 11.1 | 3.92 | 4.28 | 1.51 | 54.6% | 3.48 | 0.23 | 2.16 | 0.14 | 6.95% |
| 1991 | - | - | - | - | - | - | - | - | - | - |
| 1992 | 7.88 | -3.22 | 3.04 | -1.24 | -28.98% | 3.15 | -0.33 | 1.95 | -0.21 | -9.57% |
| 1993 | - | - | - | - | - | - | - | - | - | - |
| 1994 | - | - | - | - | - | - | - | - | - | - |
| 1995 | 3.47 | -4.41 | 1.34 | -1.7 | -56.03% | 3.12 | -0.03 | 1.94 | -0.02 | -0.99% |
| 1996 | 6.39 | 2.92 | 2.47 | 1.13 | 84.36% | 3.17 | 0.06 | 1.97 | 0.04 | 1.83% |
| 1997 | - | - | - | - | - | - | - | - | - | - |
| 1998 | 9.12 | 2.73 | 3.52 | 1.05 | 42.76% | 3.59 | 0.42 | 2.23 | 0.26 | 13.11% |
| 1999 | 4.95 | -4.17 | 1.91 | -1.61 | -45.7% | 2.99 | -0.6 | 1.86 | -0.37 | -16.58% |
| 2000 | - | - | - | - | - | - | - | - | - | - |
| 2001 | 9.97 | 5.02 | 3.85 | 1.94 | 101.41% | 3.09 | 0.1 | 1.92 | 0.06 | 3.24% |
| 2002 | - | - | - | - | - | - | - | - | - | - |
| 2003 | 5.08 | -4.89 | 1.96 | -1.89 | -49.03% | 2.96 | -0.13 | 1.84 | -0.08 | -4.17% |
| 2004 | 4.21 | -0.87 | 1.63 | -0.34 | -17.16% | 1.99 | -0.97 | 1.24 | -0.6 | -32.73% |
| 2005 | 6.48 | 2.27 | 2.5 | 0.88 | 53.9% | 2.5 | 0.51 | 1.55 | 0.31 | 25.4% |
| 2006 | 12.69 | 6.21 | 4.9 | 2.4 | 95.88% | 2.37 | -0.12 | 1.48 | -0.08 | -4.96% |
| 2007 | 7.94 | -4.75 | 3.07 | -1.83 | -37.43% | 2.75 | 0.37 | 1.71 | 0.23 | 15.67% |
| 2008 | - | - | - | - | - | - | - | - | - | - |
| 2009 | 6.18 | -1.77 | 2.38 | -0.68 | -22.25% | 1.94 | -0.8 | 1.21 | -0.5 | -29.24% |
| 2010 | 8.21 | 2.03 | 3.17 | 0.78 | 32.92% | 2.71 | 0.77 | 1.68 | 0.48 | 39.48% |
| 2011 | 5.34 | -2.86 | 2.06 | -1.11 | -34.9% | 2.41 | -0.31 | 1.49 | -0.19 | -11.25% |
| 1948-2011 | - | -5.99 | - | -2.31 | -52.86% | - | -1.26 | - | -0.78 | -34.65% |
| Rate (+-/yr) | - | -0.095 | - | -0.037 | - | - | -0.020 | - | -0.013 | - |
| Rate (%/yr) | - | - | - | - | -0.75% | - | - | - | - | -1.04% |

Changes in total areas and lengths of Saussure Glacier (1948-2011).

| Year | Area ($km^2$) | Area Change ($km^2$) | Area ($mi^2$) | Area Change ($mi^2$) | Area Change (%) | Len. (km) | Length Change (km) | Len. (mi) | Length Change (mi) | Length Change (%) |
|---|---|---|---|---|---|---|---|---|---|---|
| 1948 | 26.73 | - | 10.32 | - | - | 7.87 | - | 4.89 | - | - |
| 1961 | 25.42 | -1.32 | 9.81 | -0.51 | -4.93% | 7.5 | -0.37 | 4.66 | -0.23 | -4.7% |
| 1979 | 31.21 | 5.79 | 12.05 | 2.23 | 22.77% | 7.73 | 0.23 | 4.8 | 0.14 | 3.07% |
| 1984 | 20.84 | -10.37 | 8.05 | -4 | -33.22% | 7 | -0.72 | 4.35 | -0.45 | -9.36% |
| 1985 | - | - | - | - | - | - | - | - | - | - |
| 1986 | 21.66 | 0.82 | 8.36 | 0.32 | 3.93% | 7.02 | 0.02 | 4.36 | 0.01 | 0.24% |
| 1987 | 21.55 | -0.11 | 8.32 | -0.04 | -0.5% | 7.01 | -0.01 | 4.35 | -0.01 | -0.2% |
| 1988 | - | - | - | - | - | - | - | - | - | - |
| 1989 | 20.76 | -0.79 | 8.02 | -0.3 | -3.66% | 7.01 | 0.01 | 4.36 | 0 | 0.09% |
| 1990 | 28.97 | 8.21 | 11.18 | 3.17 | 39.52% | 7.63 | 0.61 | 4.74 | 0.38 | 8.76% |
| 1991 | - | - | - | - | - | - | - | - | - | - |
| 1992 | 20.38 | -8.58 | 7.87 | -3.31 | -29.63% | 6.98 | -0.65 | 4.34 | -0.4 | -8.47% |
| 1993 | 22.99 | 2.61 | 8.88 | 1.01 | 12.81% | 6.99 | 0.01 | 4.35 | 0.01 | 0.21% |
| 1994 | - | - | - | - | - | - | - | - | - | - |
| 1995 | 16.36 | -6.63 | 6.32 | -2.56 | -28.83% | 6.92 | -0.08 | 4.3 | -0.05 | -1.13% |
| 1996 | 18.32 | 1.95 | 7.07 | 0.75 | 11.92% | 6.9 | -0.01 | 4.29 | -0.01 | -0.17% |
| 1997 | 18.03 | -0.28 | 6.96 | -0.11 | -1.55% | 6.92 | 0.01 | 4.3 | 0.01 | 0.22% |
| 1998 | 20.31 | 2.28 | 7.84 | 0.88 | 12.62% | 6.9 | -0.02 | 4.29 | -0.01 | -0.26% |
| 1999 | 17.05 | -3.26 | 6.58 | -1.26 | -16.03% | 6.85 | -0.05 | 4.26 | -0.03 | -0.7% |
| 2000 | - | - | - | - | - | - | - | - | - | - |
| 2001 | - | - | - | - | - | - | - | - | - | - |
| 2002 | - | - | - | - | - | - | - | - | - | - |
| 2003 | - | - | - | - | - | - | - | - | - | - |
| 2004 | - | - | - | - | - | - | - | - | - | - |
| 2005 | 17.7 | 0.65 | 6.83 | 0.25 | 3.78% | 6.47 | -0.38 | 4.02 | -0.23 | -5.52% |
| 2006 | 22.77 | 5.08 | 8.79 | 1.96 | 28.68% | 6.47 | -0.01 | 4.02 | 0 | -0.09% |
| 2007 | 17.26 | -5.51 | 6.66 | -2.13 | -24.2% | 6.39 | -0.08 | 3.97 | -0.05 | -1.19% |
| 2008 | - | - | - | - | - | - | - | - | - | - |
| 2009 | 17.87 | 0.61 | 6.9 | 0.24 | 3.55% | 6.41 | 0.02 | 3.98 | 0.01 | 0.27% |
| 2010 | - | - | - | - | - | - | - | - | - | - |
| 2011 | 16.44 | -1.43 | 6.35 | -0.55 | -8.0% | 6.37 | -0.04 | 3.96 | -0.02 | -0.62% |
| 1948-2011 | - | -10.29 | - | -3.97 | -38.47% | - | -1.5 | - | -0.93 | -19.02% |
| Rate (+-/yr) | - | -0.163 | - | -0.063 | - | - | -0.024 | - | -0.015 | - |
| Rate (%/yr) | - | | | | -0.98% | - | - | - | - | -1.29% |

## REFERENCES


Allen, T.R., 1998. Topographic context of glaciers and perennial snowfields, Glacier National Park, Montana. *Geomorphology*, 21, 207-216.

Aniya, M., Sato, H., Naruse, R., Skvarca, P., and Casassa, G., 1996. The use of satellite and airborne imagery to inventory outlet glaciers of the Southern Patagonia Icefield, South America. *Photogrammetric Engineeering & Remote Sensing*, 62(12), 1361-1369.

Arendt, A.A., Echelmeyer, K.A., Harrison, W.D., Lingle, C.S, and Valentine, V.B., 2002. Rapid wastage of Alaska glaciers and their contribution to rising sea level. *Science*, 297(5580), 382-386.

Arzandeh, S. and Wang, J., 2003. Monitoring the change of phagmites distribution using satellite data. *Canadian Journal of Remote Sensing*, 29(1), 24-35.

Barnes, J.C. and Smallwood, M.D., 1975. Synopsis of current satellite snow mapping techniques with emphasis on the application of near-infrared data. In Rango, A. (ed.), *Operational Applications of Satellite Snowcover Observations*, NASA Special Publication SP-391, 199-213.

Barnett, T., Adam, J.C., and Lettenmaeir, D., 2005. Potential impacts of warming climate on water availability in snow-dominated regions. *Nature*, 438, 303-309.

Barry, R.G., 2006. The status of research on glaciers and global glacier recession: a review. *Progress in Physical Geography*, 30(3), 285-306.

Bayr, K.J., Hall, D.K., and Kovalick, W.M., 1994. Observations on glaciers in the eastern Austria Alps using satellite data. *International Journal of Remote Sensing*, 15(9), 1733-1742.

Berthier, E. and Toutin, T., 2007. SPOT5-HRS digital elevation models and the monitoring of glacier elevation changes in North-West Canada and South-East Alaska. *Remote Sensing of Environment*, 112, 2443-2454.

Binaghi, E., Madella, A., Madella, P., and Rampini, A., 1993. Integration of remote sensing images in a GIS for the study of alpine glaciers. *Proceedings, 12th EARSeL Symposium*, Hungary, Rotterdam: Balkema, 173-178.

Bitz, C.M. and Battisti, D.S., 1999. Interannual to decadal variability in climate and the glacier mass balance in Washington, Western Canada, and Alaska. *Journal of Climate*, 12(11), 3181-3196.

Bolch, T., Menounos, B., and Wheate, R., 2010. Landsat-based inventory of glaciers in western Canada, 1985-2005. *Remote Sensing of Environment*, 114, 127-137.

Bradley, R.S., Vuille, M., Diaz, H.F., and Vergara, W., 2006. Threats to water supplies in the tropical Andes. *Science*, 312, 1755-1756.

Choi, H. and Bindschadler, R., 2004. Cloud detection in Landsat imagery of ice sheets using shadow matching technique and automatic normalized difference snow index threshold value decision. *Remote Sensing of Environment*, 91, 237-242.

Civco, D.L, Hurd, J.D., Wilson, E.H., Song, M., and Zhang, Z., 2002. A comparison of land use and land cover change detection methods. In: ASPRS-ACSM Annual Conference and FIG XXII Congress, Baltimore, MD, April 22-26.

Congalton, R.G., 1991. A review of assessing the accuracy of classifications of remotely sensed data. *Remote Sensing of Environment*, 37, 35-46.

Crane, R.G. and Anderson, M.R., 1984. Satellite discrimination of snow/cloud surfaces. *International Journal of Remote Sensing*, 5, 213-223.

Della Ventura, A., Rampini, A., and Serandrei Barbero, R., 1987. Development of a satellite remote sensing technique for the study of alpine glaciers. *International Journal of Remote Sensing*, 8, 203-215.

Dowdeswell, J.A., 1986. Remote sensing of ice cap outlet glacier fluctuations on Nordaustlandet, Svalbard. *Polar Research*, 4(1), 25-32.

Dozier, J., 1987. Recent research in snow hydrology. *Reviews of Geophysics*, 25, 153-161.

Dozier, J., 1989. Spectral signature of alpine snow cover from the Landsat Thematic Mapper. *Remote Sensing of Environment*, 28, 9-22.

Dyurgerov, M.B., 2002. Glacier mass balance and regime: data of measurements and analysis, 1945-2003. *Boulder: University of Colorado Institute of Arctic and Alpine Research Occasional Paper 55*, available at http://instaar.colorado.edu/other/occ_papers.html [accessed January 17, 2013].

Dyurgerov, M.B. and Meier, M.F., 1999. Twentieth century climate change evidence from small glaciers. *Proceedings of the National Academy of Sciences of the United States of America*, 97(4), 1406-1411.

Erdenetuya, M., Khishigsuren, P., Davaa, G., and Otgontogs, M., 2006. Glacier change estimation using Landsat TM data. *International Archive of the Photogrammetry, Remote Sensing, and Spatial Information Science*, 36(6), 240-243.

Field, W.O., 1947. Glacier recession in Muir Inlet, Glacier Bay, Alaska. *The Geographical Review*, 37, 369-399.

Fitzpatrick-Lins, K., 1981. Comparison of sampling procedures and data analysis for a land-use and land-cover map. *Photogrammetric Engineering & Remote Sensing*, 47(3), 343-351.

Foody, G.M., 2002. Status of land cover classification assessment. *Remote Sensing of Environment*, 80, 185-201.

Frey, H., Paul, F., and Strozzi, T., 2012. Compilation of a glacier inventory for the western Himalayas from satellite data: methods, challenges, and results. *Remote Sensing of Environment*, 124, 832-843.

Gao, J. and Liu, Y., 2001. Applications of remote sensing, GIS, and GPS in glaciology: a review. *Progress in Physical Geography*, 25(4), 520-540.

Gratton, D.J., Howarth, P.J., and Marceau, D.J., 1990. Combining DEM parameters with Landsat MSS and TM imagery in a GIS for mountain glacier characterization. *IEEE Transactions on Geoscience and Remote Sensing*, 28(4), 766-769.

Haeberli, W., 1998. Historical evolution and operational aspects of worldwide glacier monitoring. In: Haeberli, W., Hoelze, M., Suter, S. (Eds.), *Into the Second Century of World Glacier Monitoring Prospects and Strategies*. UNESCO Publishing, Paris, pp. 35-51.

Haeberli, W. and Hoelzle, M., 1995. Application of inventory data for estimating characteristics and regional climate change effects on mountain glaciers: A pilot study with European Alps. *Annals of Glaciology*, 21, 206-212.

Haerberli, W., Cihlar, J., and Barry, R., 2000. Glacier monitoring within the Global Observing System. *Annals of Glaciology*, 31(1), 241-246.

Heid, T. and Kääb, A., 2012. Repeat optical satellite images reveal widespread and long term decrease in land-terminating glacier speeds. *The Cryosphere*, 6, 467-478.

Hall, D.K., Bayr, K.J., Schöner, W., Bindschadler, R.A., and Chien, J.Y.L., 2003. Consideration of the errors inherent in mapping historical glacier positions in Austria from the ground and space (1893-2001). *Remote Sensing of Environment*, 86, 566-577.

Hall, D.K., Benson, C.S., and Field, W.O., 1995. Changes in glaciers in Glacier Bay, Alaska, using ground and satellite measurements. *Physical Geography*, 16(1), 27-41.

Hall, D.K. and Chang, A.T.C., 1988. Reflectances of glaciers as calculated using Landsat-5 Thematic Mapper data. *Remote Sensing of Environment*, 25(3), 311-312.

Hall, D.K., Chang, A.T.C., Foster, J.L., Benson, C.S., and Kovalick.W.M., 1989. Comparison of in situ and satellite derived reflectances of Alaskan Glaciers. *Remote Sensing of Environment*, 28, 493-504.

Hall, D.K., Ormsby, J.P., Bindschadler, R.A., and Siddalingaiah, H., 1987. Characterization of snow and ice zones on glaciers using Landsat Thematic Mapper data. *Annals of Glaciology*, 9, 104-108.

Hall, D.K. and Riggs, G.A., 2010. Normalized-Difference Snow Index (NDSI). *Encyclopedia of Snow, Ice, and Glaciers*, N, 1-2.

Hung, M.C. and Wu, Y.H., 2005. Mapping and visualizing the Great Salt Lake landscape dynamics using multi-temporal satellite images, 1972-1996. *International Journal of Remote Sensing*, 26(9), 1815-1834.

Irish, R.R., Barker, J.L., Goward, S.N., and Arvidson, T., 2006. Characterization of the Landsat-7 ETM + Automated Cloud-Cover Assessment (ACCA) algorithm. *Photogrammetric Engineering & Remote Sensing*, 72(10), 1179-1188.

Jacobs, J.D., Simms, E.L, and Simms, A., 1997. Recession of the southern part of Barnes Ice Cap, Baffin Island, Canada, between 1961 and 1993, determined from digital mapping of Landsat TM. *Journal of Glaciology*, 43(143), 98-102.

Jensen, J.R., 2007. *Introductory Digital Image Processing: A Remote Sensing Perspective*. 3rd ed. Upper Saddle River, N.J.: Pearson Prentice Hall.

Jensen, J.R., Rutchey, K., Koch, M.S., and Sunil, N., 1995. Inland wetland change detection in the Everglades Water Conservation area 2A using a time series of remotely sensed data. *Photogrammetric Engineering & Remote Sensing*, 61(2), 199-209.

Kaser, G., Hardy, D.R., Mölg, T., Bradley, R.S., and Hyera, T., 2004. Modern glacier retreat on Kilimanjaro as evidence of climate change: observations and facts. *International Journal of Climatology*, 24, 324-339.

Knight, P., Weaver, R., and Sugden, D., 1987. Using Landsat MSS data for measuring ice sheet retreat. *International Journal of Remote Sensing*, 8(7), 1069-1074.

Krimmel, R., 2001. Photogrammetric data set, 1957-2000 and bathymetric measurements for Columbia Glacier, Alaska. *U.S. Geological Survey Water Resources Investigations Report*, 01, 4089.

Krimmel, R.M. and Meier, M.F., 1989. Glaciers and Glaciology of Alaska. *Field Trip Guide Book T301,* 28th Congress, Washington, D.C.: AGU.

Kulkarni, A.V., Rathore, B.P., Singh, S.K., and Bahuguna, I.M., 2011. Understanding changes in the Himalayan cryosphere using remote sensing techniques. *International Journal of Remote Sensing*, 32(3), 601-615.

Li, K., Li, Z., Gao, W., and Wang, L., 2011. Recent glacier retreat and its effect on water resources in eastern Xinjiang. *Chinese Science Bulletin*, 56(33), 3596-3604.

Li, S., Benson, C., Gens, R., and Lingle, C., 2008. Motion patterns of Nabesna Glacier (Alaska) revealed by interferometric SAR techniques. *Remote Sensing of Environment*, 112(9), 3628-36-38.

Lillesand, T.M. and Kiefer, R.W., 2000. *Remote Sensing and Image Interpretation*. New York: John Wiley & Sons, Inc.

Lopez, P., Chevallier, P., Favier, V., Pouyaud, B., Ordenes, F., and Oerlemans, J., 2010. A regional view of fluctuations in glacier length in southern South America. *Global and Planetary Change*, 71, 85-108.

Lu, D., Mausel, P., Brondizio, E., and Moran, E., 2004. Change detection techniques. *International Journal of Remote Sensing*, 25(12), 2365-2407.

Lucchitta, B.K., Mullins, K.F., Allison, A.L., and Ferrigno, J.G., 1993. Antarctic glacier-tongue velocities from Landsat images: first results. *Annals of Glaciology*, 17, 356-366.

Luckman, B.H. and Kavanaugh, T., 2000. Impact of climate fluctuations on mountain environments in the Canadian Rockies. *Ambio*, 29(7), 371-380.

Maas, G.H., 1999. The potential of height texture measures for the segmentation of airborne laser scanner data. In *Fourth International Airborne Remote Sensing Conference and Exhibition / 21st Canadian Symposium on Remote Sensing*, 21-24 June, Ottawa, Ontario, Canada.

McIver, D.K. and Friedl, M.A., 2002. Using prior probabilities in decision-tree classification of remotely sensed data. *Remote Sensing of Environment*, 81, 253-261.

Meier, M.F., 1984. Contribution of small glaciers to global sea level. *Science*, 226 (4681), 1418-1421.

Meier, M.F. and Bahr, D.B., 1996. Counting glaciers: use of scaling methods to estimate the number and size distribution of the glaciers of the world. In Colbeck, S.C., ed., *Glaciers Ice Sheets and Volcanoes*, A Tribute to Mark Meier, CRREL Special Report, 96-27, U.S. Army: Hannover, New Hampshire, 89-94.

Moik, J.G., 1980. Digital Processing of remotely sensed images. *National Aeronautics And Space Administration Technical Report SP-431*, Scientific and Technical Information Branch National Aeronautics and Space Administration, Washington D.C.

Molnia, B.F., 2008. Glaciers of North America—Glaciers of Alaska, *in* Williams, R.S., Jr., and Ferrigno, J.G. eds., Satellite image atlas of glaciers in the world: *U.S. Geological Survey Professional Paper*, 1386(K), 525p.

Moore, R.D., Fleming, S.W., Menounos, B., Wheate, R., Fountain, A., Stahl, K., Holm, K., and Jakob, M., 2009. Glacier change in western North America: influences on hydrology, geomorphic hazards, and water quality. *Hydrological Processes*, 23, 42-61.

Morisette, J.T. and Khorram, S., 2000. Accuracy assessment curves for satellite-based change detection. *Photogrammetric Engineering and Remote Sensing*, 66(7), 876-880.

Morisette, J.T., Privette, J.L., Strahler, A., Mayaux, P., and Justice, C.O., 2003. Validation of global land-cover products by the committee on Earth Observing Satellites. In Lunetta, R.L. and Lyons, J.G., eds., *Geospatial Data Accuracy Assessment*, Las Vegas, NV: U.S. Environmental Protection Agency, Report No. EPA/600/R-03/064, 335p.

Motyka, R., O'Neel, S., Connor, C.L., and Echelmeyer, K.A., 2002. Twentieth century thinning of Mendenhall Glacier, Alaska, and its relationship to climate, lake calving, and glacier run-off. *Global and Planetary Change*, 35, 93-112.

Narama, C., Kääb, A., Duishonakunov, M., and Abdrakhmatov, K., 2010. Spatial variability of recent glacier area changes in the Tien Shan Mountains, Central Asia, using Corona (~1970), Landsat (~2000), and ALOS (~2007) satellite data. *Global and Planetary Change*, 71, 42-54.

Narumalani, S., Hlady, J.T., and Jensen, J.R., 2002. Information extraction from remotely sensed data. In *Manual of Geospatial Science and Technology*, London: Taylor & Francis, 288-324.

Oerlemans, J., 1994. Quantifying global warming from the retreat of glaciers. *Science*, 264(5156), 243-245.

Oerlemans, J., 2001. *Glaciers and climate change*. A.A. Balkema Publishers, Rotterdam, Netherlands, 160pp.

Ouma, Y.O. and Tateishi, R., 2005. Optical satellite-sensor based monitoring of glacial coverage fluctuations on Mount Kenya, 1987-2000. *International Journal of Environmental Studies*, 62(6), 663-675.

Paterson, W.S.B., 1994. *The physics of glaciers*. 3rd ed. Oxford: Elsevier.

Paul, F., 2000. Evaluation of different methods for glacier mapping using Landsat TM. *Proceedings of EARSeL-SIG-Workshop Land Ice and Snow, Dresden/FRG*, June 16-17.

Paul, F., 2002. Changes in glacier area in Tyrol, Austria, between 1969 and 1992 derived from Landsat-5 Thematic Mapper and Austrian Glacier inventory. *International Journal of Remote Sensing*, 23, 487-499.

Paul, F., Kääb, A., Maisch, M., Kellenberger, T., and Haeberli, W., 2002. The new remote sensing derived Swiss glacier inventory, I: Methods. *Annals of Glaciology*, 34, 355-361.

Paul, F. and Andreeson, L.M., 2009. A new glacier inventory of the Svartisen region, Norway, from Landsat ETM+ data: challenges and change assessment. *Journal of Glaciology*, 55(192), 607-618.

Paul, F., Huggel, C., and Kääb, A., 2004. Combining satellite multispectral image data and a digital elevation model for mapping debris-covered glaciers. *Remote Sensing of Environment*, 89, 510-518.

Peduzzi, P., Herold, C., and Silverio, W., 2010. Assessing high altitude glacier thickness, volume, and area changes using field, GIS, and remote sensing techniques: the case of Nevado Coropuna (Peru). *The Cryosphere*, 4, 313-323.

Pelto, M., 2011. Utility of late summer transient snowline migration rate on Taku Glacier, Alaska. *The Cryosphere*, 5, 1127-1133.

Raj, K.B.G., 2010. Remote sensing based hazard assessment of glacial lakes: a case study in Zanskar basin, Jammu and Kashmir, India. *Geomatics, Natural Hazards, and Risk*, 1(4), 339-347.

Richards, J.A. and Jia, X., 1999. *Remote Sensing Digital Image Analysis: An Introduction*. 3rd revised ed. New York: Springer.

Romshoo, S.A. and Rashid, I., 2010. Potential and constraints of geospatial data for precise assessment of the impacts of climate change at landscape level. *International Journal of Geomatics and Geosciences*, 1(3), 386-405.

Rosenthal, W. and Dozier, J., 1996. Automated mapping of montane snow cover at subpixel resolution from the Landsat Thematic Mapper. *Water Resources*, 32(1), 115-130.

Schoner, W., Auer, I., and Bohm, R., 2000. Climate Variability and glacier reaction in the Austrian eastern Alps. *Annals of Glaciology*, 31, 31-38.

Shea, J.M., Marshall, S.J., and Livingston, J.M., 2004. Glacier distributions and climate in the Canadian Rockies. *Arctic, Antarctic, and Alpine Research*, 36(2), 272-279.

Sidjak, R.W. and Wheate, R.D., 1999. Glacier mapping of the Illecillewaet Icefield, using Landsat TM and DEM data. *International Journal of Remote Sensing*, 20(2), 273-284.

Singh, A., 1989. Digital change detection techniques using remotely-sensed data. *International Journal of Remote Sensing*, 6, 989-1003.

Solomon, S., Qin, D., Manning, M., Chen, Z., Marquis, M., Averyt, K.B., Tignor, M., and Miller, H.L. (eds), 2007. *Intergovernmental Panel on Climate Change 2007: Climate Change 2007: The physical science basis*. Contribution of working group I to the Fourth Assessment Report of the Intergovernmental Panel on climate change. Cambridge University Press, New York, USA, 996pp.

Solomina, O., Barry, R., and Bodnya, M., 2004. The retreat of Tien Shan glaciers (Kyrgyzstan) since the Little Ice Age estimated from aerial photographs, lichenometric and historical data. *Geografiska Annaler, Series A: Physical Geography*, 86(2), 205-215.

Song, C., Woodcock, C.E., Seto, K.C., Lenney, M.P., and Macomber, S.A., 2001. Classification and change detection using Landsat TM data: When and how to correct atmospheric effects?. *Remote Sensing of Environment*, 75, 230-244.

Sturm, M., Hall, D.K., Benson, C.S., and Field, W.O., 1991. Non-climatic control of glacier-terminus fluctuations in the Wrangell and Chugach Mountains, Alaska, U.S.A. *Journal of Glaciology*, 37(27), 348-356.

Tennant, C., Menounos, B., Ainsle, B., Shea, J., and Jackson, P., 2012. Comparison of modeled and geodetically derived glacier mass balance for Tiedemann and Kilnaklini glaciers, southern Coast Mountains, British Columbia, Canada. *Global and Planetary Change*, 82-83, 74-85.

United States Census Bureau, 2010. [online] Available at: http://www.census.gov/popfinder/ [Accessed 20 September 2012].

United States Geological Survey, 2013. [online] Available at: http://pubs.usgs.gov/of/2004/1216/text.html [Accessed 26 April 2013].

Veettil, B.K., 2012. Three decadal monitoring of mountain glaciers in Ecuador – a case study on ENSO impact on Andrean glaciers: A remote sensing perspective. *International Journal of Geomatics and Geosciences*, 3(1), 269-284.

Williams, Jr., R.S., 1986. Glacier inventories of Iceland: evaluation and use of sources of data. *Annals of Glaciology*, 8, 184-191.

Williams, Jr., R.S., Boovarsson, A., Friorikssson, S., Thorsteinsson, I., Palmason, G., Rist, S., Saemundsson, K., Sigtryggsson, H., and Thorarinsson, S., 1974. Environmental studies of Iceland with ERTS-1 imagery. *Proceedings of the Ninth International Symposium on Remote Sensing of the Environment*, 1, Ann Arbor, MI. Environmental Research Institute of Michigan, 31-81.

Williams, Jr., R.S. and Hall, D.K. (1998). Use of remote sensing techniques. In W. Haeberli, M. Hoelze, and S.Suter (Eds.), *Into the second century of worldwide glacier monitoring: Prospects and strategies*, Paris: UNESCO Publishing, 97-111.

Williams, Jr., R.S., Hall, D.K., Sigurdsson, O., and Chien, J.Y.L., 1997. Comparison of satellite-derived with ground-based measurements of the fluctuations of the margins of Vatnajökull, Iceland, 1973-92. *Annals of Glaciology*, 24, 72-80.

Williams, Jr., R.S., Hall, D.K., and Benson, C.S., 1991. Analysis of glacier facies using satellite techniques. *Journal of Glaciology*, 15(73), 403-415.

Wood, F.B., 1988. Global alpine glacier trends, 1960's to 1980's. *Arctic and Alpine Research*, 20 (4), 404-413.

Wu, W. and Shao, G., 2002. Optimal combination of data, classifiers, and sampling methods for accurate characterizations of deforestation. *Canadian Journal of Remote Sensing*, 28(4), 601-609.

Yuan, D., Elvidge, C.D., and Lunetta, R.S., 1998. Survey of multispectral methods for land cover change analysis. In *Remote Sensing Change Detection: Environmental Monitoring Methods and Applications*, edited by R.S. Lunetta and C.D. Elvidge, Chelsea, MI: Ann Arbor Press, pp. 21-39.

Zemp, M., Roer, I., Kaab, A., Hoelzle, M., Paul, F., and Haeberli, W., 2008. WGMS: Global Glacier Changes: facts and figures, UNEP, World Glacier Monitoring Service, Zurich, Switzerland, 88 pp., available at: http://www.grid.unep.ch/glaciers/ [Accessed 20 September 2012].